UNIVERSITAT DE BARCELONA

Resonancia magnética craneal estructural de 3 Tesla como biomarcador de neurodegeneración y pronóstico en la enfermedad de Alzheimer de inicio precoz

José Miguel Contador Muñana

Resonancia magnética craneal estructural de 3 Tesla como biomarcador de neurodegeneración y pronóstico en la enfermedad de Alzheimer de inicio precoz

Memoria de tesis doctoral presentada por José Miguel Contador Muñana para optar al grado de doctor por la Universitat de Barcelona.

Dirigida por:

Albert Lladó Plarrumaní, Unidad de Alzheimer y otros trastornos cognitivos, Hospital Clínic de Barcelona. IDIBAPS, Universitat de Barcelona y Roser Sala Llonch, Instituto de Neurociencias, Departamento de Biomedicina, Universitat de Barcelona

Tutorizada por:

Raquel Sánchez del Valle Díaz, Unidad de Alzheimer y otros trastornos cognitivos, Hospital Clínic de Barcelona. IDIBAPS, Universitat de Barcelona

Programa de doctorado de medicina e investigación traslacional. Facultad de Medicina y Ciencias de la Salud. Universitat de Barcelona

Barcelona, 22 de junio de 2022

INFORME DE LOS DIRECTORES DE TESIS

El Dr. Albert Lladó Plarrumaní, doctor en Medicina por la Universitat de Barcelona, y la Dra. Roser Sala Llonch, doctora en Neurociencias por la Universitat de Barcelona.

CERTIFICAN

Que la memoria titulada ‘Resonancia magnética craneal estructural de 3 Tesla como biomarcador de neurodegeneración y pronóstico en la enfermedad de Alzheimer de inicio precoz”, presentada por José Miguel Contador Muñana ha sido realizada bajo nuestra dirección y consideramos que reúne las condiciones necesarias para ser defendida ante el Tribunal correspondiente para optar al Grado de Doctor.

Dr. Albert Lladó Plarrumaní

Unidad de Alzheimer y

otros trastornos cognitivos,

Hospital Clínic de Barcelona.

IDIBAPS, Universitat de

Barcelona.

Dra. Roser Sala Llonch

Instituto de Neurociencias,

Departamento de

Biomedicina,

Universitat de Barcelona.

Nadie, en efecto,
ha determinado por ahora
qué puede el cuerpo

Baruch Spinoza

AGRADECIMIENTOS

Dentro de poco quedará cerrada una etapa importante a nivel académico y vital. Antes de nada, me gustaría agradecer a todas las personas que durante esta aventura *barceloní* me han acompañado y la han hecho posible, a pesar de algunos tramos accidentados. Más allá de estas palabras, espero haber demostrado a todas ellas mi gratitud durante este tiempo.

En primer lugar, quiero agradecer a todos los voluntarios que de forma desinteresada accedieron a participar en los estudios que forman parte de este proyecto. Su generosidad hace posible la investigación. Espero que este trabajo aporte, siquiera *una mica*, al conocimiento de su enfermedad.

A mis directores de tesis, el Dr. Albert Lladó Plarrumaní y la Dra. Roser Sala Llonch, los barqueros de esta aventura. Gracias por vuestro liderazgo y aliento que han sido siempre condición de posibilidad. Gracias por haberme hecho sentir tan acompañado en todo momento con vuestro apoyo y supervisión, tanto en momentos pandémicos teleconferencia mediante, como en otros más difíciles. Gracias por el trabajo y las horas dedicadas, sois todo un referente y me siento afortunado de haber aprendido tanto a vuestro lado. Albert, me gustaría darte las gracias por toda la confianza que me has depositado desde el principio. Gracias por haberme abierto la puerta para venir a Barcelona y haberme dado la oportunidad de profundizar en el campo de las demencias. Sin tu generosidad nada de esto habría sido posible. Tu saber hacer clínico y en investigación, tu claridad y las horas de discusión me han permitido sin duda progresar como médico a nivel asistencial y científico. Roser, gracias por tu confianza al tenderme una mano y aceptar codirigir este proyecto. Gracias por tu dedicación y trabajo con las imágenes que lo han hecho posible. Gracias por permitirme adentrarme en el mundo de la resonancia magnética de forma tan inteligible, tu rigor y maestría han sentado las bases de mi formación en el análisis de neuroimagen.

A la Dra. Raquel Sánchez del Valle Díaz, tutora de estas tesis y jefa de la Unidad en la que se desarrolla este proyecto, con la que he tenido la suerte y placer de trabajar. Gracias por tu confianza, sabiduría, dedicación diligente y todo lo que he podido crecer profesionalmente a tu lado. Y gracias sin duda por tus visitas y acompañamiento durante mi estancia en la 4-5

A Agnès Pérez Millán, gracias por todo el trabajo y tiempo dedicado en el análisis cuantitativo de las resonancias magnéticas, eres una parte fundamental de este proyecto. Gracias por tu ayuda y disponibilidad.

A Mircea, Sergi, Adrià, Bea, Guadalupe, Nuria, Jordi Juncà, Jordi Sarto, Óscar, Anna, Magda, Yolanda, Neus, Laura, Jaume, Miguel, es decir, a todo el equipo de la Unidad de Alzheimer y otros trastornos cognitivos del Hospital Clínic. Gracias por vuestra amabilidad y calurosa acogida. Por el acompañamiento también en momentos difíciles. Gracias por hacerlo todo tan fácil. Ha sido un verdadero placer compartir horas de hospital con vosotros y poder aprender de cada uno. Indudablemente, gracias por todo vuestro trabajo día a día, sin el cual este proyecto no habría sido posible.

A Nuria Corominas, por esta bonita amistad con la que nos venimos acompañando desde hace más de 10 años y de la que me siento afortunado. Gracias por haber estado ahí desde mi llegada a Barcelona y por todos los momentos de teatralidad.

A Esther Fernández, con la que compartí el confinamiento y he construido una amistad. Gracias por quedarte y darme la mano la noche que más lo necesité. Gracias por acompañarme y cuidarme en esta aventura.

A Marta Echaves, quien me alienta a continuar persiguiendo sueños cuando más lo necesito. Gracias por acompañarme, tanto en la virtualidad de la distancia como en el calor de la proximidad. Gracias por los cuidadosos paseos peripatéticos a la manzana y las largas conversaciones.

A Carlos Clemente, el paisano y amigo que tengo cerca. Gracias por toda la cura aquel verano y estar a mano durante este tiempo.

A Martín, Víctor, Jesús, Javi, Ulises, Chechu, J. Alejandro, Pablo, Borja, Raquel, Paula, Laura, Duna, Lucía y otros paisanos siempre presentes.

Por último, la familia. A mi hermana Rebeca, por darme lo más valioso que hay en mi vida, el amor y cariño que nos tenemos. Aunque nos separen kilómetros, nada nos aleja. A Celia, la mujer más fuerte que he conocido, que supo sostener lo insostenible, te echo de menos. A Javi, que ha estado muy presente desde bien pequeño. A Miguel Ángel, Miguel, Clara, José, Mariclara y Josefa. Y como no, a Puri y Javier, mis padres, los que más habrían disfrutado con este momento. Gracias por todo el amor con el que crecí y el gran esfuerzo que hicisteis yéndoos de Extremadura para darnos a mi hermana y a mí la formación que necesitábamos. Esta tesis es muy vuestra.

FINANCIACION

Este trabajo ha estado parcialmente financiado por el Instituto de Salud Carlos III (ISCIII) y cofinanciado por la Unión Europea (proyecto PI19/00449 Investigador Principal: Dr. Albert Lladó), PERIS 2016-2020 Departament de Salut de la Generalitat de Catalunya (proyecto SLT008 / 18/00061 Investigador Principal: Dr. Albert Lladó) y programa CERCA/Generalitat de Catalunya.

INDICE

I. LISTADO DE ABREVIATURAS

I. LISTADO DE ABREVIATURAS

Aβ42: isoforma de 42 aminoácidos de la proteína β-amiloide

ADNI: Alzheimer's Disease Neuroimaging Initiative

APOE: apolipoproteína E

CA: Cuerno de Amón

DCL: deterioro cognitivo leve

EA: enfermedad de Alzheimer

EAIP: enfermedad de Alzheimer de inicio precoz

EAIT: enfermedad de Alzheimer de inicio tardío

FDG: fluorodesoxiglucosa

LCR: líquido cefalorraquídeo

LTM: lóbulo temporal medial

NfL: neurofilamentos de cadena ligera

NIA-AA: National Institute on Aging and Alzheimer’s Association

NINCDS-ARDRA: National Institute of Neurological and Communicative Disorders and Stroke-Alzheimer’s Disease and Related Disorders Association

p-tau: proteína tau fosforilada

PET: Tomografía por emisión de positrones

PPA: proteína precursora de amiloide

PSEN: gen de la presenilina

RM: resonancia magnética

t-tau: proteína tau total

II. ENUMERACIÓN DE ARTÍCULOS QUE COMPONEN LA TESIS

II. ENUMERACIÓN DE ARTÍCULOS QUE COMPONEN LA TESIS

La tesis se presenta en formato de compendio de artículos, que son el resultado del trabajo del doctorando con la supervisión de los directores Dr. Albert Lladó Plarrumaní y Dra. Roser Sala Llonch, la tutorización de Dra. Raquel Sánchez del Valle, y la colaboración de distintos miembros de la Unidad de Alzheimer y otros trastornos cognitivos del Servicio de Neurología del Hospital Clínic.

La tesis se estructura, siguiendo la normativa del Programa de Doctorado de Medicina e investigación traslacional de la Universitat de Barcelona, como compendio de publicaciones científicas. Los artículos se enmarcan en un proyecto de investigación que, siguiendo una de las líneas de trabajo de la unidad en la cual se desarrolla, evalúa los cambios transversales y longitudinales en Resonancia Magnética (RM) craneal estructural de 3 Teslas en sujetos con enfermedad de Alzheimer de inicio precoz (EAIP) confirmada biológicamente mediante biomarcadores en líquido cefalorraquídeo (LCR). Además, se estudia la variabilidad existente en la EAIP en base al sexo en las medidas de RM craneal estructural, el deterioro cognitivo o los niveles de biomarcadores en LCR (proteína β-amiloide 42 (Aβ42), proteína tau fosforilada (p-tau), proteína tau total (t-tau) y neurofilamentos de cadena ligera (NfL)). Por otro lado, en los trabajos que la conforman también se investiga la capacidad de la RM craneal estructural de predecir la evolución cognitiva de los sujetos con EAIP y la relación entre los niveles de biomarcadores en LCR y la progresión de la atrofia, ampliando así el conocimiento sobre el valor pronóstico de los biomarcadores en la EAIP.

La tesis consta de 3 objetivos y 3 artículos:

1. Objetivo 1: estudiar, en sujetos con EAIP confirmada biológicamente, las diferencias fenotípicas en función del sexo en medidas de grosor cortical o volumen hipocampal (y sus subcampos), el deterioro cognitivo y los niveles de biomarcadores de LCR (Aβ42, p-tau, t-tau y NfL).

   Artículo 1: **Contador, José;** Pérez-Millan, Agnès; Guillen, Nuria; Sarto, Jordi; Tort-Merino, Adrià; Balasa, Mircea; Falgás, Neus; Castellví, Magdalena; Borrego-Écija, Sergi; Juncà-Parella, Jordi; Bosch, Beatriz; Fernández-Villullas, Guadalupe; Ramos-Campoy, Oscar; Antonell, Anna; Bargalló, Nuria; Sanchez-Valle, Raquel; Sala-Llonch, Roser; Lladó, Albert. Sex-differences in early-onset Alzheimer's disease. *Under review.*

2. Objetivo 2: estudiar los cambios transversales y longitudinales en grosor cortical y volumen subcortical mediante RM craneal en sujetos con EAIP

confirmada biológicamente en comparación con sujetos control, y analizar la capacidad pronóstica de los biomarcadores en LCR (Aβ42, p-tau, t-tau y NfL) en el momento del diagnóstico para predecir la evolución longitudinal de dichas medidas.

Artículo 2: **Contador, José;** Pérez-Millán, Agnès; Tort-Merino, Adrià; Balasa, Mircea; Falgàs, Neus; Olives, Jaume; Castellví, Magdalena; Borrego-Écija, Sergi; Bosch, Beatriz; Fernández-Villullas, Guadalupe; Ramos-Campoy, Oscar; Antonell, Anna; Bargalló, Nuria; Sanchez-Valle, Raquel; Sala-Llonch, Roser; Lladó, Albert Alzheimer's Disease Neuroimaging Initiative. Longitudinal brain atrophy and CSF biomarkers in early-onset Alzheimer's disease. Neuroimage: Clinical. 2021;32:102804. doi: 10.1016/j.nicl.2021.102804. IF: 4.881; Q2 Neuroimaging

3. Objetivo 3: estudiar la capacidad para predecir los cambios cognitivos longitudinales de las alteraciones en grosor cortical y volumen subcortical en RM craneal que presentan en el momento del diagnóstico los sujetos con EAIP confirmada biológicamente en comparación con sujetos control.

   Artículo 3: **Contador, José**; Pérez-Millan, Agnès; Guillen, Nuria; Tort-Merino, Adrià; Balasa, Mircea; Falgás, Neus; Olives, Jaume; Castellví, Magdalena; Borrego-Écija, Sergi; Bosch, Beatriz; Fernández-Villullas, Guadalupe; Ramos-Campoy, Oscar; Antonell, Anna; Bargalló, Nuria; Sanchez-Valle, Raquel; Sala-Llonch, Roser; Lladó, Albert. Baseline MRI atrophy predicts 2-year cognitive outcomes in early-onset Alzheimer's disease. Journal of Neurology 2022;269(5):2573-2583. doi: 10.1007/s00415-021-10851-9. IF: 4.849. Q1, Clinical neurology

III. INTRODUCCION

III. INTRODUCCION

a) Enfermedad de Alzheimer y enfermedad de Alzheimer de inicio precoz

En 1906, Alois Alzheimer presentó los hallazgos histopatológicos de una mujer con deterioro cognitivo progresivo de inicio a los 51 años consistente en pérdida de memoria, dificultades con el lenguaje, desorientación y alucinaciones, y que falleció a los 56 años en un estadio de demencia avanzada (1). Unos años más tarde, en 1910, Emil Kraepelin reconoce como una entidad clínico-patológica lo que llamó Enfermedad de Alzheimer (EA), causante de demencia de inicio precoz o presenil, diferenciada de la demencia senil, de inicio tardío y que se creía propia del envejecimiento. Estudios posteriores en los años 60-70 demostraron que la mayoría de las personas con demencia senil presentaban los hallazgos neuropatológicos de la EA. Desde entonces, la investigación se centró en el estudio de las presentaciones tardías, más frecuentes, quedando relegadas a un segundo plano las presentaciones precoces de la enfermedad inicialmente descritas por Alois Alzheimer.

En el año 2019, se estima que la prevalencia mundial de demencia fue de 57,4 millones de personas, con la previsión de que en 2050 el número de personas con demencia ascenderá a los 152,8 millones (2). Demencia es un concepto que de forma general se refiere a la pérdida de habilidades cognitivas que interfieren en las actividades de la vida diaria. Dentro de las posibles etiologías, la EA es la causa más frecuente de demencia, responsable del 60-80% de los casos (3). Habitualmente se presenta con un cuadro de afectación de la memoria episódica anterógrada que se acompaña en la evolución de otros síntomas cognitivos, como afectación de las capacidades visoespaciales, lenguaje o función ejecutiva/atencional. Su prevalencia e incidencia están en aumento en los últimos años debido sobre todo al envejecimiento de la población, y sin un tratamiento efectivo que detenga la evolución de la enfermedad, la EA se ha convertido en una epidemia mundial con una gran repercusión socioeconómica (4).

Siguiendo el punto de corte arbitrario de 65 años, la EA se puede clasificar según la edad de inicio en EA de inicio precoz (EAIP, <65 años) y EA de inicio tardío (EAIT, >65 años). A pesar de que la edad es el principal factor de riesgo conocido para la EA y la incidencia y la prevalencia de la enfermedad aumentan de forma exponencial a partir de los 65 años, el 5-10% de los casos inicia a edades más jóvenes (5,6), estimándose la prevalencia de la EAIP en 41,1 por 100.000 individuos (7). Igual que ocurre en la demencia de inicio tardío, la EAIP es también la causa

neurodegenerativa más frecuente en jóvenes, suponiendo hasta el 50% de las etiologías neurodegenerativas en una consulta especializada en demencia de inicio precoz (8). Además del retraso diagnóstico que conlleva la EAIP (9), la enfermedad sobreviene en un periodo de la vida en el que las personas que la sufren y, en general, sus cuidadores, aún tienen muchas responsabilidades familiares, laborales, económicas y sociales, y los recursos disponibles para este grupo de edad son limitados (10).

Como ya describió Alois Alzheimer, la EA se define a nivel neuropatológico por el depósito extracelular de placas de proteína β-amiloide y el acúmulo intracelular de proteína tau fosforilada (p-tau) en forma de ovillos neurofibrilares. El depósito de proteína β-amiloide comenzaría en regiones neocorticales y se extendería por el sistema límbico, diencéfalo, tronco del encéfalo y finalmente el cerebelo. Por el contrario, la patología tau inicialmente progresaría desde la corteza transentorrinal hacia el sistema límbico (hipocampo) y, por último, regiones neocorticales (11,12), correlacionándose de forma estrecha con los síntomas, severidad y progresión clínica de la enfermedad (13). Según la "hipótesis de la cascada amiloide", el proceso patológico se iniciaría 15-20 años antes de la aparición de los síntomas en lo que se conoce como fase preclínica de la enfermedad (14). Así, el acúmulo de la proteína β-amiloide desencadenaría distintos procesos de respuesta inflamatoria, estrés oxidativo, formación de ovillos neurofibrilares de proteína tau, disfunción neuronal y, finalmente, muerte celular, los cuales conducirían a la pérdida cognitiva primero en forma de deterioro cognitivo leve (DCL) y, posteriormente, demencia. Ambas, la EAIT y la EAIP, comparten el depósito de proteína β-amiloide y ovillos neurofibrilares como marcador patológico de la enfermedad, aunque algunos autores sostienen que podríamos estar ante dos formas diferentes de la enfermedad (15). En este sentido, la EAIP presenta cambios neuropatológicos más severos con una mayor carga de patología tau en regiones parietales, precuneus y lóbulo frontal (16,17). Además, el hipocampo parece estar afectado con menos frecuencia en la EAIP, sobre todo en las presentaciones no-amnésicas. Por otro lado, las personas con EAIP podrían presentar una forma patológica más pura de EA, en la que la sintomatología observada no estaría tan influencia por otros procesos neuropatológicos que se observan con más frecuencia en las presentaciones tardías (18).

Por último, si bien la mayoría de los individuos con EA se presentan con una forma esporádica de la enfermedad, menos del 1% presentan una forma genética autosómica dominante asociada a mutaciones en uno de los 3 genes conocidos: presenilina 1 (PSEN1), presenilina 2 (PSEN2) o proteína precursora de amiloide (PPA). Este porcentaje asciende al 10-15% en la EAIP (6,19), ya que habitualmente el inicio de los síntomas de estas formas

genéticas suele producirse por debajo de los 65 años. Además de las variantes genéticas autosómicas dominantes, se han identificado varios genes que confieren un riesgo poligénico para la enfermedad. El más estudiado es el alelo ε4 del gen de la apolipoproteína E (*APOE*), cuya presencia disminuye la edad de inicio en EA, siendo más frecuente en la EAIP que en la EAIT (20). La presencia del alelo ε4 también se ha relacionado con la atrofia del lóbulo temporal medial (LTM) característica de las presentaciones amnésicas de EA. Por el contrario, su ausencia predispondría a una afectación más allá del LTM y a presentaciones no-amnésicas en la EAIP (21), si bien algunos estudios neuropatológicos en EAIP no han encontrado diferencias en la frecuencia de los genotipos de *APOE* entre los dos tipos de presentaciones (22).

b) Diagnóstico de la enfermedad de Alzheimer y biomarcadores

La EA tradicionalmente ha sido considerada una entidad clínico-patológica, en la que el diagnóstico de certeza de un síndrome clínico compatible sólo podía ser confirmado mediante la anatomía patológica. Los primeros criterios diagnósticos de EA del National Institute of Neurological and Communicative Disorders and Stroke-Alzheimer's Disease and Related Disorders Association (NINCDS-ARDRA) en 1984 se basaban exclusivamente en criterios clínicos, siendo imprescindible cumplir criterios de demencia e incluyendo pruebas complementarias únicamente para descartar otras causas de demencia (23). Además, no se tenía en cuenta la variabilidad fenotípica de la enfermedad más allá de las presentaciones amnésicas. La precisión diagnóstica de estos criterios es relativamente baja, alcanzando una sensibilidad en torno al 80% y una especificidad del 70% (24), con el 30% de los sujetos diagnosticados en vida no presentando la enfermedad en estudios anatomopatológicos (25).

En los últimos 30 años, el paradigma de la enfermedad ha cambiado con el desarrollo de biomarcadores que demuestran *in vivo* los procesos patológicos de la EA, incluyendo el depósito de proteínas β-amiloide y tau, así como la progresiva neurodegeneración. La EA es considerada hoy en día una entidad biológica en la que el continuum clínico de la enfermedad puede diagnosticarse sin necesidad de estudios anatomopatológicos. Inicialmente, en los criterios diagnósticos de demencia debida a EA de 2011 del National Institute on Aging y la Alzheimer's Association (NIA-AA) (26) se definieron niveles de certeza en base a la demostración mediante biomarcadores del depósito de proteína β-amiloide y/o neurodegeneración, y además la EA pasó a poderse diagnosticar en su fase de DCL (27). Se permitía el diagnóstico de EA en individuos sintomáticos en cualquier fase de la enfermedad y no sólo con presentaciones amnésicas, si bien la definición de la enfermedad aún no estaba separada de criterios clínicos.

Posteriormente, la NIA-AA define en 2018 un marco de investigación en EA (28) que reconoce, además de las fases de DCL y demencia de la enfermedad, una fase preclínica de detección de cambios biológicos en sujetos asintomáticos. Así el término de EA pasa a referirse completamente a una entidad que es biológica y no clínica. La nueva clasificación de 2018 propone el sistema ATN según la cual el continuo clínico de la enfermedad se categoriza mediante: a) biomarcadores llamados “A” de depósito de amiloide, cuya positividad determina si alguien se encuentra en el continuo de Alzheimer; b) biomarcadores de patología tau, denominados “T”, que indican cuando son positivos si alguien en el continuo de Alzheimer presenta EA; y c) biomarcadores de neurodegeneración “(N)”, entre paréntesis por su menor especificidad, pues también pueden aparecer en otras patologías distintas de la EA (29), si bien son de un valor innegable al relacionarse estrechamente con la sintomatología. De esta manera, las diferentes fases clínicas de la enfermedad pueden ser caracterizadas en base a un perfil ATN que es evaluado mediante biomarcadores en líquido cefalorraquídeo (LCR) o técnicas de neuroimagen. No obstante, con el nuevo marco de investigación, se deja la puerta abierta a incorporar otros biomarcadores que puedan ser validados en el futuro (30). A continuación, se detallan los principales biomarcadores de la enfermedad disponibles:

- Biomarcadores de LCR:

Al encontrarse en contacto directo con el cerebro, el LCR es capaz de reflejar de forma estrecha la producción y aclaramiento de diferentes proteínas y es útil para evaluar los cambios patológicos de la EA. Niveles bajos del péptido β-amiloide 42 (Aβ42) o elevados de p-tau en LCR son biomarcadores validados que traducen, respectivamente, la presencia de depósito de proteína β-amiloide u ovillos neurofibrilares (31,32). Según el modelo actual de la enfermedad, serían los que se alteran más precozmente (33). Por otro lado, los niveles elevados de tau total (t-tau) se relacionan con la neurodegeneración secundaria a la pérdida neuronal, sin ser específicos de la EA. Además, otros biomarcadores en LCR como los neurofilamentos de cadena ligera (NfL), de origen axonal, también se incluyen en los nuevos criterios de 2018 de la NIA-AA como medida de neurodegeneración inespecífica.

El principal inconveniente del análisis del LCR es que requiere de una técnica invasiva como es la punción lumbar, lo que puede limitar su aceptación por parte de algunos sujetos. Sin embargo la seguridad del procedimiento es ampliamente respaldada (34) y podría no ser peor tolerada que otras pruebas (35). En este sentido, el desarrollo e implantación de técnicas de análisis de biomarcadores en plasma en los últimos años promete ser una herramienta diagnóstica de gran utilidad en la EA (36,37),

presentando la ventaja de que su obtención es mínimamente invasiva y fácil en la práctica clínica.

- Biomarcadores de neuroimagen:

Las técnicas de neuroimagen ofrecen la posibilidad de evidenciar los cambios patológicos de la EA y además caracterizar espaciotemporalmente la distribución de la enfermedad. Dentro de este grupo se encuentran la Resonancia Magnética (RM) y la tomografía por emisión de positrones (PET):

- RM craneal:

La RM craneal es una prueba de imagen no invasiva que no usa radiación ionizante y que además presenta las ventajas de ser de bajo coste y estar instaurada en la mayoría de los centros. Es una herramienta de uso habitual para el estudio de sujetos que se presentan con deterioro cognitivo, ya sea para descartar otras entidades o evaluar la presencia de comorbilidades como la patología vascular cerebral. Por otro lado, la RM craneal llamada estructural, y concretamente la secuencia 3D potenciada en T1, es un biomarcador disponible para analizar la morfología cerebral. En la EA, los estudios de RM craneal estructural permiten definir espacialmente la neurodegeneración a través de la atrofia cerebral, obteniéndose patrones que se relacionan estrechamente con los síntomas observados y siendo útil para caracterizar los distintos fenotipos de la enfermedad. Tradicionalmente, la RM de 1.5 Teslas ha sido utilizada en la práctica clínica. No obstante, los equipos de RM de 3 Teslas están cada vez más presentes y otorgan una mayor resolución para diferenciar entre sustancia gris y blanca, facilitando así la detección de la atrofia cerebral en la EA (38). Además, los equipos de RM de 7 Teslas disponibles por el momento en investigación, junto al desarrollo de nuevas secuencias, permiten adquirir una imagen aún más detallada de las estructuras.

Según el modelo actual de la EA (33,39), la atrofia cerebral sería el biomarcador que más cerca se encuentra temporalmente de la aparición de los síntomas cognitivos, y sucedería al acúmulo de proteína tau, con el que se relaciona topográficamente, reflejando la neurodegeneración asociada a este depósito (40). Así, en sujetos con EA, la neurodegeneración seguiría un patrón característico de atrofia, con regiones que muestran atrofia en etapas precoces de la enfermedad y otras que se afectan en etapas avanzadas. Al ser una herramienta con la que se pueden realizar medidas repetidas con relativa facilidad, permite además monitorizar la progresión de la neurodegeneración y capturar la

secuencia temporal de atrofia a través de estudios longitudinales, relacionándose la tasa de cambio en diferentes estructuras con los cambios cognitivos (41). De cara a evaluar transversal y longitudinalmente los cambios en RM estructural se pueden usar diferentes enfoques (escalas visuales de atrofia o bien métodos basados en el vértice craneal, regiones de interés o vóxeles), y a día de hoy, existen varios softwares automatizados de segmentación cerebral (Freesurfer- https://surfer.nmr.mgh.harvard.edu/, FSL, SPM) que proporcionan medidas cuantitativas que han mostrado una correlación alta con las medidas histológicas (42).

El LTM, y particularmente la corteza entorrinal y el hipocampo, se han establecido como regiones que se afectan de forma específica y precoz en la EA. De la misma manera, se ha descrito un patrón de atrofia cortical característico de la enfermedad que, siguiendo la distribución de los estudios anatomopatológicos, incluiría la corteza del LTM, temporal posterior, parietal y algunas regiones del lóbulo frontal. Este patrón se relaciona con la severidad de los síntomas y puede ser detectado incluso en sujetos asintomáticos amiloide positivo (43,44). Además, la atrofia en estas regiones es útil en discriminar sujetos con EA de sujetos sanos o con otras demencias (45). Sin embargo, la sensibilidad y especificidad son bajas para considerar los hallazgos en RM craneal estructural un biomarcador diagnóstico de EA (46). Aquí es importante tener en cuenta que, si bien se ha producido un cambio de paradigma en la EA que permite su diagnóstico *in vivo*, la mayoría de los estudios han incluido sujetos sin confirmación biológica de la enfermedad. Por otro lado, existe cierta heterogeneidad en las mediciones de RM utilizadas y muchas veces no han separado los distintos fenotipos clínicos, lo que ha podido añadir variabilidad a los hallazgos.

Por último, usando otras modalidades de RM como la RM de difusión, la cual permite obtener medidas de la microestructura de la sustancia blanca cerebral, se han detectado cambios en los tractos cerebrales de personas con EA, incluyendo tractos límbicos y cortico-corticales (47). Además, la RM funcional, que utiliza la medida de la señal BOLD (*blood level oxygen dependent*), permite estudiar los cambios en la actividad cerebral durante la ejecución de tareas, así como los cambios en la conectividad funcional en reposo, medida como las fluctuaciones espontáneas de dicha señal (48). En este sentido, se han descrito alteraciones en la red neuronal por defecto o en la conectividad del hipocampo que preceden a los cambios estructurales en EA y podrían permitir un diagnóstico precoz y diferencial frente a otras patologías (49).

- PET cerebral:

El PET es una técnica capaz de proporcionar *in vivo* información sobre procesos biológicos como el metabolismo cerebral o el depósito de proteínas. Es una prueba mínimamente invasiva que presenta la desventaja del uso de radiación ionizante. Su disponibilidad sigue siendo bastante limitada a algunos centros ya que los trazadores han de producirse en las inmediaciones debido al tiempo limitado con el que emiten radiación. Además, es una prueba relativamente cara, sobre todo en comparación con otros biomarcadores disponibles como los biomarcadores en LCR. Por un lado, utilizando un análogo de la glucosa (fluorodesoxiglucosa – FDG) se puede mapear el metabolismo de la glucosa en el cerebro, relacionado con la neurodegeneración. La localización espacial del déficit metabólico se relaciona con los síntomas clínicos y difiere entre diversos fenotipos clínicos de la EA, aunque su resolución espacial es baja (50). Posteriormente, la aparición de diferentes trazadores ha permitido estudiar la presencia de los marcadores patológicos de la EA. Así, los trazadores de proteína β-amiloide (florbetapir, florbetaben o flutemetamol), y más recientemente de proteína tau (flortaucipir, MK-6420, PI2620, RO948 F 18), han demostrado ser capaces de detectar *in vivo* la distribución anatómica del depósito de estas proteínas (51,52).

c) Variantes fenotípicas y diferencias en biomarcadores en la enfermedad de Alzheimer: edad y sexo

A pesar de que en los últimos años el uso de los biomarcadores y de los nuevos criterios han mejorado de forma significativa la certeza diagnóstica de la EA, las investigaciones estudiando los biomarcadores exclusivamente en la EAIP son limitadas. Por otro lado, existe un interés creciente en evaluar el desarrollo y la expresión de la enfermedad dependiendo del sexo (53), siendo la EA 2 veces más prevalente en mujeres que hombres (4), aunque en el caso de la EAIP no parece que la prevalencia difiera entre sexos (7). El estudio de las diferencias fenotípicas en función a la edad de inicio o el sexo de los sujetos es crucial para una medicina personalizada que incluya herramientas diagnósticas y de monitorización específicas que faciliten el desarrollo de tratamientos eficaces. Algunas de las diferencias fenotípicas o en biomarcadores dependiendo de la edad de inicio o el sexo son las siguientes:

- Manifestaciones clínicas:

La presentación amnésica o típica es la más frecuente en la EAIT (94%) y en la EAIP, aunque en menor proporción (68%). Las presentaciones no-

amnésicas o atípicas, aquellas que involucran inicialmente a dominios que no son la memoria, son infrecuentes en la EAIT, pero en la EAIP pueden suponer hasta el 30-40% de las presentaciones de la enfermedad (54,55), reflejando la mayor afectación patológica de regiones neocorticales (17) y contribuyendo en parte al retraso diagnóstico de la EAIP por su menor reconocimiento (22). Por otro lado, el curso clínico de la enfermedad es, en general, más agresivo en la EAIP que en la EAIT, con un menor tiempo de evolución hasta llegar a la fase demencia y una menor supervivencia (20,56,57).

En cuanto a las diferencias clínicas según el sexo, la evidencia sugiere que las mujeres con EA presentan un curso clínico más agresivo (58), acorde con la mayor carga neuropatológica de proteína tau encontrada en mujeres (59,60).

- Biomarcadores de LCR:

Al igual que en la EAIT, la EAIP muestra la disminución de los niveles de Aβ42 y el aumento de p-tau y t-tau en LCR característicos de la EA (61,62). Por el momento, no hay evidencia de que los niveles en la EAIP difieran de las presentaciones tardías, salvo algún estudio aislado reportando niveles más bajos de Aβ42 en la EAIP (63). En cambio, los niveles de NfL aumentan con la edad en sujetos con y sin EA (64). El sexo de los sujetos tampoco parece influenciar las concentraciones de Aβ42 o tau en la EAIP (61), aunque la interacción entre el sexo femenino y el alelo ε4 de *APOE* podría resultar en niveles más altos de proteína tau en el espectro de la EA (65). Por el contrario, algún estudio sugiere que los hombres con EA presentarían niveles más altos de NfL que las mujeres (64).

- Estudios de RM craneal:

A pesar de que la literatura investigando los cambios en RM debidos a la EA es extensa, como se ha comentado, la mayoría de la evidencia disponible se basa en estudios en los que se incluyen personas sin confirmación biológica de la enfermedad, y los trabajos en este sentido centrados en la EAIP son escasos, sobre todo a nivel longitudinal.

Tradicionalmente, la afectación del hipocampo ha sido considerada característica de la EA, incluyéndose en los criterios de la enfermedad como un biomarcador diagnóstico (26,27). Sin embargo, su utilidad en el diagnóstico de la EAIP podría ser limitado (66). A diferencia de la EAIT, más limitada a regiones temporales mediales, los estudio transversales en EAIP muestran una atrofia global más extensa, incluyendo regiones neocorticales fuera del LTM (67–71), siendo las conclusiones sobre el patrón de atrofia longitudinal en sujetos diagnosticados mediante el uso de biomarcadores

más limitadas (72–74). Por otro lado, estudios recientes analizando los cambios en los distintos subcampos del hipocampo en la EAIP han demostrado cambios específicos para variantes amnésicas y no-amnésicas a nivel transversal (75). Tomados en conjunto, los hallazgos sugieren un proceso patológico más agresivo en sujetos con EAIP que se traduce en un patrón topográfico característico al compararlo con sujetos con EAIT.

En cuanto a las diferencias por sexos en la EA, los resultados previos que investigan los patrones de atrofia entre mujeres y hombres con EA son variables. Así, en la EA, menor volumen hipocampal se ha descrito tanto en mujeres (76) como en hombres (77) y las mujeres parecen presentar una tasa de progresión mayor de la atrofia (78–80).

- Estudios PET craneal:

La captación cortical de trazadores para placas de β-amiloide (florbetapir, florbetaben o flutemetamol) no muestra diferencias dependiendo de la edad de inicio (81,82) o el sexo (83), aunque algunos estudios han mostrado que los sujetos con EAIP presentan mayor retención en estructuras subcorticales como el tálamo o el globo pálido (84). El PET-amiloide, al igual que el estudio de biomarcadores en LCR, es una herramienta de gran utilidad en el diagnóstico diferencial de la EAIP. Dicha utilidad disminuye en edades más avanzadas, dado que la positividad de PET-amiloide en sujetos asintomáticos aumenta con la edad (hasta 35% a los 80 años) (83).

El escenario con los distintos trazadores de PET-tau es diferente (Flortaucipir, MK-6420, PI2620, RO-948). La captación del trazador en la EA refleja estrechamente la distribución espaciotemporal de la patología tau desde el LTM a regiones neocorticales. Además, se relaciona con la posterior neurodegeneración y los síntomas clínicos (85), especialmente en la EAIP (86). Consistente con los hallazgos anatomopatológicos, la EAIP presenta mayor acúmulo progresivo de patología tau (87) y mayor captación extratemporal del trazador de tau comparada con la EAIT (88–90), tanto en presentaciones amnésicas como no-amnésicas. Además, los sujetos con EAIP parecen tolerar una mayor carga de tau que podría relacionarse con una mayor resiliencia cognitiva (91) o con la menor presencia de copatología en personas jóvenes (18,92). Por otro lado, estudios recientes han puesto de manifiesto una mayor captación del trazador de tau en mujeres con EA (93,94), sugiriendo una mayor susceptibilidad a la patología tau, pero mayor resiliencia cognitiva a los efectos de su acúmulo (91).

d) Biomarcadores de progresión en la enfermedad de Alzheimer

El estudio de los biomarcadores de la EA en los últimos años ha mejorado sin duda la comprensión de la fisiopatología de la enfermedad, aunque

también se ha puesto de manifiesto la gran complejidad y los numerosos matices que resultan de la interacción entre las proteínas β-amiloide y tau en el cerebro. A pesar de los avances, los mecanismos que contribuyen a la velocidad de progresión de la enfermedad son poco conocidos. Particularmente, las relaciones que se establecen entre distintos biomarcadores y la clínica no son del todo comprendidas, y en los criterios de 2018 de la NIA-AA se subraya la importancia de combinar diferentes biomarcadores para estudiar los diferentes procesos patológicos.

Conocer a qué velocidad progresará la EA es de gran relevancia para otorgar, en primer lugar, un pronóstico certero a los sujetos con la enfermedad y sus allegados de cara a planificar el futuro. Además, conocer con precisión la evolución de la enfermedad es de utilidad en ensayos clínicos, en los que identificar sujetos con una rápida progresión permitiría disminuir la variabilidad y demostrar eficacia con un menor número de participantes y en un menor intervalo de tiempo (103,104). Se sabe que los sujetos con DCL A+T+N+ y A+T+N- son los que presentan mayor riesgo de progresión a fase de demencia a corto plazo, comparado con otros perfiles de biomarcadores (95,96). Por otro lado, estudios en sujetos con evidencia biológica de la enfermedad, han mostrado que los niveles de proteína tau o NfL en LCR podrían predecir los cambios cognitivos y la pérdida cerebral en RM craneal (97–99). Además, la atrofia en RM (100,101) o la captación en PET-tau (102) podrían ser útiles para predecir los cambios cognitivos en el futuro. Sin embargo, la evidencia sobre el riesgo de progresión en la EIAP es prácticamente nula.

En este contexto, la RM no sólo es una herramienta que puede ayudar a comprender la fisiopatología de la EAIP, sino que también puede proporcionar datos de pronóstico útiles en la práctica clínica e investigación. Como biomarcador de neurodegeneración no invasivo, accesible y económico, la RM craneal estructural permitiría caracterizar la topografía de la atrofia progresiva, mostrando hallazgos que serían específicos para la EAIP, diferentes a las presentaciones tardías y que dependerían del sexo de los sujetos. Además, dada la estrecha relación entre la neurodegeneración y los síntomas cognitivos, la RM craneal podría ser un biomarcador pronóstico que predijera los futuros cambios cognitivos en la EAIP, menos influenciada por otras patologías. Por otro lado, integrando los cambios estructurales en RM con otros biomarcadores se podrían poner de manifiesto relaciones que permitan predecir la evolución de la pérdida neuronal, identificándose así sujetos con una evolución más agresiva.

IV. HIPÓTESIS

IV. HIPÓTESIS

1. El sexo de los sujetos con EAIP podría influir en la extensión espacial de la neurodegeneración de la enfermedad medida por RM craneal estructural, el grado de deterioro cognitivo o los niveles de biomarcadores en LCR.
2. Los estudios de RM craneal estructural permitirían evaluar la progresión de la atrofia cerebral en sujetos con EAIP, lo que puede contribuir al conocimiento de la fisiopatología de la EAIP y al desarrollo de medidas específicas para monitorizar la evolución de la enfermedad. Además, los niveles de biomarcadores en LCR en el momento del diagnóstico podrían predecir la progresión longitudinal de la atrofia en estos sujetos.
3. En la EAIP, los cambios en RM craneal estructural en el momento del diagnóstico podrían predecir los cambios cognitivos longitudinales.

V. OBJETIVOS

V. OBJETIVOS

1. Estudiar, en sujetos con EAIP confirmada biológicamente, las diferencias fenotípicas en función del sexo en medidas de grosor cortical o volumen hipocampal (y sus subcampos), el deterioro cognitivo y los niveles de biomarcadores de LCR (Aβ42, p-tau, t-tau y NfL).

2. Estudiar los cambios transversales y longitudinales en grosor cortical y volumen subcortical mediante RM craneal en sujetos con EAIP confirmada biológicamente en comparación con sujetos control, y analizar la capacidad pronóstica de los biomarcadores en LCR (Aβ42, p-tau, t-tau y NfL) en el momento del diagnóstico para predecir la evolución longitudinal de dichas medidas.

3. Estudiar la capacidad para predecir los cambios cognitivos longitudinales de las alteraciones en grosor cortical y volumen subcortical en RM craneal que presentan en el momento del diagnóstico los sujetos con EAIP confirmada biológicamente en comparación con sujetos control.

VI. MATERIALES, MÉTODOS Y RESULTADOS

VI. MATERIALES, MÉTODOS Y RESULTADOS

OBJETIVO 1

Estudiar, en sujetos con EAIP confirmada biológicamente, las diferencias fenotípicas en función del sexo en medidas de grosor cortical o volumen hipocampal (y sus subcampos), el deterioro cognitivo y los niveles de biomarcadores de LCR (Aβ42, p-tau, t-tau y NfL).

Título del trabajo:

"Sex-differences in early-onset Alzheimer's disease."

Autores: Contador, José; Pérez-Millan, Agnès; Guillen, Nuria; Sarto, Jordi; Tort-Merino, Adrià; Balasa, Mircea; Falgás, Neus; Castellví, Magdalena; Borrego-Écija, Sergi; Juncà-Parella, Jordi; Bosch, Beatriz; Fernández-Villullas, Guadalupe; Ramos-Campoy, Oscar; Antonell, Anna; Bargalló, Nuria; Sanchez-Valle, Raquel; Sala-Llonch, Roser; Lladó, Albert.

-Under review-

Sex differences in early-onset Alzheimer's disease

José Contador[a]*, Agnès Pérez-Millan[a, b]*, Nuria Guillen[a], Jordi Sarto[a], Adrià Tort-Merino[a], Mircea Balasa[a, c], Neus Falgàs[a, c], Magdalena Castellví[a], Sergi Borrego-Écija[a], Jordi Juncà-Parella[a], Beatriz Bosch[a], Guadalupe Fernández-Villullas[a], Oscar Ramos-Campoy[a], Anna Antonell[a], Nuria Bargalló[d, e], Raquel Sanchez-Valle[a], Roser Sala Llonch[b, f]§, Albert Lladó[a]§, ¶

a. Alzheimer's Disease and Other Cognitive Disorders Unit, Neurology Service, Hospital Clínic de Barcelona, Institut d'Investigacions Biomèdiques August Pi i Sunyer (IDIBAPS), Universitat de Barcelona, Barcelona, Spain

b. Institute of Neurosciences. Department of Biomedicine, Faculty of Medicine, University of Barcelona, Barcelona, Spain

c. Atlantic Fellow for Equity in Brain Health, Global Brain Heath Institute.

d. Image Diagnostic Centre Radiology Department, Hospital Clínic de Barcelona, Magnetic Resonance Image Core facility Institut d'Investigacions Biomèdiques August Pi i Sunyer (IDIBAPS), Barcelona, Spain

e. Centro de Investigación Biomédica en Red de Salud Mental. CIBERSAM. Spain

f. Biomedical Imaging Group, Biomedical Research Networking Center in Bioengineering, Biomaterials and Nanomedicine (CIBER-BBN), Barcelona, Spain

* These authors contributed equally to this work.

§ These authors share senior authorship

¶ Corresponding author: Albert Lladó, MD, PhD, Alzheimer's disease and other cognitive disorders unit, Neurology Service, Hospital Clínic, IDIBAPS. Carrer Villarroel, 170, Barcelona, 08036, Spain. Tel: +34 932275785; fax: +34 932275783. Email address: allado@clinic.cat.

ABSTRACT

INTRODUCTION: Sex is believed to drive heterogeneity in Alzheimer's disease (AD), although evidence in early-onset AD (<65 years, EOAD) is scarce.

METHODS: We included 62 EOAD patients and 44 healthy controls (HC) with cerebrospinal fluid (CSF) AD's core biomarkers and neurofilament light chain levels, neuropsychological assessment, and 3T-MRI. We measured cortical thickness (CTh) and hippocampal subfield volumes (HpS) using Freesurfer. Adjusted linear models were used to analyze sex-differences and the relationship between atrophy and cognition.

RESULTS: Compared to same-sex HC, female-EOAD showed greater cognitive impairment and broader atrophy burden than male-EOAD. In a direct female-EOAD and male-EOAD comparison, there were slight differences in temporal CTh, with no differences in cognition or HpS. CSF tau levels were higher in female-EOAD than in male-EOAD. Greater atrophy was associated with worse cognition in female-EOAD.

DISCUSSION: At diagnosis, there are sex-differences in the pattern of cognition impairment, atrophy burden and CSF tau in EOAD.

Keywords: Alzheimer Disease, Early onset Alzheimer Disease, Sex Characteristics, cognition, biomarkers, atrophy, cerebrospinal fluid, MRI.

Abbreviations: Aβ, amyloid-β; AD, Alzheimer's disease; APOE, Apolipoprotein E; CA, cornus ammonis; CSF, cerebrospinal fluid; CTh, cortical thickness; EOAD, early-onset AD GC-ML-DG, granule cell and molecular layer of dentate gyrus; HC, healthy controls; HATA, hippocampus–amygdala transition area; LM, Linear Models; LOAD, late-onset AD MRI, magnetic resonance imaging; MCI, mild cognitive impairment; ML, molecular layer; NfL, neurofilament light chain; p-tau, phosphorylated tau; PET, positron emission tomography; t-tau, total tau; YOE, years of education.

1. INTRODUCTION

Alzheimer's disease (AD) is the leading cause of neurodegenerative dementia globally. According to age at onset, AD is classified in early-onset AD (<65 years; EOAD) and late-onset AD (>65 years; LOAD), both sharing the neuropathological hallmarks of the disease but presenting different clinical and neurobiological characteristics (1). In both presentations, AD is 2 times more prevalent in women, even after considering their greater life expectancy (2,3). Women are the epicenter of AD's pandemic, but also increasing evidence supports that sex is a factor driving clinical and pathological heterogeneity in the disease, and sex-differences have become a research priority for the development of precision medicine approaches (4). However, whether sex should be considered when predicting disease onset, prognosis and treatment response remain unclear. Difficulties in this field included the fact that most of the studies assessing sex-differences are based on a clinical diagnosis, with rates of 30% of patients not having AD pathology at autopsy (5). Nevertheless, in the last decade, biomarkers have allowed the shift from a clinical to a biological construct, reflected in the 2018 criteria of the National Institute on Aging and Alzheimer's Association Research Framework (6), and nowadays, their use is recommended for supporting AD diagnosis in early-onset individuals.

Therefore, identifying sex influence in AD biomarkers, and how these change across different AD's presentations like EOAD, is critical for understanding the pathophysiology of the disease. Neuropathological studies have demonstrated that women present more neurofibrillary tangles compared to men (7,8), but a similar amount of amyloid-β (Aβ) plaques. Evidence suggests that women present greater cognitive impairment than men (9), in line with the close relationship between tau and cognition. On the other hand, prior findings showed variability in the specific atrophy patterns and atrophy progression rates found between women and men in AD, probably explained by the lack of systematic approach (i.e., brain volume normalization) and patient heterogeneity across studies, being these potential differences still controversial. For instance, smaller hippocampal volume has been reported in both women (10) and men(11), but the evidence of sex-differences in the pattern of hippocampal subfield atrophy is scarce. Furthermore, sex seems to have no impact on CSF concentrations of Aβ42 or tau in patients with AD (12,13), including EOAD patients(14). However, an interaction of female sex and Apolipoprotein E (APOE) influencing higher tau levels in women has been reported (13). In contrast, male patients exhibit higher CSF levels of neurofilament light chain (NfL) compared with females (15). Overall, further studies investigating sex-differences in clinical and biomarker features by using well-characterized cohorts are warranted.

Here, we aimed to study the sex influence on cognition, CSF biomarkers levels (Aβ42, phosphorylated tau(p-tau), total tau (t-tau) and NfL), cortical thickness (CTh), hippocampus and hippocampal subfield volumes in an EOAD cohort with a biomarkers-based diagnosis. In addition, we explored sex-differences in the association between atrophy and cognition.

2. METHODS

2.1 Study participants

We included 106 participants, 62 EOAD patients and 44 healthy controls (HC), recruited from a prospective cohort at the “Alzheimer’s disease and Other Cognitive Disorders Unit”, at the Hospital Clínic de Barcelona. At the beginning of the study, all participants underwent a clinical and physical examination, a lumbar puncture for analysis of CSF AD’s core biomarkers, a structural brain 3T-MRI scan and APOE genotyping. 54 EOAD and 43 HC also performed a comprehensive neuropsychological evaluation. In addition, CSF NfL levels were analyzed in 54 EOAD patients and 40 HC.

All EOAD patients presented AD biomarkers profile suggesting underling AD neuropathology (A+T+) with neurodegeneration (N+) according to the NIA-AA Research Framework 2018(6) and a Mini-Mental State Examination (MMSE) score>15. They also fulfilled diagnostic criteria for mild cognitive impairment (MCI) due to AD or AD mild dementia (16,17). HC presented normal cognition and normal AD biomarkers (A−T−N−).

Ethical approval was obtained from the Hospital Clínic Ethics Committee (HCB/2019/0054) and written informed consent was obtained from all the participants

2.2 Cognitive assessment

A detailed cognitive battery was administered by a trained neuropsychologist, including sixteen cognitive tests for the assessment of five cognitive domains: memory, language, praxis, visual-spatial perception and executive and attention functions. MMSE was used as a measure of global cognition. All scores were z-normalized using the mean and standard deviation of HC. For each participant, we created a mean z-score composite for each of the cognitive domains in addition to a mean global composite of all of them. Details on the cognitive assessments for each domain can be found in Supplementary Table S1.

2.3 CSF biomarkers and APOE genotype

We used commercially available single-analyte enzyme-linked immunosorbent assay to determine levels of AD’s core biomarkers

(INNOTEST, Fujirebio) and NfL (IBL International). CSF samples were collected and processed according to our lab protocol (18). The APOE genotype was determined through the analysis of rs429358 and rs7412 by Sanger sequencing. Participants were categorized according to the presence of at least one APOE ε4 allele (carriers) or the absence of APOE ε4 alleles (non-carriers).

2.4 Imaging acquisition protocol

Structural MRI scans for each subject were acquired at a field strength of 3 Tesla with a T1-weighted magnetization-prepared rapid gradient-echo (MPRAGE) sequence (repetition time = 2.30 milliseconds, echo time = 2.98 milliseconds, 240 slices, field-of-view = 256 mm, voxel size = 1 × 1 × 1 mm) using a 3T Magnetom Trio Tim scanner (Siemens Medical Systems, Germany). In addition, 6 subjects were scanned in a comparable 3T Prisma scanner (Siemens Medical Systems, Germany) using the same protocol. All studies were performed at the Magnetic Resonance Image Core Facility of IDIBAPS using the MRI scans located in Hospital Clínic Barcelona.

2.5 Image processing

2.5.1 Cortical thickness

We processed T1-weighted acquisitions using the stream available in FreeSurfer version 6.0 (http://surfer.nmr.mgh.harvard.edu/). FreeSurfer preprocessing steps are fully reported elsewhere (19,20). The summary measures of mean CTh in 68 cortical parcellations (21) were obtained in addition to hemispheric measures of mean CTh. Furthermore, we calculated the mean parietotemporal CTh z-score of both hemispheres using the HC group as a reference (Supplementary Table S2), taking into account the characteristic atrophy of these lobes in AD. All the images were visually inspected and manually corrected if needed.

2.5.2 Hippocampal subfields

Following recent hypotheses on hippocampal regional specificity, the entire hippocampal formation was segmented using the routine volumetric FreeSurfer 6.0 pipeline (22,23). The whole hippocampus volume and 12 subfields were obtained for each hemisphere: hippocampal tail, parasubiculum, presubiculum, subiculum, cornus ammonis (CA)1, CA2-3, CA4, hippocampus–amygdala transition area (HATA), molecular layer (ML) and granule cell and molecular layer of dentate gyrus (GC-ML-DG), fimbria, and hippocampal fissure. All images were visually checked to detect errors in segmentation. Volumes were normalized by the estimated intracranial volume and scaled with a factor of 100 for visualization purposes. In addition,

the bilateral hippocampal volume mean z-score was calculated using the HC group as a reference.

2.6 Statistical analyses

2.6.1 Demographics and clinical characteristics of the sample

EOAD and HC were compared using t Student tests for continuous variables and $\chi 2$ tests for the sex and APOE. ANOVA with post hoc analysis and Fisher's tests were used to analyze differences across sex groups. All statistical analyses in this study were conducted using R 4.0.2.

2.6.2 Cognitive measures

We used Linear Models (LM) to compare z-scores between EOAD and HC in separate group-comparisons for male and female, adjusted by age and years of education (YOE). We also directly compared female-EOAD and male-EOAD using adjusted LMs. Furthermore, we tested sex by group interactions in the whole sample with age and YOE as covariates. All p values were adjusted for multiple comparisons using Bonferroni correction and we used a significant threshold of corrected $p < 0.05$.

2.6.3 CSF biomarkers levels

Differences between EOAD and HC in CSF biomarkers levels were analyzed using t Student tests and ANOVA with post hoc analysis. In the EOAD group, we performed separated LM adjusted by APOE status and age at lumbar puncture to test sex-differences in CSF levels (Aβ42, p-tau and t-tau and NfL). We also tested the sex x APOE status interaction on CSF biomarkers levels. A significant threshold of $p < 0.05$ after Bonferroni correction was used. Ten EOAD subjects were excluded from the analysis of Aβ42 level differences due to variations in our laboratory's standard protocol.

2.6.4 MRI measures

We first performed separate comparisons between female and male EOAD patients and HC of the same sex for CTh and hippocampal volume differences, including hippocampal subfields. We created LM for each measure, with age at MRI, APOE status and MRI scanner as covariates. Next, we performed the direct comparison between female-EOAD and male-EOAD, including MMSE as a covariate and the covariates used in the previous analysis. Finally, we evaluated the sex by group interaction in the whole sample. A significant threshold of $p < 0.05$ Bonferroni corrected was used in all analyses.

2.6.5 Association between atrophy and cognitive performance

In female-EOAD and male-EOAD, we fitted separate LM with each of the cognitive z- scores as the response variable and the mean parietotemporal CTh or the mean hippocampal volume z-score as a predictor. Age at neuropsychological assessment and YOE were introduced as covariates.

3. RESULTS

3.1 Demographics and clinical characteristics of the sample

Age at MRI, LP or cognitive assessment and education were similar between women and men with EOAD/HC and between participants with EOAD and HC ($p>0.05$, Table 1). No differences in age at onset were found between female-EOAD and male-EOAD ($p>0.05$). APOEε4 carriers' frequency was higher in EOAD than HC due to higher frequency in female-EOAD and male-EOAD than female-HC ($p<0.001$). As expected from the group's conformation, significant differences in raw MMSE scores were observed between EOAD and HC and between female-EOAD or male-EOAD and HC of the same sex ($p<0.001$).

3.2 Sex-differences in cognition

Female-EOAD showed lower z-scores than female-HC in all the domains, global composite and MMSE. In contrast, male-EOAD showed lower z-scores than male-HC only in memory, attentional and executive functions, global composite and MMSE (all $p<0.05$ Bonferroni corrected, Figure 1). No differences were found between female-EOAD and male-EOAD nor group by sex interactions including all EOAD and HC ($p>0.05$). Detailed neuropsychological information for each group can be found in Supplementary Table S3 and Table S4.

3.3 Sex-differences in CSF biomarkers levels

As expected from the selection criteria, significant differences in the levels of CSF biomarkers between EOAD and HC were found, in the whole sample and separated by sexes ($p<0.05$, Supplementary Table S5).

Female-EOAD showed significantly higher CSF t-tau and p-tau levels than male-EOAD, after adjusting for age at lumbar puncture and APOE status ($p<0.05$, Bonferroni corrected, Figure 2). CSF Aβ42 and NfL levels showed no significant sex-differences. No sex by APOE-status associations were observed in CSF biomarkers levels.

3.4 Sex-differences in MRI measures

3.4.1 Cortical thickness

Female-EOAD and male-EOAD showed reduced CTh in parietotemporal regions when compared to HC of the same sex ($p<0.05$ Bonferroni corrected, Figure 3A and 3B), extended to the frontal lobe in male-EOAD. In female-EOAD, cortical loss was observed in bilateral banks of superior temporal sulcus, fusiform, middle and inferior temporal, inferior parietal and precuneus regions; the left posterior cingulate, supramarginal and superior temporal regions; and the right superior parietal region. In male-EOAD, cortical loss was found in bilateral banks of superior temporal sulcus, inferior parietal and precuneus regions; and the left caudal middle frontal, middle and inferior temporal, parahippocampal, isthmus cingulate, superior parietal and supramarginal regions. In a direct female-EOAD and male-EOAD comparison, male-EOAD showed reduced CTh in the left parahippocampal region ($p<0.05$, Bonferroni corrected, Figure 3C), and no significant sex by group interactions were found in the whole sample ($p>0.05$).

Regarding hemispheric CTh, female-EOAD showed reduced CTh in both hemispheres when compared to same-sex HC, while male-EOAD only did in the left hemisphere ($p<0.05$, Bonferroni corrected, Figure 3D and 3E). No differences were found between female-EOAD and male-EOAD in hemispheric CTh ($p>0.05$, Figure 3F) neither significant sex by group interactions were observed in the whole sample ($p>0.05$).

3.4.2 Hippocampal subfields

Compared to HC of the same sex, female-EOAD showed volume differences in all the subfields and in bilateral hippocampus, except for bilateral parasubiculum and right CA 2/3. Male-EOAD showed differences in the bilateral hippocampal tail and left presubiculum and left hippocampus (all $p<0.05$, Bonferroni corrected, Table 2 and Figures S1&S2). No differences were found between EOAD-female and EOAD-male or sex by group interactions in the whole sample ($p>0.05$).

3.5 Association between atrophy and cognitive performance

In female-EOAD, parietotemporal CTh showed a positive association with MMSE, global composite and praxis and perception functions z-scores, whereas mean hippocampus volume showed a positive association with memory ($p<0.05$ uncorrected, Supplementary Figure 3). Results did not survive after multiple comparison correction. No significant associations were found in male-EOAD. Additional information can be found in Supplementary Table S6.

4. DISCUSSION

We investigated the impact of sex in cognitive impairment, CSF biomarkers levels, CTh and hippocampal subfield volumes in an EOAD cohort with a biomarkers-based diagnosis. In a direct comparison between female-EOAD and male-EOAD, we found that, at the time of diagnosis, there are no sex-differences in cognition, hippocampal volume or hippocampal subfield volume. Slight differences in cortical thickening in the medial temporal lobe were observed. However, female-EOAD presented more widespread atrophy burden and greater cognitive impairment than male-EOAD when compared to sex-matched HC. On the other hand, we observed that CSF levels of tau were higher in female-EOAD than male-EOAD, independently of the APOE status, and no differences were found in Aβ42 or NfL levels. Finally, we found that parietotemporal CTh and hippocampal volume were associated with cognition in female-EOAD but not in male-EOAD. Although previous works have investigated the influence of sex in AD, this is the first study exclusively centered on EOAD, the most common early-onset neurodegenerative dementia.

In addition to the direct comparison between female-EOAD and male-EOAD, we conducted a separate analysis comparing each group with HC of the same sex to avoid introducing sex as a covariate. At diagnosis, women presented greater cognitive impairment than men when compared to same-sex HC, in five cognitive domains and global cognition. These findings are in concordance with prior reports studying LOAD patients that showed that cognitive functions are more severely and widely affected in women (9,24,25). Also, previous evidence in normal aging points to a cognitive advantage in verbal memory tests in women and in motor and visuospatial tasks in men (26,27) that remains stable until the MCI stage(11) and seems to disappear or even reverses in AD(25). According to this, women would require more neurodegenerative burden than men to be diagnosed and, at this point, they may be more susceptible to the clinical manifestation of AD (7,28).

In line with the observed multidomain cognitive decline in female-EOAD, we found, a broader atrophy pattern in female-EOAD than in male-EOAD when they were compared to controls of the same sex. While the atrophy pattern in women EOAD covered parietotemporal regions of both hemispheres, in male-EOAD the pattern was more limited to the left hemisphere. Both sex patterns of cortical atrophy in female and male patients are consistent with the EOAD literature (29,30). From the visual exploration of the patterns, it is observable that regions like the precuneus seem to capture atrophy equally in both sexes at diagnosis, while the medial temporal lobe cortex might show

sexual dimorphism in EOAD, which was confirmed statistically, as male patients presented lower thickness than women in the left parahippocampal region. In previous studies, no sex-differences in CTh have been found among amyloid-positive patients (31), although females seem to present greater temporoparietal tau-PET retention than males. On the other hand, women with AD have shown more accelerated longitudinal cortical thinning (32–35) and more severe neurofibrillary degeneration and brain loss associated with faster cognitive progression(7). In line with our findings in CTh, we observed that female-EOAD showed bilateral hippocampus volume loss and atrophy of most hippocampal subfields compared to same-sex HC. In contrast, male-EOAD showed relative hippocampal subfields preservation. As previously described in AD (11), no sex-effect on hippocampal volume was found in EOAD when directly comparing both sexes. However, a symmetrical and generalized hippocampal subfield volume loss has been demonstrated in typical EOAD (36), similar to our findings in female-EOAD, with CA1 being one of the regions of early neurofibrillary tangles deposition in AD(37). In healthy aging, the female sex confers selective vulnerability of specific hippocampal subfields to volume loss (38). Here we observed that, in male-EOAD, differences in hippocampal volume were limited to left presubiculum and bilateral tail, which might reflect regions that are more vulnerable in male-EOAD with reciprocal connections with the medial temporal regions (39,40). Moreover, the hippocampal-sparing AD subtype has been previously linked to the male sex in AD (41). On the other hand, the effect of APOE ε4 allele on hippocampal atrophy seems stronger in women than men (42). Although the proportion of APOE ε4 carriers was similar between women and men with EOAD, the number of carriers was lower in the female-HC group. Whether an amyloid-independent effect of APOE in normal aging mediates our results is still controversial, as cognition seems to remain relatively preserved over time when amyloid pathology is not present (43). Taken all together, our findings suggest sex-related differences in atrophy spreading in EOAD subjects due to selective vulnerability. Women have previously shown higher tau burden than men in many regions (7,44) and hippocampus(8), while men might present a more located pattern of neurodegeneration at the time of diagnosis, consistent with the idea that tau pathology is influenced by sex-specific genetic, chromosomal and hormonal mechanisms (45). Furthermore, we have also observed that AD pathology might be more likely to result in cognitive dysfunction in females than in males (46), although our results did not survive after correction for multiple comparisons. Cognitive symptoms might be more attributable to the atrophy burden in women, according to previous evidence in which women may show stronger relationships between tau distribution and cognition (47), and other non-tau pathways might be linked with the cognitive decline in men, making it less specific of AD pathology.

Finally, previous studies of CSF Aβ42, p-tau and t-tau concentrations generally have not found differences between women and men (12–14). However, these studies were not restricted to A+T+N+ participants, and never in EOAD. We found elevated tau levels in women with EOAD that were not explained by the presence of the APOE ε4 allele, as previously indicated (13). Our data suggest that the APOE ε4 effect in women on CSF tau might not be a sex-specific risk marker for AD at younger ages, similar to previous evidence showing a strong sex-specific association between APOE ε4 and AD in women between ages 65–75(42). Furthermore, some studies show that women present greater increase in CSF tau levels than men longitudinally (48). On the other hand, no differential effect of APOE ε4 has been found on tau-PET retention (31), and testosterone levels might mediate the influence of APOE ε4 on CSF tau(49). In contrast, higher CSF NfL levels among men with AD were previously reported, and sex-specific reference intervals have been proposed (15). However, we observed similar levels of CSF NfL between women and men with EOAD, maybe pointing to sex-differences in white matter integrity and vascular burden between EOAD and LOAD patients, while the observed higher tau levels in female-EOAD could reflect the greater neurodegeneration specific to AD pathology.

There are limitations to this study. Here we have only focused on biological sex, but we have not assessed whether other factors like gender, neuropsychiatric symptoms, vascular factors or individual hormonal history are mediating our results. The study is also limited by the cross-sectional design, where longitudinal studies can better capture the temporal order of sex-differences. Our sample derived from a memory clinic cohort and the relatively small sample size makes it necessary for our findings to be replicated in larger multicentric samples. Studies investigating sex-differences between EOAD and LOAD patients are also still needed. Furthermore, the approach used for measuring hippocampal subfields also has some limitations: the segmentations only approximate the histology and there is an extensive debate regarding volume normalization for the study of sex-differences.

5. CONCLUSION

We have described different patterns of cognitive impairment, brain atrophy burden and CSF biomarkers levels in women and men with EOAD at the time diagnosis. In subjects with a biomarkers-based diagnosis, our results suggest that there are sex-differences in pathology spreading and susceptibility to the disease in EOAD and that these can contribute to disease prevention, diagnosis, and monitoring treatment response in clinical trials. Further studies are needed towards precision medicine in early-onset dementia patients.

ACKNOWLEDGMENTS: We thank patients and their relatives for their participation in the research. We are indebted to the Magnetic Resonance Image core of the IDIBAPS for the technical help. This work has been performed thanks to the 3T Equipment of Magnetic Resonance at IDIBAPS (project IBPS15-EE-3688 co-funded by MCIU and ERDF).

SOURCES OF FUNDING: This work has been funded by Instituto de Salud Carlos III (ISCIII) and co-funded by the European Union (project PI19/00449 to A Lladó) and PFIS grants (FI18/00121 to O Ramos, FI20/00076 to N Guillén and FI21/00015 to J Sarto), PERIS 2016-2020 Departament de Salut de la Generalitat de Catalunya (SLT008 / 18/00061 to Dr A Lladó) and CERCA Programme/Generalitat de Catalunya.

CONFLICTS OF INTEREST: Dr. Raquel Sanchez-Valle reports personal fees from Wave pharmaceuticals for attending Advisory board meetings, personal fees from Roche diagnostics, Janssen and Neuraxpharm for educational activities, and research grants to her institution from Biogen and Sage Therapeutics outside the submitted work. The remaining authors have no conflicts of interest to declare.

REFERENCES

1. Mendez MF. Early-onset Alzheimer's Disease: Nonamnestic Subtypes and Type 2 AD. Arch Med Res [Internet]. 2012;43(8):677–85. Available from: https://www.ncbi.nlm.nih.gov/pmc/articles/PMC3624763/pdf/nihms412728.pdf

2. Peeters G, Katelekha K, Lawlor B, Demnitz N. Sex differences in the incidence and prevalence of young-onset Alzheimer's disease: A meta-analysis. Int J Geriatr Psychiatry. 2021;37(1).

3. 2021 Alzheimer's disease facts and figures. Alzheimers Dement [Internet]. 2021;17(3):327–406. Available from: https://alz-journals.onlinelibrary.wiley.com/doi/abs/10.1002/alz.12328

4. Ferretti MT, Iulita MF, Cavedo E, Chiesa PA, Dimech AS, Chadha AS, et al. Sex differences in Alzheimer disease — The gateway to precision medicine. Nat Rev Neurol [Internet]. 2018;14(8):457–69. Available from: http://dx.doi.org/10.1038/s41582-018-0032-9

5. Nelson PT, Head E, Schmitt FA, Davis PR, Neltner JH, Jicha GA, et al. Alzheimer's disease is not "brain aging": Neuropathological, genetic, and epidemiological human studies. Acta Neuropathol. 2011;121(5):571–87.

6. Jack CR, Bennett DA, Blennow K, Carrillo MC, Dunn B, Haeberlein SB, et al. NIA-AA Research Framework: Toward a biological definition of

Alzheimer's disease. Alzheimers Dement [Internet]. 2018;14(4):535–62. Available from: https://linkinghub.elsevier.com/retrieve/pii/S1552526018300724

7. Filon JR, Intorcia AJ, Sue LI, Vazquez Arreola E, Wilson J, Davis KJ, et al. Gender differences in Alzheimer disease: Brain atrophy, histopathology burden, and cognition. J Neuropathol Exp Neurol. 2016;75(8):748–54.

8. Liesinger AM, Graff-Radford NR, Duara R, Carter RE, Hanna Al-Shaikh FS, Koga S, et al. Sex and age interact to determine clinicopathologic differences in Alzheimer's disease. Acta Neuropathol [Internet]. 2018;136(6):873–85. Available from: https://doi.org/10.1007/s00401-018-1908-x

9. Irvine K, Laws KR, Gale TM, Kondel TK. Greater cognitive deterioration in women than men with Alzheimer's disease: A meta analysis. J Clin Exp Neuropsychol. 2012;34(9):989–98

10. Apostolova LG, Dinov ID, Dutton RA, Hayashi KM, Toga AW, Cummings JL, et al. 3D comparison of hippocampal atrophy in amnestic mild cognitive impairment and Alzheimer's disease. Brain [Internet]. 2006;129(11):2867–73. Available from: https://academic.oup.com/brain/article-lookup/doi/10.1093/brain/awl274

11. Sundermann EE, Biegon A, Rubin LH, Lipton RB, Mowrey W, Landau S, et al. Better verbal memory in women than men in MCI despite similar levels of hippocampal atrophy. Neurology [Internet]. 2016;86(15):1368– 76. Available from: https://www.neurology.org/lookup/doi/10.1212/WNL.0000000000002570

12. Mattsson N, Lönneborg A, Boccardi M, Blennow K, Hansson O, Geneva Task Force for the Roadmap of Alzheimer's Biomarkers. Clinical validity of cerebrospinal fluid Aβ42, tau, and phospho-tau as biomarkers for Alzheimer's disease in the context of a structured 5-phase development framework. Neurobiol Aging. 2017;52:196–213.

13. Hohman TJ, Dumitrescu L, Barnes LL, Thambisetty M, Beecham G, Kunkle B, et al. Sex-specific association of apolipoprotein e with cerebrospinal fluid levels of tau. JAMA Neurol. 2018;75(8):989–98.

14. Schoonenboom NSM, Pijnenburg YAL, Mulder C, Rosso SM, Van Elk E-J, Van Kamp GJ, et al. Amyloid β(1–42) and phosphorylated tau in CSF as markers for early-onset Alzheimer disease. Neurology [Internet]. 2004;62(9):1580–4. Available from: http://www.neurology.org/lookup/doi/10.1212/01.WNL.0000123249.58898.E0

15. Bridel C, Van Wieringen WN, Zetterberg H, Tijms BM, Teunissen CE, Alvarez-Cermeño JC, et al. Diagnostic Value of Cerebrospinal Fluid Neurofilament Light Protein in Neurology: A Systematic Review and Meta-analysis. JAMA Neurol. 2019;76(9):1035–48.

16. Albert MS, DeKosky ST, Dickson D, Dubois B, Feldman HH, Fox NC, et al. The diagnosis of mild cognitive impairment due to Alzheimer's disease: Recommendations from the National Institute on Aging- Alzheimer's Association workgroups on diagnostic guidelines for Alzheimer's disease. Alzheimers Dement [Internet]. 2011;7(3):270–9. Available from: http://doi.wiley.com/10.1016/j.jalz.2011.03.008

17. McKhann GM, Knopman DS, Chertkow H, Hyman BT, Jack CR, Kawas CH, et al. The diagnosis of dementia due to Alzheimer's disease: Recommendations from the National Institute on Aging-Alzheimer's Association workgroups on diagnostic guidelines for Alzheimer's disease. Alzheimers Dement [Internet]. 2011;7(3):263–9. Available from: http://doi.wiley.com/10.1016/j.jalz.2011.03.005

18. Antonell A, Tort-Merino A, Ríos J, Balasa M, Borrego-Écija S, Auge JM, et al. Synaptic, axonal damage and inflammatory cerebrospinal fluid biomarkers in neurodegenerative dementias. Alzheimers Dement. 2020;16(2):262–72.

19. Fischl B, Dale AM. Measuring the thickness of the human cerebral cortex from magnetic resonance images. Proc Natl Acad Sci U S A. 2000;97(20):11050–5.

20. Fischl B, van der Kouwe A, Destrieux C, Halgren E, Ségonne F, Salat DH, et al. Automatically Parcellating the Human Cerebral Cortex. Cereb Cortex [Internet]. 2004;14(1):11–22. Available from: http://cercor.oxfordjournals.org/content/14/1/11.abstract

21. Desikan RS, Ségonne F, Fischl B, Quinn BT, Dickerson BC, Blacker D, et al. An automated labeling system for subdividing the human cerebral cortex on MRI scans into gyral based regions of interest. Neuroimage. 2006;31(3):968–80.

22. Leemput K Van, Bakkour A, Benner T, Wiggins G, Wald LL, Augustinack J, et al. Automated Segmentation of Hippocampal Subfields From Ultra-High Resolution In Vivo MRI. Hippocampus. 2009;19(6):549–57.

23. Eugenio J, Augustinack JC, Nguyen K, Player CM, Player A, Wright M, et al. NeuroImage A computational atlas of the hippocampal formation using ex vivo , ultra-high resolution MRI : Application to adaptive segmentation of in

vivo MRI. Neuroimage [Internet]. 2015;115:117–37. Available from: http://dx.doi.org/10.1016/j.neuroimage.2015.04.042

24. Lin KA, Choudhury KR, Rathakrishnan BG, Marks DM, Petrella JR, Doraiswamy PM, et al. Marked gender differences in progression of mild cognitive impairment over 8 years. Alzheimers Dement (N Y) [Internet]. 2015;1(2):103–10. Available from: http://dx.doi.org/10.1016/j.trci.2015.07.001

25. Sundermann EE, Biegon A, Rubin LH, Lipton RB, Landau S, Maki PM, et al. Does the Female Advantage in Verbal Memory Contribute to Underestimating Alzheimer's Disease Pathology in Women versus Men? J Alzheimers Dis. 2017;56(3):947–57.

26. Herlitz A, Nilsson LG, Bäckman L. Gender differences in episodic memory. Mem Cognit. 1997;25(6):801–11.

27. McCarrey AC, An Y, Kitner-Triolo MH, Ferrucci L, Resnick SM. Sex differences in cognitive trajectories in clinically normal older adults. Psychol Aging. 2016;31(2):166–75.

28. Digma LA, Madsen JR, Rissman RA, Jacobs DM, Brewer JB, Banks SJ, et al. Women can bear a bigger burden: ante- and post-mortem evidence for reserve in the face of tau. Brain Commun. 2020;2(1):fcaa025

29. Cho H, Jeon S, Kang SJ, Lee JM, Lee JH, Kim GH, et al. Longitudinal changes of cortical thickness in early- versus late-onset Alzheimer's disease. Neurobiol Aging. 2013;34(7):1921.e9-15.

30. Falgàs N, Ruiz-Peris M, Pérez-Millan A, Sala-Llonch R, Antonell A, Balasa M, et al. Contribution of CSF biomarkers to early-onset Alzheimer's disease and frontotemporal dementia neuroimaging signatures. Hum Brain Mapp [Internet]. 2020;41(8):2004-13.

31. Edwards L, La Joie R, Iaccarino L, Strom A, Baker SL, Casaletto KB, et al. Multimodal neuroimaging of sex differences in cognitively impaired patients on the Alzheimer's continuum: greater tau-PET retention in females. Neurobiol Aging [Internet]. 2021;105:86–98. Available from: https://doi.org/10.1016/j.neurobiolaging.2021.04.003

32. Lee J, Cho H, Jeon S, Kim HJ, Kim YJ, Lee J, et al. Sex-Related Reserve Hypothesis in Alzheimer's Disease: Changes in Cortical Thickness with a Five-Year Longitudinal Follow-Up. J Alzheimers Dis. 2018;65(2):641–9.

33. Hua X, Hibar DP, Lee S, Toga AW, Jack CR, Weiner MW, et al. Sex and age differences in atrophic rates: An ADNI study with n=1368 MRI scans. Neurobiol Aging. 2010;31(8):1463–80.

34. Skup M, Zhu H, Wang Y, Giovanello KS, Lin J, Shen D, et al. Sex differences in grey matter atrophy patterns among AD and aMCI patients: Results from ADNI. Neuroimage [Internet]. 2011;56(3):890–906. Available from: https://www.ncbi.nlm.nih.gov/pmc/articles/PMC3624763/pdf/nihms412728.pdf

35. Koran MEI, Wagener M, Hohman TJ, Alzheimer's Neuroimaging Initiative. Sex differences in the association between AD biomarkers and cognitive decline. Brain Imaging Behav. 2017;11(1):205–13.

36. Parker TD, Slattery CF, Yong KXX, Nicholas JM, Paterson RW, Foulkes AJM, et al. Differences in hippocampal subfield volume are seen in phenotypic variants of early onset Alzheimer's disease. NeuroImage Clin [Internet]. 2019;21:101632. Available from: https://doi.org/10.1016/j.nicl.2018.101632

37. Lace G, Savva GM, Forster G, De Silva R, Brayne C, Matthews FE, et al. Hippocampal tau pathology is related to neuroanatomical connections: An ageing population-based study. Brain. 2009;132(5):1324–34

38. Veldsman M, Nobis L, Alfaro-Almagro F, Manohar S, Husain M. The human hippocampus and its subfield volumes across age, sex and APOE e4 status. Brain Commun. 2020;3(1):fcaa219.

39. Ding SL. Comparative anatomy of the prosubiculum, subiculum, presubiculum, postsubiculum, and parasubiculum in human, monkey, and rodent. J Comp Neurol. 2013;521(18):4145–62.

40. Insausti R, Muñoz-López M, Insausti AM, Artacho-Pérula E. The human periallocortex: Layer pattern in presubiculum, parasubiculum and entorhinal cortex. A review. Front Neuroanat. 2017;11:84.

41. Ferreira D, Nordberg A, Westman E. Biological subtypes of Alzheimer disease: A systematic review and meta-analysis. Neurology. 2020;94(10):436–48.

42. Fleisher A, Grundman M, Jack CR, Petersen RC, Taylor C, Kim HT, et al. Sex, apolipoprotein E ε4 status, and hippocampal volume in mild cognitive impairment. Arch Neurol [Internet]. 2005;62(6):953–7. Available from: http://archneur.jamanetwork.com/article.aspx?doi=10.1001/archneur.62.6.953

43. Lim YY, Kalinowski P, Pietrzak RH, Laws SM, Burnham SC, Ames D, et al. Association of ß-Amyloid and apolipoprotein e e4 with memory decline in preclinical Alzheimer disease. JAMA Neurol. 2018;75(4):488–94.

44. Buckley RF, Scott MR, Jacobs HIL, Schultz AP, Properzi MJ, Amariglio RE, et al. Sex Mediates Relationships Between Regional Tau Pathology and Cognitive Decline. Ann Neurol. 2020;88(5):921–32.

45. Davis EJ, Solsberg CW, White CC, Miñones-Moyano E, Sirota M, Chibnik L, et al. Sex-Specific Association of the X Chromosome with Cognitive Change and Tau Pathology in Aging and Alzheimer Disease. JAMA Neurol. 2021;78(10):1249–54.

46. Barnes LL, Wilson RS, Bienias JL, Schneider JA, Evans DA, Bennett DA. Sex differences in the clinical manifestations of Alzheimer disease pathology. Arch Gen Psychiatry. 2005;62(6):685–91.

47. Banks SJ, Andrews MJ, Digma L, Madsen J, Reas ET, Caldwell JZK, et al. Sex differences in Alzheimer's disease: do differences in tau explain the verbal memory gap? Neurobiol Aging [Internet]. 2021;107:70–7. Available from: https://doi.org/10.1016/j.neurobiolaging.2021.05.013

48. Buckley RF, Mormino EC, Chhatwal J, Schultz AP, Rabin JS, Rentz DM, et al. Associations between baseline amyloid, sex, and APOE on subsequent tau accumulation in cerebrospinal fluid. Neurobiol Aging. 2019;78:178–85.

49. Sundermann EE, Panizzon MS, Chen X, Andrews M, Galasko D, Banks SJ, et al. Sex differences in Alzheimer's-related Tau biomarkers and a mediating effect of testosterone. Biol Sex Differ. 2020;11(1):33.

Table 1 Characteristics of the participants

	EOAD			HC		
	Female-EOAD (N=34)	Male-EOAD (N=28)	All-EOAD (N=62)	Female-HC (N=32)	Male-HC (N=12)	All-HC (N=44)
Age at onset (years)	57.5 (4.3)	56.3 (3.8)	56.9 (4.1)	N/A	N/A	N/A
Age at MRI (years)	60.6 (4.1)	59.4 (4.3)	60.1 (4.2)	58.6 (4.5)	57.8 (6.0)	58.3 (4.9)
MMSE score	22.4 (4.0)†,‡	23.9 (3.3)†,‡	23.1 (3.8)*	28.7 (1.7)§,¶	29 (1.0)§,¶	28.8 (1.5)*
APOEε4 carriers (N)	19†	15†	34*	4§,¶	3	7*
Age at LP (years)	60.7 (4.6)	59.3 (4.3)	60.1 (4.5)	58.5 (4.6)	57.7 (6.0)	58.3 (5.0)
Age at cognitive assessment (years)	60.6 (4.2)	59.1 (4.2)	59.9 (4.2)	58.4 (4.6)	58 (6.2)	58.3 (5.0)
Education (years)	10.4 (3.5)	12.5 (3.2)	11.4 (3.5)	11.3 (3.5)	12.8 (3.7)	11.7 (3.6)
Time between MRI and cognitive assessment (years)	0.4 (0.8)	0.2 (0.4)	0.3 (0.6)	0.1 (0.1)	0.2 (0.4)	0.1 (0.2)

* Significant differences between EOAD and HC using t Student or χ2.
Between sexes comparisons were performed using ANOVA with post hoc analysis and Fisher's tests: †, significantly different from HC-female; ‡, significantly different from HC-male; §, significantly different from EOAD-female; ¶, significantly different from EOAD-male.
Kay: EOAD, early-onset Alzheimer's disease; HC healthy control; LP, lumbar puncture; MMSE, Mini-Mental State examination; MRI, magnetic resonance imaging.

Figure 1. Neuropsychological z-scores differences between groups and sexes (*p<0.05, Bonferroni corrected, Lineal Models using age at neuropsychological assessment, APOE and education as covariates). Key: EOAD early-onset AD; HC healthy controls; MMSE Mini-Mental State Examination.

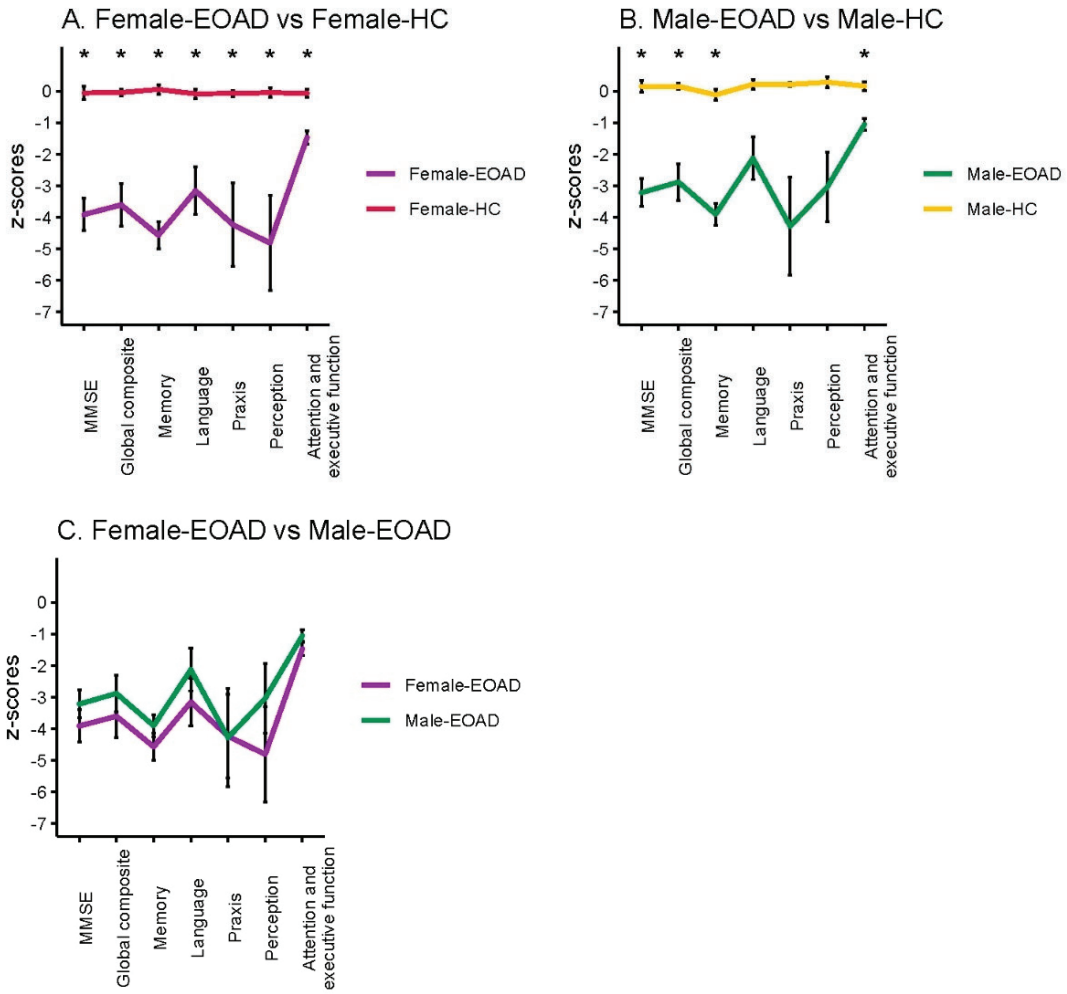

Figure 2. Sex-differences in CSF biomarkers in EOAD (*p<0.05, Bonferroni corrected). Lineal Models using age at lumbar puncture and APOE as covariates. Key: EOAD early-onset AD; Aβ42: amyloid-β 42; P-tau, phosphorylated tau; T-Tau, total tau; NfL, neurofilaments light chain.

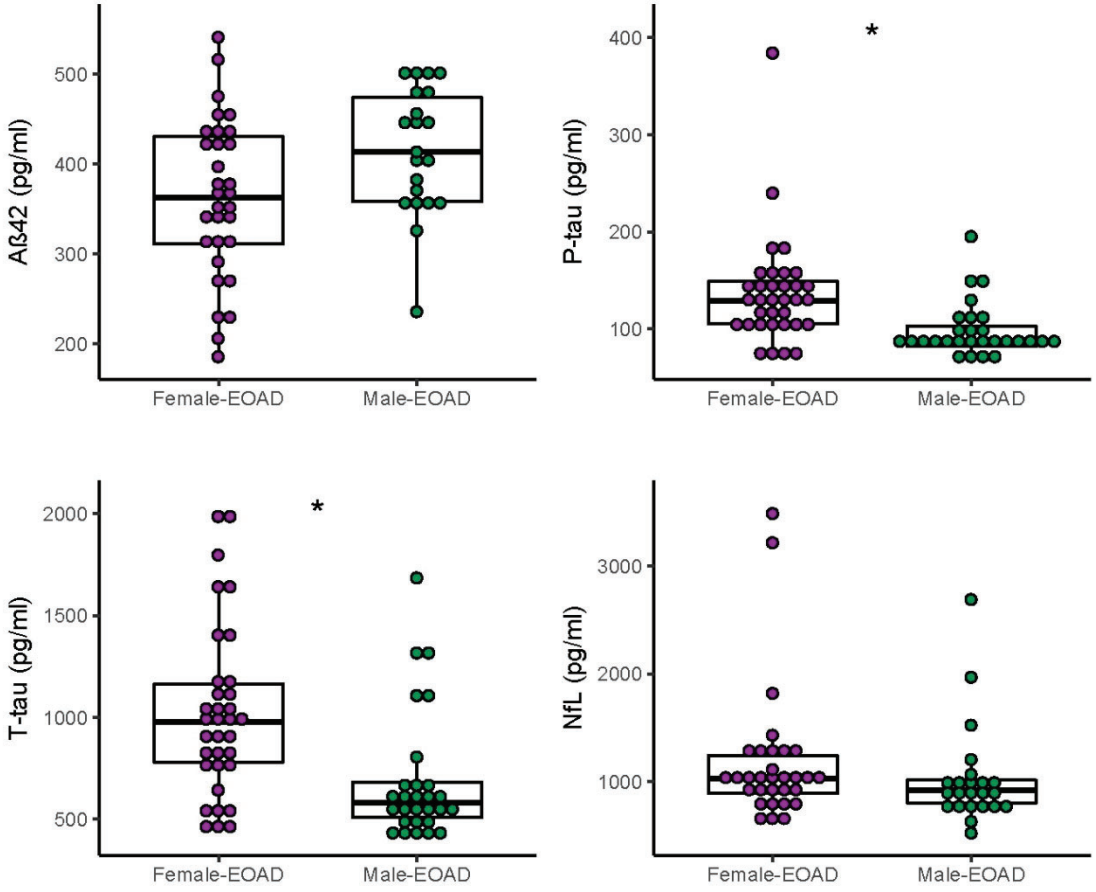

Figure 3. (A-C) Group differences in regional cortical thickness. We only show standardized β coefficients of regions with statistically significant results (p<0.05, Bonferroni corrected). **(D-F)** Group differences in hemispheric cortical thickness (*p<0.05, Bonferroni corrected). Key: EOAD early-onset AD; HC healthy control; Std. β, standardized β coefficients.

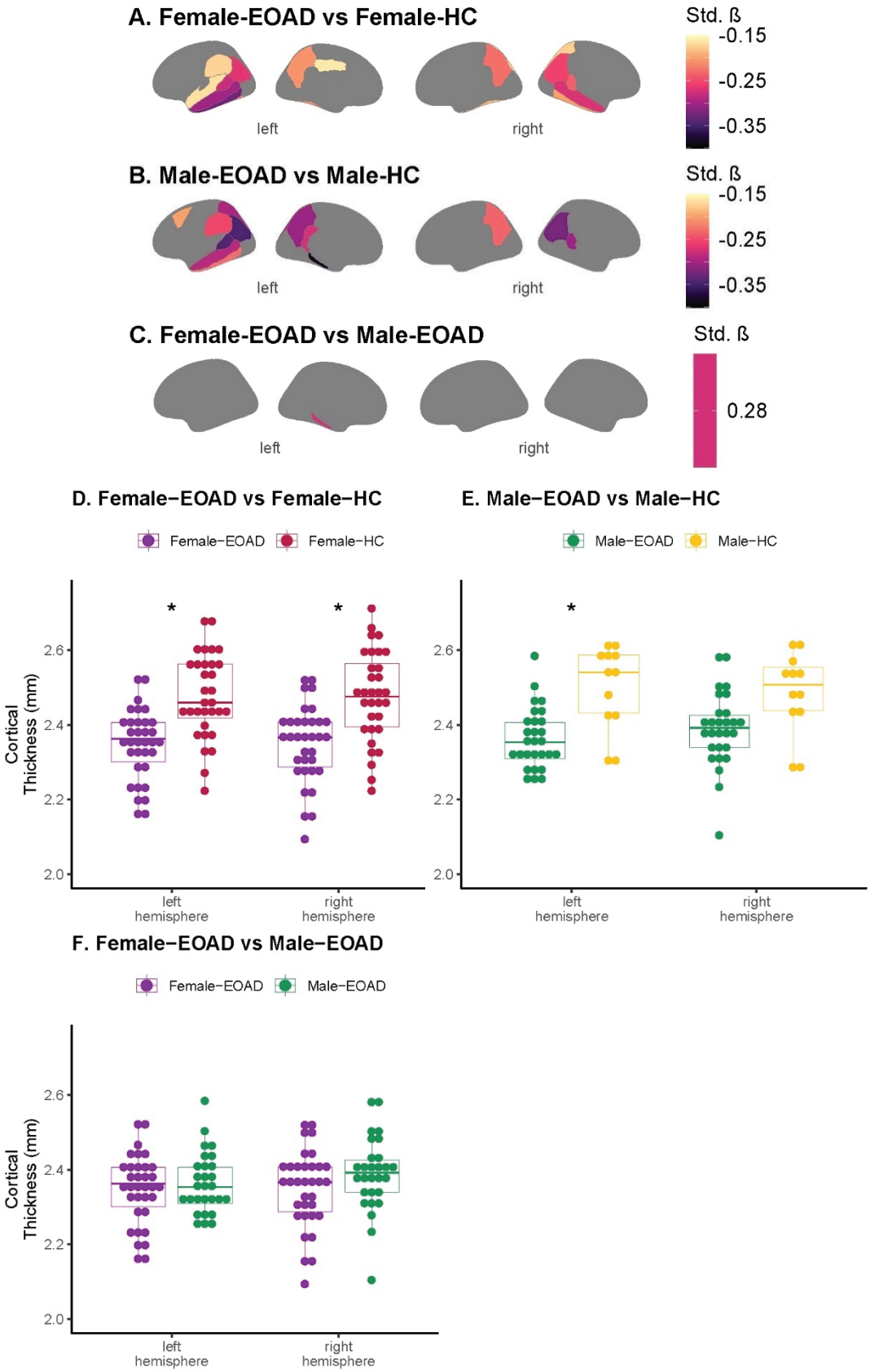

Supplementary material:

Supplementary Table S1. Cognitive composites

Cognitive domain	Test
Memory	FCSRT - free learning
	FCSRT - total learning
	FCSRT - delayed free recall
	FCSRT - delayed total recall
	Landscape test
Language	Boston Naming Test
	Semantic fluency: animals
	comprehension subtest of BDAE
Praxis	WAB ideomotor praxis
	CERAD constructional praxis
Visuospatial	VOSP incomplete letters
	VOSP number location
Executive	Trail Making Test-A
	Letter fluency test: F, A and S
	WAIS digit span forwards
	WAIS digit span backwards

The sign of Trail Making Test-A seconds was reversed to represent lower score, lower performance.
Key: BDAE, Boston Diagnostic Aphasia Examination; CERAD, Consortium to Establish a Registry for Alzheimer's Disease; FCSRT, Free and Cued Selective Reminding Test; VOSP, Visual Object and Space Perception; WAB, Western Aphasia Battery; WAIS, Wechsler Adult Intelligence Scale.

Supplementary Table S2. Regions included in the parietotemporal composite

Lobe	Region (left and right hemisphere)
Parietal	Inferior parietal
	Isthmus cingulate
	Postcentral
	Posterior cingulate
	Precuneus
	Superior parietal
	Supramarginal
Temporal	Banks of superior temporal sulcus
	Entorhinal
	Fusiform
	Inferior temporal
	Middle temporal
	Parahippocampal
	Superior temporal
	Temporal pole
	Transverse temporal

Supplementary Table S3. Cognitive z-scores by groups

	EOAD			HC		
Cognitive measure	Female-EOAD (N=28)	Male-EOAD (N=26)	All-EOAD (N=54)	Female-HC (N=31)	Male-HC (N=12)	All-HC (N=43)
zMMSE(SD)	-3.9(2.6)	-3.2(2.3)	-3.6(2.5)	-0.1(1.1)	0.2(0.6)	0(1)
zGlobal composite(SD)	-3.6(3.5)	-2.9(3.0)	-3.3(3.3)	-0.04(0.6)	0.1(0.3)	0.01 (0.5)
zMemory(SD)	-4.6(2.2)	-3.9(1.8)	-4.2(2.0)	0.1(0.8)	-0.1(0.6)	0.005 (0.8)
zLanguage(SD)	-3.2(4)	-2.1(3.5)	-2.7(3.7)	-0.1(0.9)	0.2(0.5)	-0.002 (0.8)
zPraxis(SD)	-4.2(7.1)	-4.3(7.9)	-4.3(7.4)	-0.1(0.5)	0.2(0.2)	0.01 (0.5)
zVisuospatial(SD)	-4.8(7.9)	-3(5.7)	-3.9(6.9)	-0.1(0.8)	0.3(0.6)	0.04 (0.8)
zExecutive and attentional function(SD)	-1.5(1.1)	-1.1(0.9)	-1.3(1.0)	-0.1(0.8)	0.2(0.5)	-0.005 (0.7)

Key: EOAD, early-onset Alzheimer's disease; HC, healthy controls; MMSE, Mini-Mental State examination; SD=standard deviation.

Supplementary Table S4. Standardized coefficients of the differences in cognition between EOAD and HC of the same sex

Cognitive measure		Female-EOAD vs Female-HC	Male-EOAD vs Male-HC
zMMSE	Std. β (SD)	-3.8(0.5)*	-3.3(0.6)*
zGlobal composite	Std. β (SD)	-3.4(0.6)*	-3(0.9)*
zMemory	Std. β (SD)	-4.4(0.4)*	-3.7(0.5)*
zLanguage	Std. β (SD)	-2.7(0.8)*	-2.3(1.0)
zPraxis	Std. β (SD)	-4.1(1.3)*	-4.4(2.4)
zVisuospatial	Std. β (SD)	-4.9(1.5)*	-3.5(1.6)
zExecutive and attentional function	Std. β (SD)	-1.2(0.2)*	-1.2(0.3)*

The cognitive battery was available in 28 female-EOAD, 26 male-EOAD, 31 female-HC and 12 male-HC. *p<0.05, Bonferroni corrected, using Linear Models. Age and years of education were introduced as covariates in the models. Key: EOAD, early-onset Alzheimer's disease; HC, healthy controls; MMSE, Mini-Mental State examination; SD=standard deviation; Std. β, standardized β coefficient

Supplementary Table S5. Cerebrospinal fluid biomarkers differences between EOAD and HC

	EOAD			HC		
	Female-EOAD (N=34)	Male-EOAD (N=28)	All-EOAD (N=62)	Female-HC (N=32)	Male-HC (N=12)	All-HC (N=44)
CSF Aβ42 levels (pg/ml)*	362.7 (88.6)§,¶	415.3 (70.7)§,¶	383.9 (85.2)‡	820.8 (179.8)#,**	865.3 (290.6)#,**	832.9 (212.9)‡
CSF p-tau levels (pg/ml)	136.6 (55.6)§,¶	97.9 (28.3)§,¶	119.1 (49.0)‡	48 (9.7)#,**	44.8 (9.9)#,**	47.1 (9.8)‡
CSF t-tau levels (pg/ml)	1021.2 (416.1)§,¶	692.5 (318.0)§,¶	872.7 (407.0)‡	205.9 (52.8)#,**	199.5 (67.2)#,**	204.1 (56.4)‡
CSF NfL levels (pg/ml)†	1175.3 (631.8)§,¶	1026.5 (469.3)§,¶	1112 (568.2)‡	422.1 (136.1)#,**	553.2 (161.3)#,**	458.2 (153.2)‡

* CSF Aβ42 levels of 31 female-EOAD, 21 male-EOAD and 44 HC were included in the analysis. †CSF NfL levels were available 31 female-EOAD, 23 male-EOAD, 29 female-HC and 11 male-HC. ‡ Significant differences between EOAD and HC using t Student. Comparisons between EOAD and HC sexes were performed using ANOVA with post hoc analysis: §, significantly different from HC-female; ¶ significantly different from HC-male; # significantly different from EOAD-female; ** Significantly different from EOAD-male. Key: Aβ, amyloid-β; EOAD, early-onset Alzheimer's disease; HC healthy control; NfL, neurofilament light chain; p-tau, phosphorylated tau; t-tau, total tau.

Supplementary Table S6. Association between parietotemporal CTh or hippocampal volume and cognition z-scores

Cognition z-score		Parietotemporal CTh z-score		Hippocampal volume z-score	
		Std. β (SD)	p	Std. β (SD)	p
zMMSE	Female-EOAD	1.7(0.7)*	0.02	0.9(0.6)	0.14
	Male-EOAD	0.2(0.6)	0.72	0.7(0.6)	0.22
zGlobal composite	Female-EOAD	2.5(0.9)*	0.01	1.02(0.76)	0.19
	Male-EOAD	1.2(0.9)	0.21	-0.3(0.9)	0.70
zMemory	Female-EOAD	0.2(0.4)	0.60	0.7(0.3)*	0.03
	Male-EOAD	-0.4(0.5)	0.47	0.6(0.5)	0.20
zLanguage	Female-EOAD	1.2(1.1)	0.30	1.1(0.9)	0.22
	Male-EOAD	1.0(1.1)	0.35	-1.3(1.0)	0.19
zPraxis	Female-EOAD	5.5(1.7)*	0.003	1.8(1.6)	0.26
	Male-EOAD	1.0(1.1)	0.35	-0.1(2.4)	0.95
zPerception	Female-EOAD	4.7(2.0)*	0.03	0.8(1.8)	0.67
	Male-EOAD	2.9(1.6)	0.09	-0.8(1.6)	0.64
zAttentional and executive function	Female-EOAD	0.4(0.2)	0.14	0.1(0.2)	0.65
	Male-EOAD	-1.7(2.3)	0.48	-0.2(0.2)	0.54

Standardized β coefficients and p-values from Linear Models to analyze the association between parietotemporal cortical thickness or hippocampal volume z-scores and cognition z-scores. Age at neuropsychological assessment and years of education were introduced as covariates.

Key: EOAD, early-onset Alzheimer's disease; HC, healthy controls; MMSE, Mini-Mental State examination; SD=standard deviation; Std. β, standardized β coefficient

Supplementary Figure 1. Differences between groups and sexes in left hippocampus and hippocampal subfields volumes adjusted by total intracranial volume (*p<0.05, Bonferroni corrected). Key: CA, cornus ammonis; EOAD early-onset AD; GC-ML-DG, granule cell and molecular layer of dentate gyrus; HATA, hippocampus - amygdala transition area; HC healthy control.

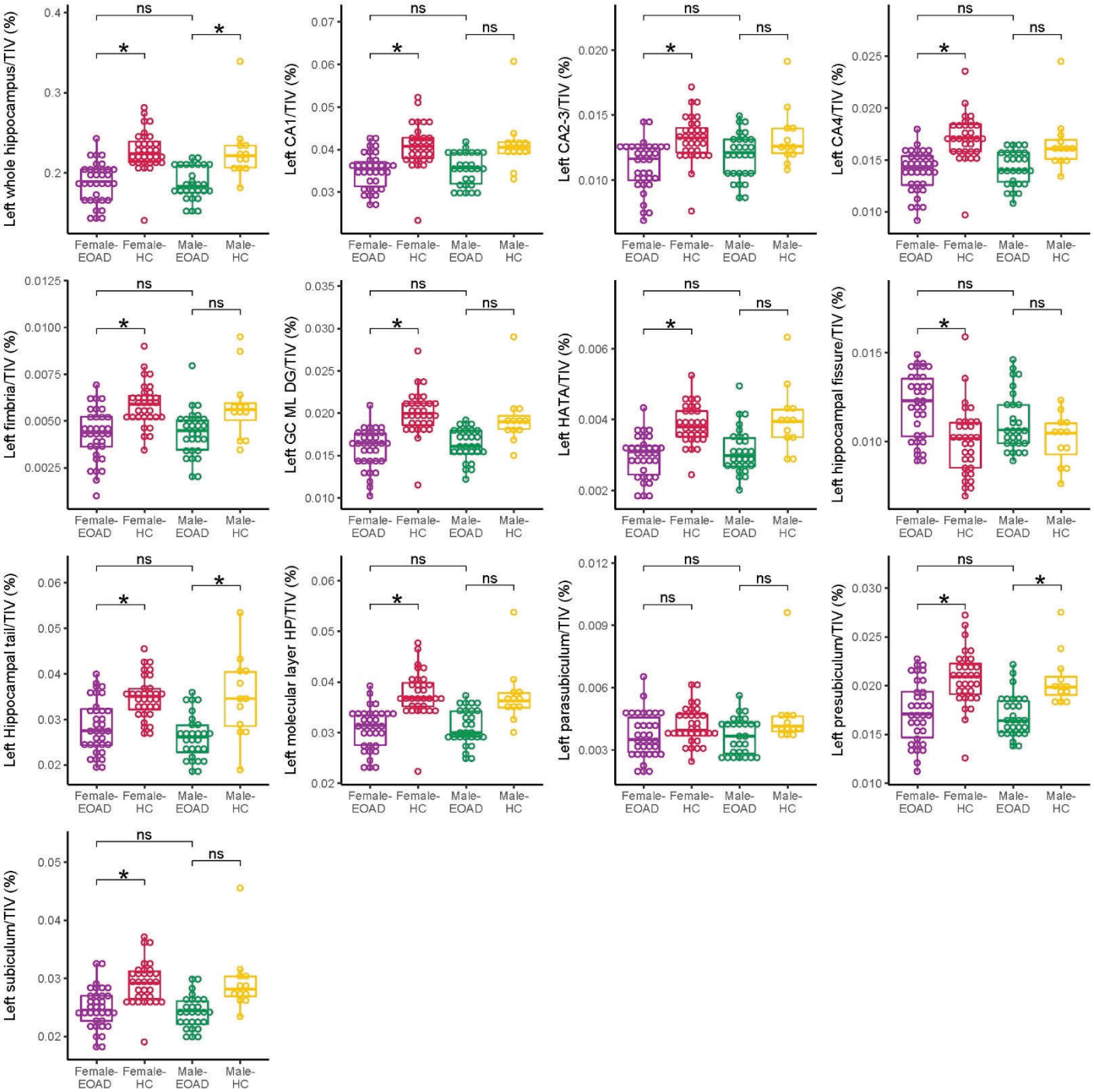

Supplementary Figure 2. Differences between groups and sexes in right hippocampus and hippocampal subfields volumes adjusted by total intracranial volume (*p<0.05, Bonferroni corrected). Key: CA, cornus ammonis; EOAD early-onset AD; GC-ML-DG, granule cell and molecular layer of dentate gyrus; HATA, hippocampus - amygdala transition area; HC healthy control.

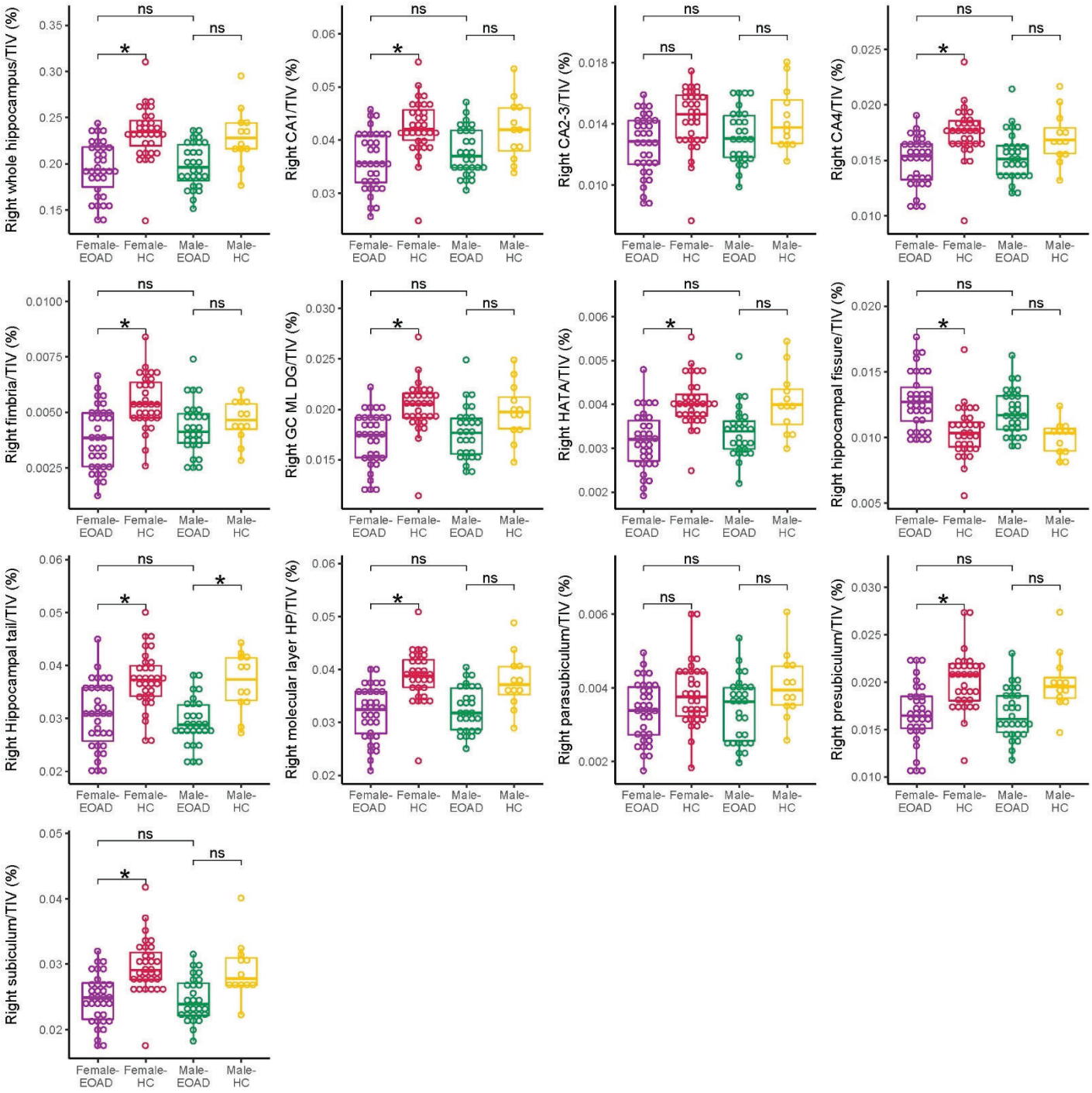

Supplementary figure 3. Association between parietotemporal cortical thickness or hippocampal volume and cognition in female-EOAD and male-EOAD. Dashed lines represent a significant association between cognition and MRI measures ($p<0.05$, uncorrected, in separated by sex Lineal Models using age and education as covariates). Key: CTh, cortical thickness; EOAD early-onset AD.

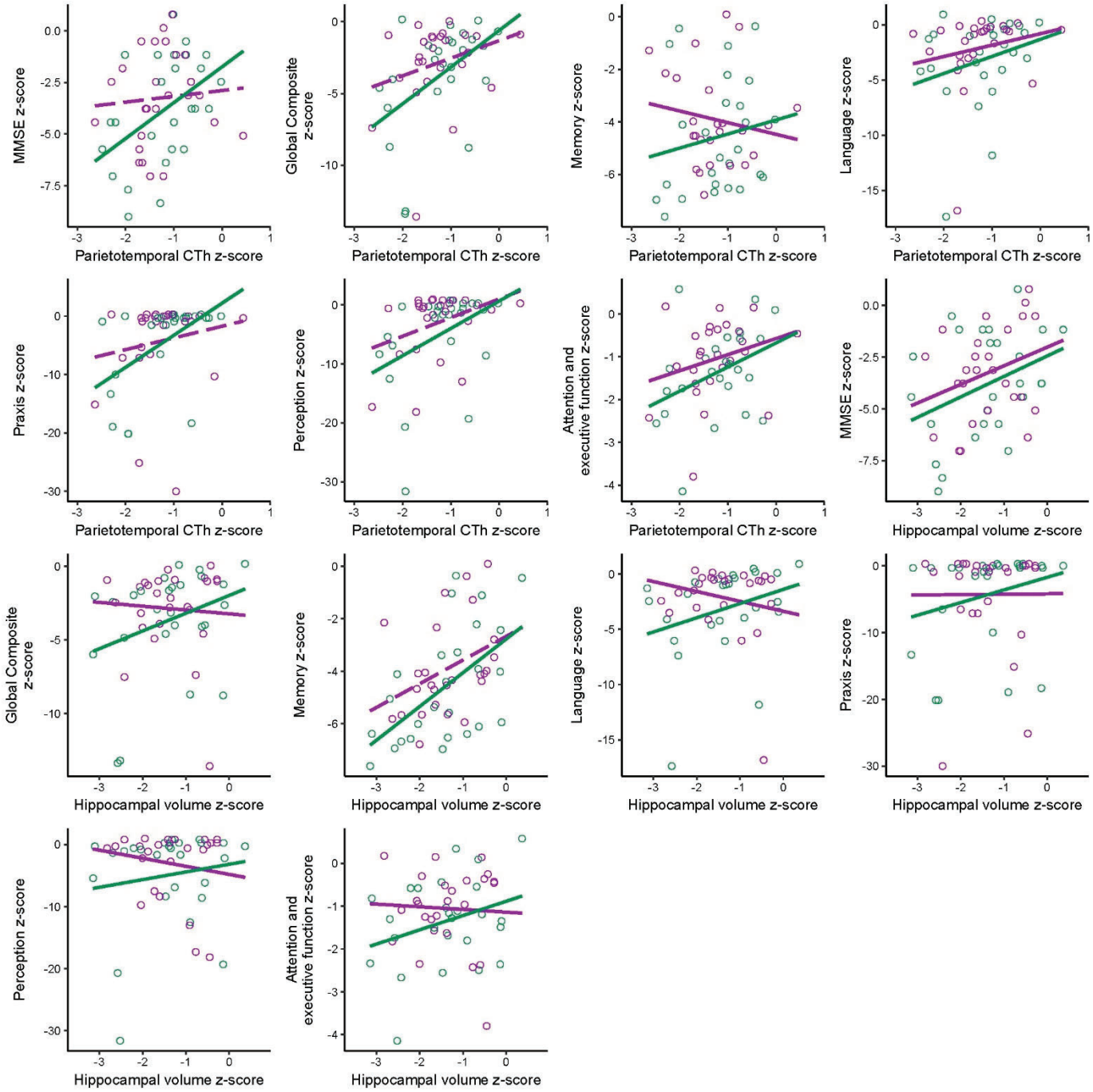

OBJETIVO 2

Estudiar los cambios transversales y longitudinales en grosor cortical y volumen subcortical mediante RM craneal en sujetos con EAIP confirmada biológicamente en comparación con sujetos control, y analizar la capacidad pronóstica de los biomarcadores en LCR (Aβ42, p-tau, t-tau y NfL) en el momento del diagnóstico para predecir la evolución longitudinal de dichas medidas.

Título del trabajo:

"Longitudinal brain atrophy and CSF biomarkers in early-onset Alzheimer's disease."

Autores: Contador, José; Pérez-Millán, Agnès; Tort-Merino, Adrià; Balasa, Mircea; Falgàs, Neus; Olives, Jaume; Castellví, Magdalena; Borrego-Écija, Sergi; Bosch, Beatriz; Fernández-Villullas, Guadalupe; Ramos-Campoy, Oscar; Antonell, Anna; Bargalló, Nuria; Sanchez-Valle, Raquel; Sala-Llonch, Roser; Lladó, Albert

Neuroimage:Clinical 2021;32:102804.
doi: 10.1016/j.nicl.2021.102804
IF: 4.881; Q2 Neuroimaging

NeuroImage: Clinical 32 (2021) 102804

Contents lists available at ScienceDirect

NeuroImage: Clinical

journal homepage: www.elsevier.com/locate/ynicl

Longitudinal brain atrophy and CSF biomarkers in early-onset Alzheimer's disease

José Contador [a], Agnès Pérez-Millán [a], Adrià Tort-Merino [a], Mircea Balasa [a,b], Neus Falgàs [a,b,c], Jaume Olives [a], Magdalena Castellví [a], Sergi Borrego-Écija [a], Beatriz Bosch [a], Guadalupe Fernández-Villullas [a], Oscar Ramos-Campoy [a], Anna Antonell [a], Nuria Bargalló [d], Raquel Sanchez-Valle [a,e], Roser Sala-Llonch [f,g,1], Albert Lladó [a,e,1,*], for the Alzheimer's Disease Neuroimaging Initiative[2]

[a] Alzheimer's Disease and Other Cognitive Disorders Unit, Neurology Service, Hospital Clínic of Barcelona, Institut d'Investigacions Biomèdiques August Pi i Sunyer (IDIBAPS), Universitat de Barcelona, Barcelona 08036, Spain
[b] Atlantic Fellow for Equity in Brain Health, Global Brain Heath Institute
[c] Department of Neurology, Memory & Aging Center, Weill Institute for Neurosciences, University of California, 675 Nelson Rising Lane, Suite 190, San Francisco, CA 94158, USA
[d] Image Diagnostic Centre, IDIBAPS, Hospital Clínic de Barcelona, Barcelona, Spain
[e] Centro de Investigación Biomédica en Red de Enfermedades Neurodegenerativas. CIBERNED, Spain
[f] Institute of Neurosciences. Department of Biomedicine, Faculty of Medicine, University of Barcelona, Barcelona, 08036, Spain
[g] Biomedical Imaging Group, Biomedical Research Networking Center in Bioengineering, Biomaterials and Nanomedicine (CIBER-BBN), Barcelona, Spain

ARTICLE INFO

Keywords:
Early-onset Alzheimer's disease
Longitudinal
MRI
Atrophy
Cerebrospinal fluid
Biomarkers

ABSTRACT

There is evidence of longitudinal atrophy in posterior brain areas in early-onset Alzheimer's disease (EOAD; aged < 65 years), but no studies have been conducted in an EOAD cohort with fluid biomarkers characterization. We used 3T-MRI and Freesurfer 6.0 to investigate cortical and subcortical gray matter loss at two years in 12 EOAD patients (A + T + N +) compared to 19 controls (A-T-N-) from the Hospital Clínic Barcelona cohort. We explored group differences in atrophy patterns and we correlated atrophy and baseline CSF-biomarkers levels in EOAD. We replicated the correlation analyses in 14 EOAD (A + T + N +) and 55 late-onset AD (LOAD; aged ≥ 75 years; A + T + N +) participants from the Alzheimer's disease Neuroimaging Initiative. We found that EOAD longitudinal atrophy spread with a posterior-to-anterior gradient and beyond hippocampus/amygdala. In EOAD, higher initial CSF NfL levels correlated with higher ventricular volumes at baseline. On the other hand, higher initial CSF Aβ42 levels (within pathological range) predicted higher rates of cortical loss in EOAD. In EOAD and LOAD subjects, higher CSF t-tau values at baseline predicted higher rates of subcortical atrophy. CSF p-tau did not show any significant correlation. In conclusion, posterior cortices, hippocampus and amygdala capture EOAD atrophy from early stages. CSF Aβ42 might predict cortical thinning and t-tau/NfL subcortical atrophy.

Abbreviations: AD, Alzheimer's disease; EOAD, early-onset AD; CSF, cerebrospinal fluid; Aβ42, amyloid β1-42; t-tau, total Tau; MRI, magnetic resonance imaging; p-tau, phosphorylated Tau; NfL, neurofilament light chain; LOAD, late-onset AD; NFT, neurofibrillary tangle; MTL, medial temporal lobe; NIA-AA, National Institute on Aging-Alzheimer's Association; GM, gray matter; ADNI, Alzheimer's disease Neuroimaging initiative; HC, healthy controls; HCB, Hospital Clinic Barcelona; MMSE, Mini-Mental State Examination; MCI, mild cognitive impairment; PET, positron emission tomography; CTh, cortical thickness; spc, symmetrized percent change; FWHM, full-width at half maximum; GLM, general linear model; FWE, family-wise error; Bankssts, banks of the superior temporal sulcus.

* Corresponding author at: Alzheimer's Disease and other Cognitive Disorders Unit, Neurology Service, Hospital Clínic, IDIBAPS. Carrer Villarroel, 170, Barcelona 08036, Spain.
E-mail address: allado@clinic.cat (A. Lladó).

[1] These authors contributed equally to this work.

[2] Some of the data used in this study were obtained from the ADNI database (www.loni.ucla.edu/ADNI). As such, the investigators within the ADNI contributed to the design and implementation of ADNI and/or provided data but did not participate in analysis or writing of this report. A complete listing of ADNI investigators is available at: www.loni.ucla.edu/ADNI/Collaboration/ADNI_Authorship_list.pdf).

https://doi.org/10.1016/j.nicl.2021.102804
Received 19 April 2021; Received in revised form 17 August 2021; Accepted 20 August 2021
Available online 25 August 2021

1. Introduction

According to the arbitrary cut-off age of 65 years, Alzheimer's disease (AD) is classified as early-onset AD (EOAD, aged < 65 years) or late-onset AD (LOAD, aged > 65 years). Both variants share the same pathological landmarks, such as underlying amyloid plaques, neurofibrillary tangles (NFT) and progressive neurodegeneration. However, early-onset presentations might constitute a distinct and more severe variant of AD (Mendez, 2012) in which AD-pathology distributes differently. While the limbic areas are predominantly affected in LOAD, EOAD patients show a higher burden of NFT in neocortical regions (Marshall et al., 2007; Murray et al., 2011).

These neuropathological features go along with higher rates of non-amnestic symptoms (Koedam et al., 2010) and faster cognitive decline in EOAD (Wattmo and Wallin, 2017). On the other hand, cross-sectional studies using magnetic resonance imaging (MRI) reveal a pattern of widespread atrophy in EOAD particularly marked in parietal areas, whereas in LOAD, atrophy is restricted to temporal regions (Aziz et al., 2017; Harper et al., 2017; Möller et al., 2013; Ossenkoppele et al., 2015a). Longitudinal MRI studies suggest that, in EOAD, the associative cortices are more vulnerable to atrophy than the medial temporal lobe (MTL), and that the atrophy rates are faster than those in LOAD (Cho et al., 2013a; Fiford et al., 2018; Joie et al., 2020; Migliaccio et al., 2015). However, the conclusions drawn by prior studies regarding a specific pattern of longitudinal atrophy for EOAD are not clear as many of them include subjects in whom the clinical diagnosis of AD was not supported by the use of biomarkers or who were not obtained from specific EOAD cohorts.

In 2018, the National Institute on Aging-Alzheimer's Association (NIA-AA) Research Framework redefined the AD continuum in terms of three groups of biomarkers: amyloid (A), tau (T) and neurodegeneration (N) (Jack et al., 2018), namely the ATN profile. The ATN profile can be evaluated through neuroimaging or biofluids (e.g. cerebrospinal fluid (CSF)). In this context, longitudinal patterns of progressive atrophy could help to identify regions of early neurodegeneration in EOAD, in whom the MTL seems to not optimally reflect the spread of the disease (Falgàs et al., 2019; Murray et al., 2011).

There is a poor understanding of how longitudinal changes in MRI interact with other biomarkers, especially in EOAD. Similar to LOAD patients, the presence of low levels of CSF amyloid-β1-42 (Aβ42) with high levels of phosphorylated Tau (p-tau) and total Tau (t-tau) define the diagnosis in EOAD (Jack et al., 2018; McKhann et al., 2011). Some studies have suggested that baseline CSF Tau and neurofilament light chain (NfL) levels could predict longitudinal atrophy in AD (Fjell et al., 2010; Tarawneh et al., 2015; Zetterberg et al., 2016), and baseline Aβ42 levels have been previously correlated with the pattern of atrophy in EOAD (Falgàs et al., 2020; Ossenkoppele et al., 2015b).

In this prospective study, we aim to describe the pattern of progressive atrophy in a well-characterized EOAD cohort over two years. We hypothesized that the longitudinal cortical loss in EOAD would follow a posterior gradient of cortical thinning and that the subcortical gray matter (GM) loss would extend beyond MTL structures. Secondly, we aim to define the relationship between baseline CSF levels of Aβ42, p-tau, t-tau and NfL, and the longitudinal rates of atrophy in EOAD. To confirm our results, we additionally analyze these parameters in EOAD and LOAD subjects from the Alzheimer's disease Neuroimaging Initiative (ADNI) database.

2. Methods

2.1. Participants

2.1.1. Discovery sample: Hospital Clínic of Barcelona cohort

We selected EOAD patients and age-matched healthy controls (HC) from a prospective cohort collected at the "Alzheimer's disease and Other Cognitive Disorders Unit" in Hospital Clínic, Barcelona (HCB). Participants met the following inclusion criteria: having two available 3 T-MRI scans (one at baseline and one after 2 years), Mini Mental State Examination (MMSE) >= 15, available CSF biomarkers levels and multiple clinical and neuropsychological evaluations. Subjects with previous psychiatric or neurological conditions, autosomal dominant pattern of AD inheritance or gross brain pathology (i.e., stroke, tumor) were excluded. According to clinical and biomarker data (Jack et al., 2018), participants were classified in two groups:

- EOAD-HCB (N = 12): EOAD patients with AD core CSF biomarkers levels in the range suggesting the presence of AD neuropathology (A + T +) with neurodegeneration (N +). Patients also fulfilled NIA-AA diagnostic criteria for mild cognitive impairment (MCI) due to AD with high likelihood, or AD mild dementia with high evidence of AD pathophysiology process (Albert et al., 2011; McKhann et al., 2011). All subjects that fulfilled the inclusion criteria in this study presented an amnestic or multidomain neuropsychological profile at the time of the first MRI.
- HC (N = 19): research volunteers with cognitive performance within normative range and normal CSF levels of core AD biomarkers (A-T-N-).

This study was approved by HCB Ethics Committee and all the individuals gave written informed consent for their clinical data to be used for research purposes.

2.1.2. Replication sample: Alzheimer's disease Neuroimaging initiative (ADNI) cohort

To further investigate the interaction between CSF biomarkers levels and progressive GM loss, as well as a possible influence of age, we used two groups of patients obtained from the ADNI GO/2 database (adni.loni.usc.edu). The ADNI was launched in 2003 as a public–private partnership, led by Principal Investigator Michael W. Weiner, MD, with a primary goal to test whether different biomarkers can be combined to measure the progression of MCI and early AD. For up-to-date information, see www.adni-info.org.

The selection criteria for the EOAD-ADNI and LOAD-ADNI samples were identical to those of our discovery sample: a baseline diagnosis of MCI/AD, two 3 T-MRI scans with appropriate quality (baseline and at 2 years point), MMSE >= 15 and available CSF biomarkers at baseline. We selected patients with an A + T + N + profile in CSF and we excluded those with discordant Florbetapir-PET information. We included subjects < 65 years in the EOAD group (EOAD-ADNI: N = 14) and subjects >=75 years in the LOAD group (LOAD-ADNI: N = 55), to avoid a potential overlap between groups. In addition, we used available information in ADNI regarding CSF biomarkers rate of change at two years and baseline Florbetapir-PET Standardized Uptake Value Ratio (SUVR).

2.2. Cerebrospinal fluid biomarkers and APOE genotype

For the discovery cohort, all CSF samples were collected before the MRI scan except for one patient in EOAD-HCB and five subjects in HC. We used commercially available single-analyte enzyme-linked immunosorbent assay (ELISA) to determine levels of CSF Aβ42, p-tau, t-tau (INNOTEST, Fujirebio Europe N.V., Gent, Belgium) and Nfl. (IBL International, Hamburg, Germany). CSF samples in the ADNI cohort were collected after first MRI scan. Details regarding the CSF samples in the ADNI cohort are described elsewhere (Shaw et al., 2009). For the discovery cohort, we used the CSF Aβ42 (A), p-tau (T) and t-tau (N) cut-off values determined by our laboratory (Antonell et al., 2020). For the ADNI cohort, we used pre-defined cut-off points (Aβ42 < 980 pg/mL, p-tau > 21.8 pg/dl and t-tau > 245) to determine the ATN status.

APOE genotype was determined through the analysis of rs429358 and rs7412 by Sanger sequencing in the discovery cohort. *APOE* genotyping in ADNI has been outlined previously (Risacher et al., 2010). APOE status was analyzed according to the presence or absence of at

least one *APOE* ε4 allele.

2.3. Imaging acquisition

A 3 T Magnetom Trio Tim scanner (Siemens Medical Systems, Germany) at Hospital Clínic was used to collect the MR data of the discovery sample. A high-resolution 3D structural data set (T1-weighted, MP-RAGE, repetition time = 2,300 ms, echo time = 2.98 ms, 240 slices, field-of- view = 256 mm, voxel size = 1 × 1 × 1 mm) was acquired for all subjects at each time point. The ADNI brain MRI and Florbetapir-PET protocols have been reported in detail elsewhere (Jack et al., 2008; Landau et al., 2013).

2.4. Imaging processing

For the discovery sample, we first performed cortical reconstruction and volumetric segmentation of MRI scans using the longitudinal stream in FreeSurfer 6.0 (http://surfer.nmr.mgh.harvard.edu/). It creates a specific subject template in order to minimize the bias between time-points, leading to good reliability and reproducibility scores (Reuter et al., 2012). All the images in this study were visually inspected and manually corrected when needed.

Using the FreeSurfer longitudinal stream, we obtained cortical thickness (CTh) maps and subcortical volumes at each time-point. We used the symmetrized percent change (spc) to evaluate longitudinal changes in CTh, calculated as the rate of thickness change (CTh at time2 – CTh at time1) divided by the average thickness ((CTh at time2 + CTh at time1)/2). Before statistics, all CTh maps were registered to a common space and smoothed using a full-width at half maximum (FWHM) kernel of 15 mm. In addition, we obtained global CTh measures for each hemisphere (mean CTh across all the vertices) and summary measures within the atlas-based parcellations available in FreeSurfer (34 cortical regions in each hemisphere) (Desikan et al., 2006).

For the subcortical structures, we obtained volumetric measures at baseline and at two years for the 23 atlas-based subcortical GM regions available (Seidman et al., 1997) and we calculated the spc, using the same method described for the CTh maps.

For the replication samples, we downloaded the summary table of longitudinal measurements for subcortical volumes and CTh, which have been calculated within the ADNI pipeline. We calculated the spc at two years point as previously described. In addition, we downloaded the summary table of SUVR calculations for amyloid-PET.

2.5. Statistical analysis demographics, clinical data and CSF biomarkers levels

To compare differences between groups at baseline, the Mann-Whitney *U* test was used for continuous variables and the Fisher's exact tests for the sex and *APOE* ε4 distributions. In addition, we performed a cross-correlation correlation analysis between the CSF biomarkers levels in each of the different AD samples. All the statistical analyses were conducted using R version 4.0.2 (http://www.R-project.org/)

2.6. Cortical thickness analysis

For the discovery sample (EOAD-HCB), we used tools available in FreeSurfer to obtain vertexwise differences between groups, using different general linear model (GLM) designs. We obtained group CTh differences at baseline, as well as differences in CTh spc maps, using age and sex as covariates. Information on baseline atrophy was included to describe which regions were preserved or atrophied at baseline and presented (or not) atrophy over two years. All maps were corrected for multiple comparisons using a permutation-based method, as implemented in Freesurfer. This method corrects for family-wise error (FWE) while accounting for the distribution of the data using Monte Carlo permutations at the cluster level. Significance level for the group differences was set at $p < 0.01$. In addition, we used global CTh measures for each hemisphere and atlas-based parcellations to further study cortical differences across groups, using Mann-Whitney *U* test. To better compare our results across cohorts, and to explore a possible bias results towards regions that might have severe atrophy at baseline, we also studied differences in longitudinal cortical loss across groups using the rate of change (CTh at time2 - CTh at time1/Time 2 - Time 1).

Within the EOAD-HCB group, we performed correlations between initial CSF biomarker levels (Aβ42, p-tau, t-tau, and NfL) and whole CTh spc maps. The resulting correlation maps were corrected for multiple comparisons as stated above and thresholded at $p < 0.05$. After the correlation analysis between the spc map and the initial CSF levels, we used Spearman's coefficients to correlate separately the spc of the regions that were identified in the previous clusters and the corresponding levels of CSF biomarkers (for interpretation purposes). We then correlated separately the spc of these regions with CSF biomarker levels in the EOAD-ADNI and the LOAD-ADNI groups. In addition, to better understand this relationship, we performed the same analysis using the measures of the regions that showed atrophy in EOAD-HCB at baseline. We also correlated CTh spc with initial CSF biomarkers levels using the full sample of EOAD-HCB and HC subjects in the analysis. Finally, we performed a cross-correlation analysis between the CSF biomarkers in the different AD samples. Since we found differences between the interval between the first MRI and the lumbar puncture in EOAD-HCB, EOAD-ADNI and LOAD-ADNI, we tested a possible influence of this interval in CSF levels or the spc decline.

2.7. Subcortical volume analysis

For the discovery sample, we used the Mann-Whitney *U* test to calculate group differences in volume at the time of the first scan and the differences in spc longitudinally. For volume analyses, significance level was set at $p < 0.002$, which was the result of adjusting an initial p level of 0.05 to account for all the independent tests assessed, according to the Bonferroni criteria for multiple comparisons correction. In addition, we repeated the cross-sectional analysis after intracranial volume adjustment. The longitudinal analysis for subcortical GM loss was also repeated using the rate of change as previously described.

We then used Spearman's coefficients to correlate initial CSF biomarker levels and the spc in the structures that showed significant longitudinal atrophy. Later, we repeated the analysis using the previously identified significant regions but in the ADNI cohort. Also, the volume of the structures that exhibited baseline atrophy was correlated with initial biomarkers level and the spc was correlated including EOAD-HCB and HC in a single correlation analysis. The influence of the interval between MRI scan and lumbar puncture in spc was also investigated.

3. Results

3.1. EOAD-HCB cohort: Baseline demographics, clinical data and CSF biomarkers levels

Demographics, MMSE scores, *APOE* genotype and CSF biomarkers levels are shown in Table 1. As expected from the groups' conformation, EOAD-HCB presented lower Aβ42 and higher t-tau, p-tau and NfL levels and scored worse in MMSE than HC. There were no differences between groups in age at the first MRI scan, time between scans, time between the first MRI scan and the lumbar puncture, sex or *APOE* ε4 status. In addition, we found that higher levels of Aβ42, p-tau and NfL correlated with higher levels of t-tau in EOAD-HCB. P-tau also correlated with NfL ($p < 0.05$, Supplementary Fig. 1).

Table 1
Demographic, clinical characteristics, and CSF biomarkers levels for groups included in analysis.

Variable	EOAD-HCB	HC	EOAD-ADNI	LOAD-ADNI
N	12	19	14	55
Female/Male	8/4	16/3	8/6	24/31
Age at onset, years	57.25(4.86)	N/A	NE	NE
Age at first MRI, years	60.64 (4.58)	57.96 (4.68)	60.7 (3.38)	79.41 (3.45)‡
Time to second MRI, years	1.99 (0.17)	2.02 (0.25)	2.06 (0.1)†	2.08 (0.09)‡
Time between MRI and CSF, years	0.66 (1.17)	1.15 (1.05)	0.13 (0.13)†	0.08 (0.05)‡
APOE ε4 carriers/ non carriers	3/9	3/16	13/1†	21/34‡
MMSE, mean	20.83 (3.43)*	29.27 (1.06)	26.07 (3.08)†	26.55 (2.73)‡
Aβ42, mean pg/mL	387.65 (73)*	892.26 (217.88)	653.14 (181.43)	674.72 (166.85)
p-tau, mean pg/mL	103.65 (24.29)*	53.27 (11.20)	45.18 (15.21)	37(16.5)
t-tau, mean pg/mL	740.28 (282.44)*	227.29 (50.91)	438.89 (127.25)	364.54 (145.53)
NfL, mean pg/mL	914.94 (219)*	416.50 (109.12)	NE	NE

NOTE. Data are presented as mean (standard deviation). *$p < 0.05$ for the comparisons between EOAD-HCB and HC; †$p < 0.05$ for the comparisons between EOAD-HCB and EOAD-ADNI; ‡$p < 0.05$ for the comparisons between EOAD-HCB versus LOAD-ADNI. Abbreviations: EOAD, early-onset AD; HCB, Hospital Clinic; HC, healthy controls; LOAD, late-onset AD; N/A, not applicable; NE, not evaluated; MRI, Magnetic resonance imaging; CSF; cerebrospinal fluid; MMSE, Mini-Mental State Examination; Aβ42, amyloid β42; p-tau, phosphorylated tau; t-tau, total tau; NfL, neurofilament light chain.

3.2. EOAD-ADNI cohort: Baseline demographics, clinical data and CSF biomarkers levels

Data from the EOAD-ADNI and LOAD-ADNI samples are presented in Table 1. Compared to EOAD-HCB, we found no differences in age at first MRI scan in the EOAD-ADNI, while the LOAD-ADNI group was older, as expected. Compared to EOAD-HCB, EOAD-ADNI and LOAD-ADNI showed differences in MMSE score, proportion of *APOE* ε4 carriers, time between scans and the time between the first MRI scan and the lumbar puncture. No sex differences were found. Higher CSF levels of p-tau correlated with higher t-tau levels in EOAD-ADNI and LOAD-ADNI ($p < 0.05$, Supplementary Fig. 2).

3.3. EOAD-HCB baseline analyses

3.3.1. Cortical thickness

The EOAD-HCB group showed lower CTh than HC in global CTh of left and right hemispheres ($p = 0.00072$ and $p = 0.0042$, respectively), with no differences between them ($p = 0.55$). With the vertex-wise analyses, we found a pattern of reduced CTh in EOAD-HCB compared to HC ($p < 0.01$ cluster-wise corrected, Fig. 1A). These differences comprised the bilateral precuneus, the posterior and isthmus cingulate regions, areas surrounding the temporoparietal junction - including the bilateral supramarginal, the superior and inferior parietal, banks of the superior temporal sulcus (bankssts) - as well as the superior, middle and inferior temporal regions. These differences also extended into the right lateral occipital cortex. However, the EOAD-HCB group did not show differences in CTh in the MTL, the temporal pole or the frontal lobe compared to HC.

When analyzing the CTh of atlas-based parcellations, we found that the bilateral middle temporal, the precuneus and the inferior parietal regions showed the greatest reduction in CTh in EOAD-HCB compared to HC, in addition to the left inferior temporal and left supramarginal (all $p < 0.00074$, Supplementary Table 1).

3.3.2. Subcortical volumes

EOAD-HCB group showed lower volume in bilateral hippocampus and amygdala and greater volume of inferior-lateral ventricles when compared to HC (all $p < 0.002$; Fig. 2A, Supplementary Table 2). Results did not differ after adjusting for total intracranial volume.

3.4. EOAD HCB longitudinal analysis

3.4.1. Longitudinal changes in cortical thickness

EOAD-HCB showed longitudinal cortical thinning in posterior rather than anterior regions compared to HC ($p < 0.01$ cluster-wise corrected; Fig. 1B). Areas affected at baseline continued changing over 2 years and additional longitudinal atrophy was found in the bilateral MTL, including the entorhinal and parahippocampal regions, fusiform, insular, lateral occipital and lingual regions.

Using global CTh measures, we observed greater longitudinal CTh

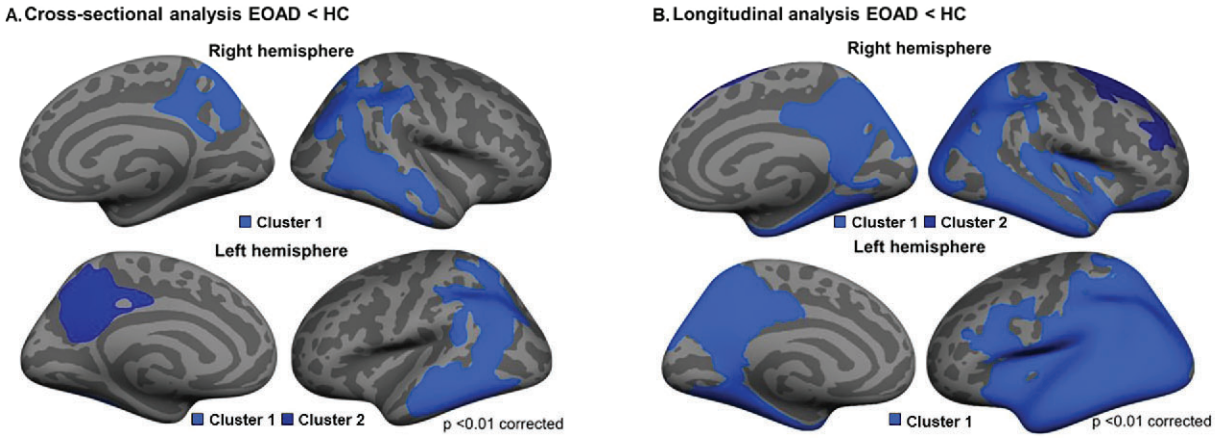

Fig. 1. Vertex-wise maps of the differences between EOAD-HCB and HC in (A) cortical thickness at baseline and (B) cortical thickness spc at two years. Significant clusters of gray matter loss are shown in light and dark blue, EOAD < HC with a corrected $p < 0.01$. The results are represented on the fsaverege model. At baseline (A), the EOAD-HCB participants exhibited lower CTh than HC in three clusters, one in the right hemisphere (size 13,262.72 mm^2) and two in the left hemisphere (light blue 3,182.41 mm^2 and dark blue 1,2555.52 mm^2). At two years (B), EOAD-HCB showed lower spc in three cluster, two in the right hemisphere (dark blue 3,777.76 mm^2 and light blue 30,742.5 mm^2) and one in the left hemisphere (size 44424.55 mm^2). Abbreviations: EOAD, early-onset AD; HCB, Hospital Clinic Barcelona; HC, healthy controls; CTh, cortical thickness; spc, symmetrized percent change. (For interpretation of the references to colour in this figure legend, the reader is referred to the web version of this article.)

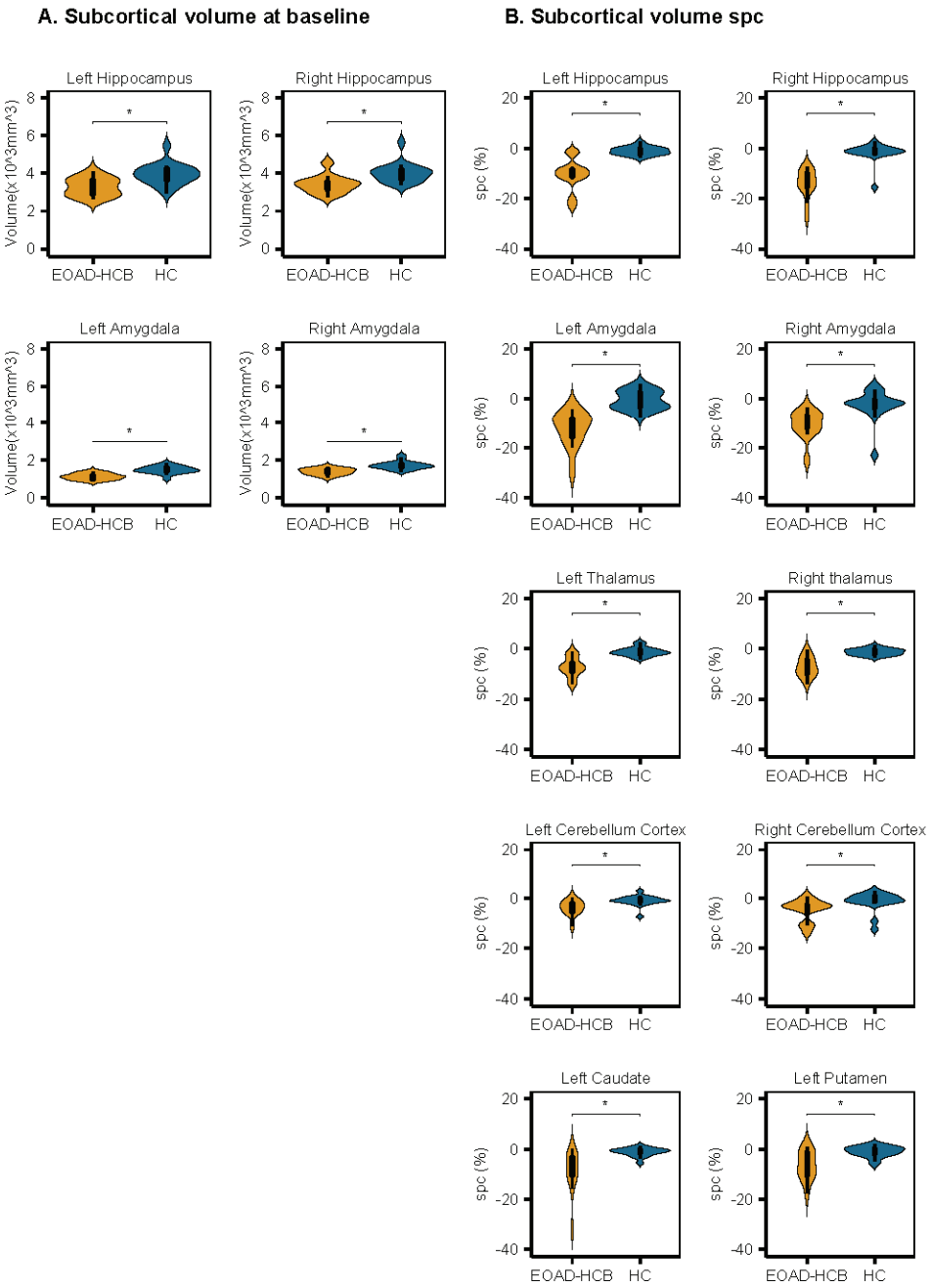

Fig. 2. Significant differences between EOAD-HCB and HC in (A) subcortical gray matter volume at baseline and (B) subcortical volume spc at two years. *p-values < 0.002. Statistical analyses have been performed with Mann-Whitney *U* test and corrected for multiple comparisons with the Bonferroni's method. Abbreviations: EOAD, early-onset AD; HCB, Hospital Clinic Barcelona; HC, healthy controls; spc, symmetrized percent change.

loss in both hemispheres in EOAD-HCB compared to HC ($p < 0.000001$), with no differences between hemispheres ($p = 0.59$). However, we observed asymmetries in the topography of longitudinal atrophy in the spc maps. In the left hemisphere, cortical loss involved language-related areas such as the pars opercularis and the transverse temporal gyri, while right atrophy spread further into the visual cortex (cuneus) and prefrontal areas. Compared to HC, the greatest rates of cortical thinning in EOAD-HCB were found in the bilateral entorhinal, right fusiform, left precuneus and bilateral parahippocampal regions (all $p < 0.00074$; Table 2, Supplementary Table 3). When using the rate of change as measure of longitudinal CTh loss results did not change (all $p < 0.00074$, Supplementary Table 4).

3.4.2. *Symmetrized percent change in subcortical volume*

In two years, the EOAD-HCB group showed volume loss in regions beyond the MTL, including the bilateral hippocampus, amygdala, thalamus, cerebellum GM, and left caudate and putamen regions. This loss was accompanied by a bilateral enlargement in the lateral and inferior-lateral ventricles (all $p < 0.002$, Bonferroni-corrected; Fig. 2B, Supplementary Table 5). The greatest reductions were observed in the bilateral hippocampus, amygdala, thalamus and left caudate regions (Table 2). Using the rate of change instead of the spc, the subcortical regions that exhibited longitudinal atrophy remained the same (all $p < 0.002$, Supplementary Table 6), except the left pallidum ($p = 0.0025$).

Table 2
Symmetrized percent change (%) of regions that exhibited greater longitudinal atrophy.

Region	EOAD-HCB	HC	p value
Right entorhinal	−12.5(4.3)	−0.4(2.9)	0.00000005
Left entorhinal	−12.1(5.3)	−0.6(1.9)	0.00000003
Right fusiform	−8.9(4.7)	−0.1(1.8)	0.00000009
Left precuneus	−8.6(4.5)	−0.7(2.2)	0.00000032
Right parahippocampal	−8.5(6.4)	0.1(1.8)	0.000011
Left parahippocampal	−8.2(4.2)	0(2.5)	0.0000048
Right hippocampus	−14(5.9)	−1.5(3.7)	0.000001
Left Amygdala	−12.3(7.3)	−0.5(3.8)	0.0000002
Left hippocampus	−10.4(6.3)	−1(1.7)	0.0000084
Right amygdala	−10.4(5.8)	−2.2(6)	0.0000184
Left Caudate	−8.9(8.8)	−1.2(1.6)	0.0002964
Left Thalamus	−7.3(3.9)	−1.2(1.7)	0.0000084
Right thalamus	−7.3(3.9)	−1.3(1.3)	0.0000064

NOTE. Data are presented as mean (standard deviation). Abbreviations: EOAD, early-onset AD; HCB, Hospital Clinic; HC, healthy controls. Additional information can be found in Supplementary.

3.5. Correlation between baseline and longitudinal GM changes and initial CSF biomarkers

3.5.1. Baseline and longitudinal CTh changes and initial CSF biomarkers in EOAD-HCB cohort

At baseline, no correlations were found between the regions that exhibited cortical loss and the CSF biomarkers levels in EOAD-HCB ($p > 0.05$). At two years, initial CSF Aβ42 levels showed a negative correlation with longitudinal CTh loss in areas of the right hemisphere (corrected $p < 0.05$; Fig. 3A). CSF p-tau, t-tau or NfL levels did not yield any significant results ($p > 0.05$).

High levels of Aβ42 in EOAD patients correlated with accelerated cortical thinning in two clusters, covering the right superiorparietal, precuneus, lingual and isthmus cingulate cortices (cluster 1: $\rho = -0.85$); and the right precuneus, posterior cingulate and paracentral cortices (cluster 2: $\rho = -0.83$). When we studied the spc within these regions, as obtained with the atlas-based measures, high CSF Aβ42 levels in EOAD-HCB correlated with faster cortical thinning in the right precuneus ($\rho = -0.78$, $p = 0.0047$) and superior parietal regions ($\rho = -0.59$, $p = 0.049$) (Fig. 3B).

In addition, when including EOAD-HCB and HC subjects in a single correlation analysis, we found that baseline levels of CSF biomarkers (Aβ42, t-tau, p-tau, NfL) correlated with the CTh spc measures in the majority of cortical regions. In this case, higher CSF Aβ42 levels were correlated with less atrophy over two years in all regions that showed longitudinal atrophy, except left cuneus and left putamen; higher t-tau, p-tau and NfL levels were correlated with higher longitudinal atrophy in all regions (all $p < 0.05$, Supplementary Table 7).

3.5.2. Baseline and longitudinal changes in subcortical volumes and initial CSF biomarkers in EOAD-HCB cohort

In EOAD-HCB, higher initial CSF NfL levels were correlated with higher volume of the left lateral ventricle at baseline ($\rho = 0.59$, $p = 0.049$; Supplementary Fig. 3). In contrast, higher baseline CSF t-tau levels correlated with greater volume loss over two years in left amygdala ($\rho = -0.601$, $p = 0.042$; Fig. 3B ($\rho = 0.59$, $p = 0.049$; Supplementary Fig. 3). CSF Aβ42 or p-tau levels did not showed any significant correlation with baseline measures or longitudinal atrophy. On the other hand, when including EOAD-HCB and HC in the analysis, initial CSF biomarkers correlated with longitudinal atrophy. As expected, higher CSF Aβ42 were correlated with less atrophy over two years, except left putamen; higher t-tau levels were correlated with higher longitudinal atrophy in all the regions except left caudate; higher p-tau levels were correlated with higher longitudinal atrophy except left cerebellum cortex; higher NfL were correlated with higher longitudinal atrophy in all the regions (all $p < 0.05$, Supplementary Table 8).

3.5.3. Longitudinal GM changes and initial CSF biomarkers in ADNI cohort

In EOAD-ADNI but not in LOAD-ADNI, higher CSF Aβ42 levels at baseline correlated with accelerated cortical loss over the next two years in the right precuneus ($\rho = -0.6$, $p = 0.026$) and right superior parietal regions ($\rho = -0.54$, $p = 0.048$) (Fig. 3B). In contrast, we found that high CSF t-tau values at baseline correlated with greater volume loss in the left amygdala in LOAD-ADNI ($\rho = -0.374$, $p = 0.0051$; Fig. 3B), but not in EOAD-ADNI.

The available 18F-AV-45 (Florbetapir) PET SUVR in right precuneus and superior parietal regions, parietal lobes and whole brain did not correlated with the atrophy rates of the above regions in EOAD-ADNI ($n = 14$, Supplementary Table 9). In EOAD-ADNI ($n = 8$), the annualized rate of change in CSF Aβ42 levels (mean = -30.6, standard deviation = 61.8) did not show significant correlation with right precuneus or superiorparietal spc. Furthermore, the CSF t-tau annualized rate of change (mean = 3.9, standard deviation = 28) was also not correlated with left amygdala ($p > 0.05$) in LOAD-ADNI ($n = 33$). No significant correlations were observed between the interval between the first MRI and the lumbar puncture and CSF levels or spc decline, neither in EOAD-HCB nor in EOAD-ADNI/LOAD-ADNI ($p > 0.05$).

4. Discussion

We performed a prospective 3T-MRI study to track CTh and GM volume changes in EOAD. First, we analyzed the pattern of initial atrophy in EOAD to describe which regions were preserved or atrophied at baseline and which presented longitudinal atrophy. We showed that posterior cortices, together with the hippocampus and the amygdala, were the most affected regions at the time of diagnosis. The longitudinal analysis at 2 years showed that progressive atrophy spreads throughout the neocortex with a posterior-to-anterior gradient and beyond the initial subcortical structures. Finally, we observed that, within the pathological range, initial CSF Aβ42 levels closer to the to the normality threshold were associated with accelerated cortical loss in posterior regions in EOAD whereas higher baseline t-tau levels correlated with greater rates of volume loss in MTL subcortical structures in EOAD and LOAD samples.

At baseline, we described lower CTh in EOAD in the bilateral parietal, precuneus, and posterior cingulate as well as in the lateral temporal lobes and right occipital cortices. Previous cross-sectional MRI studies have also found widespread brain atrophy in EOAD, particularly in parietotemporal areas when compared to LOAD (Aziz et al., 2017; Falgàs et al., 2020; Harper et al., 2017; Möller et al., 2013; Ossenkoppele et al., 2015a). We found that the thickness of the entorhinal and parahippocampal cortices was preserved at the time of diagnosis, in consonance with studies describing greater pathological burden (Murray et al., 2011; Whitwell et al., 2012) and greater Tau deposit outside the MTL at younger ages (Joie et al., 2020; Schöll et al., 2017). In addition, our results describing lower volumes in the hippocampus and amygdala in EOAD also agree with previous studies on subcortical structures (Cavedo et al., 2014; van de Pol et al., 2006).

Amyloid deposits are first observed in the isocortex and then in subcortical structures while NFTs accumulate in the MTL before neocortical involvement (Braak and Braak, 1991; Hyman et al., 2012). We found that EOAD patients show atrophy in isocortical areas whereas the entorhinal/parahippocampal cortices were spared at early stages. This suggests a specific pattern of atrophy for patients with EOAD in which the MTL might be less influenced by other processes associated with aging (Savva et al., 2009). The posterior-to-anterior gradient is consistent with previous longitudinal MRI studies analyzing structural changes according to age at onset (Fiford et al., 2018; Joie et al., 2020; Thijssen et al., 2020). In subjects without biomarkers characterization, Cho et al. found cortical loss throughout the cortex over three years (Cho et al., 2013a) whereas Migliaccio et al. found that volume loss spread from the hippocampus and parietotemporal cortices to the precuneus and isthmus cingulate regions, and the MTL cortices were spared over

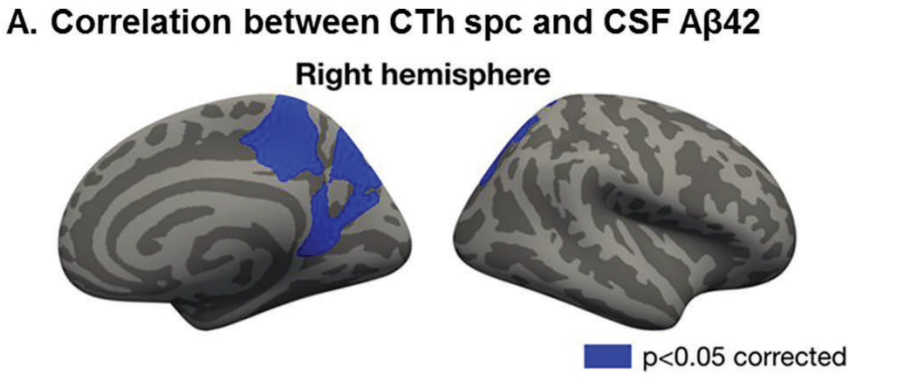

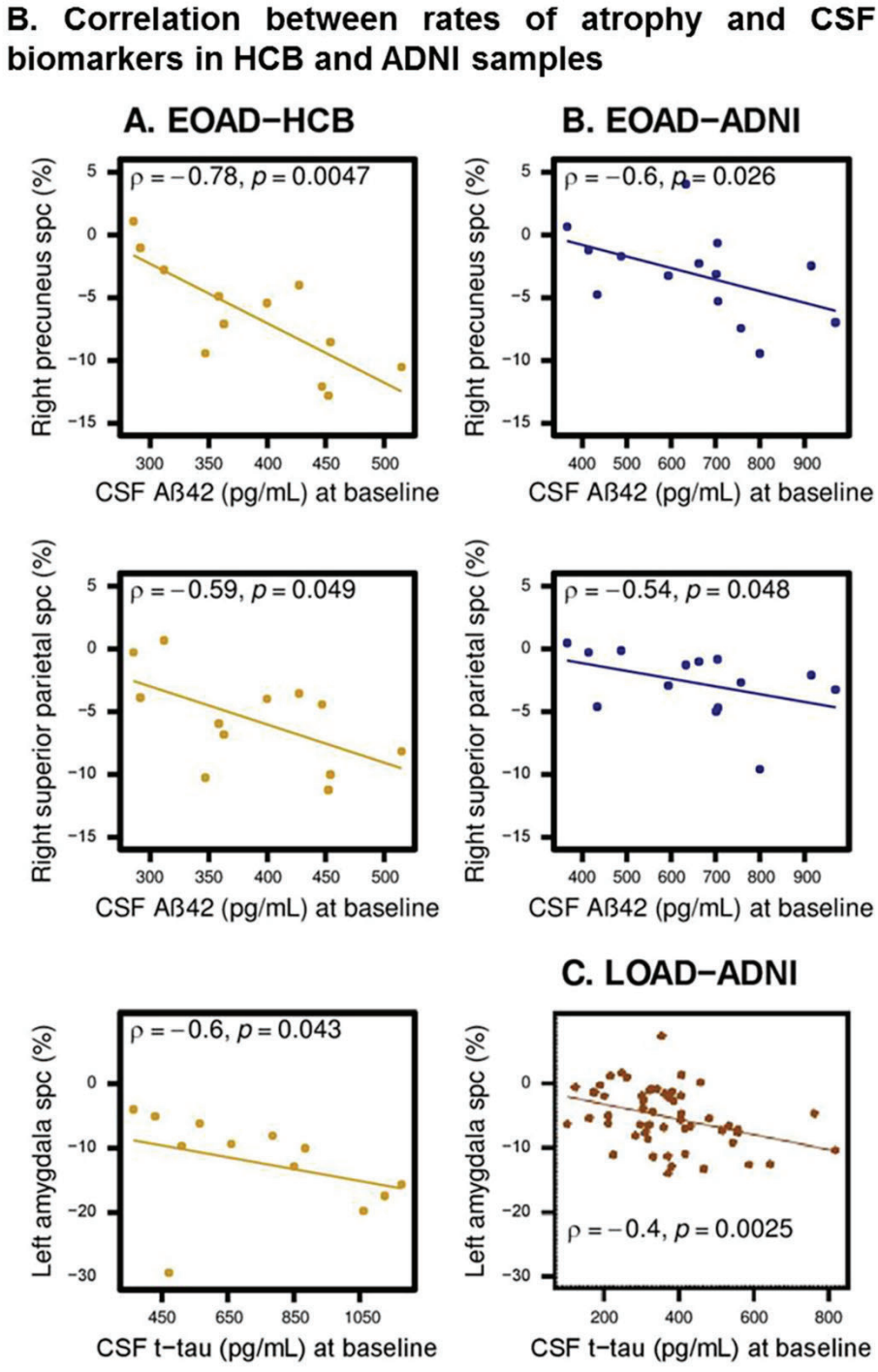

Fig. 3. (A) Vertex-wise maps of correlations between the cortical thickness spc and baseline cerebrospinal fluid Aβ42 levels in EOAD-HCB ($p < 0.05$ cluster-wise corrected; cluster1 size = 3461.18 mm^2; cluster2 size = 1891.24 mm^2). (B) Significant correlations between the regional rates of gray matter atrophy in EOAD-HCB, EOAD-ADNI and LOAD-ADNI and the baseline cerebrospinal fluid biomarkers levels. Abbreviations: CTh, cortical thickness; spc, symmetrized percent change; Aβ42, amyloid β42; EOAD, early-onset AD; HCB, Hospital Clinic Barcelona; ADNI, Alzheimer's disease neuroimaging initiative; t-tau, total tau.

one year (Migliaccio et al., 2015). Volume loss in subcortical structures beyond the MTL is in line with previous reports (Cho et al., 2013b; Fiford et al., 2018) and some authors even suggest specific pathomechanisms for subcortical atrophy in EOAD (Lee et al., 2020).

Although the MTL presented the greatest rates of CTh and subcortical GM loss at the longitudinal level, atrophy was only detectable in subcortical structures at the time of diagnosis. The precuneus, isthmus cingulate, and lateral parietotemporal regions had reduced CTh at the time of the diagnosis and accelerated cortical loss over two years. Here, we reinforce the idea that the posterior associative regions might better capture cortical loss in EOAD than the MTL (Hamelin et al., 2015). The precuneus and posterior cingulate are early sites of amyloid deposition and had been implicated in changes of the default mode network at early AD phases (Palmqvist et al., 2017). In addition to an age effect, the more focally posterior GM changes in the neocortex could be influenced by the low number of *APOE* ε4 carriers in our cohort (Mattsson et al., 2018).

Higher CSF Aβ42 levels, within pathological range, were associated with faster cortical loss in precuneus and superior parietal cortices in the two EOAD cohorts, but not in LOAD subjects. CSF Aβ42 levels have been related to EOAD GM loss in cross-sectional studies (Falgàs et al., 2020; Ossenkoppele et al., 2015b). Although AD biomarkers of neurodegeneration become abnormal after amyloid biomarkers (Jack et al., 2018), rates of atrophy might accelerate before the conventional thresholds of CSF Aβ42 positivity (Insel et al., 2016). In preclinical stages, transitional CSF Aβ42 values are related to increased CTh in temporoparietal and precuneus regions (Fortea et al., 2011) and a reduction in the rates of brain atrophy is followed by an acceleration of cortical loss once CSF Tau levels increase (Pegueroles et al., 2017). Here, we found a counterintuitive correlation between amyloid and CTh spc for the two EOAD samples. One possible explanation could be that the rates of cortical loss observed in subjects close to the Aβ42 positivity threshold reflect greater inflammation in vulnerable regions due to accelerated deposit of amyloid once levels become abnormal (Kreisl et al., 2013; Ossenkoppele et al., 2012). Amyloid pathology precedes and activates microglia (Parbo et al., 2018) and the dual peak hypothesis of neuroinflammation in AD suggests that an early peak in activated microglia is initially protective, attempting to remove Aβ, whereas a later peak is detrimental (Fan et al., 2017). On the other hand, higher inflammation in medial temporal regions and the hippocampus has been negatively associated with hippocampal volume in [11C]PK11195-PET and MRI studies (Femminella et al., 2016). Here, initial CSF Aβ42 levels might correlate with neuroinflammation in EOAD, predicting an acceleration of atrophy due to activated microglia. In addition, in our cohort, EOAD subjects that exhibited higher pathological levels of Aβ42 also presented higher t-tau levels, maybe suggesting higher degree of neurodegeneration. Our results cannot indicate cause-effect relationships but suggest that amyloid-dependent neurodegeneration might be related to the observed progressive cortical thinning in EOAD subjects. Both EOAD samples showed differences in the proportion of *APOE* carriers and MMSE scores. This suggests that the relationship between CSF Aβ42 levels and the cortical thinning could be observed in EOAD patients with MCI and mild dementia regardless of the *APOE* genotype. Although previous studies have reported a dose-dependent CSF Aβ42 effect in APOE ε4 LOAD patients, the available evidence exploring this effect in EOAD is limited (Kaur et al., 2020). In addition, previous studies have reported that the correlation between amyloid-PET and cortical thickness is typically poor (Whitwell et al., 2018). Although both CSF Aβ42 and amyloid PET are valid biomarkers of brain Aβ-plaque load, our findings, as whole, contribute to highlight the complex relationships at the regional level between atrophy and amyloid biomarkers. Novel image coregistration techniques might improve the sensitivity of the detection of a correlation between amyloid PET and longitudinal atrophy in MRI (Pillai et al., 2020).

We also observed that NfL or t-tau might be associated with subcortical volume loss independently of subjects' age. As previously proposed across the AD continuum (Fjell et al., 2010), we observed that higher t-tau levels at baseline correlated with accelerated atrophy in the left amygdala in EOAD and LOAD, although not replicated in the two EOAD samples. In addition, we observed that higher NfL levels at baseline were related to cross-sectional ventricular enlargement. T-tau/NfL levels have shown low correlation with cortical thickness, regardless of the time interval, and these biomarkers might be more related with other neurodegeneration processes rather than cortical thinning (Boerwinkle et al., 2021). Despite of CSF t-tau and NfL levels represent N biomarkers, t-tau might reflect Aβ42-dependent subcortical atrophy while NfL might indicate neurodegeneration independently of amyloid pathology (Tarawneh et al., 2015; Zetterberg et al., 2016). On the other hand, we found that p-tau was not correlated with MRI atrophy. However, p-tau was highly correlated with t-tau and NfL levels, supporting the notion that p-tau is related with the abnormal phosphorylated state of tau in AD whereas t-tau reflects the intensity of brain damage (Jack et al., 2018). Still, p-tau, and the rest of CSF biomarkers used in this study, correlated with the degree of atrophy over time when EOAD and healthy subjects were analyzed together. Whether CSF biomarkers represent a marker of future atrophy associated with underlying pathology must be assessed in further studies.

Similar to other EOAD studies, our main limitation is the relatively small sample size, which might limit the power to detect further differences in atrophy or correlations between CSF biomarkers and atrophy. For this reason, we replicated the correlation analysis in two independent cohorts. The selection criteria in the ADNI cohort might account for the observed differences between EOAD-ADNI/LOAD-ADNI and EOAD patients in memory clinic setting, exemplified by higher number of *APOE* ε4 + cases and better cognitive status in ADNI. Another strength of our study is the use of CTh measures that may reflect changes more specific to AD than the previous volumetric analysis which are more influenced by the effect of aging or other pathologies on white matter loss (Feczko et al., 2009). Studies in larger EOAD cohorts and selecting preclinical subjects can expand our results and define the sequence of early atrophy.

5. Conclusion

We characterized progressive cortical thinning and subcortical volume loss in biologically well-characterized EOAD patients and young controls. We showed that posterior cortices, hippocampus and amygdala capture better the progressive atrophy in EOAD at early stages than the MTL. Our study narrows the field of brain areas for disease tracking, providing a valuable prior constraint on future hypothesis testing. More research is required to understand age-related mechanisms for atrophy spreading and the relationship between the pattern of atrophy and CSF biomarkers.

CRediT authorship contribution statement

José Contador: Conceptualization, Methodology, Investigation, Formal analysis, Writing – original draft, Visualization, Data curation, Resources. **Agnès Pérez-Millán:** Methodology, Software, Formal analysis, Writing - review & editing. **Adrià Tort-Merino:** Writing - review & editing. **Mircea Balasa:** Writing - review & editing. **Neus Falgàs:** Writing - review & editing. **Jaume Olives:** Writing - review & editing. **Magdalena Castellví:** Writing - review & editing. **Sergi Borrego-Écija:** Writing - review & editing. **Beatriz Bosch:** Writing - review & editing. **Guadalupe Fernández-Villullas:** Writing - review & editing. **Oscar Ramos-Campoy:** Writing - review & editing. **Anna Antonell:** Writing - review & editing. **Nuria Bargalló:** Writing - review & editing. **Raquel Sanchez-Valle:** Writing - review & editing. **Roser Sala-Llonch:** Conceptualization, Methodology, Software, Formal analysis, Investigation, Resources, Writing - review & editing, Visualization, Supervision. **Albert Lladó:** Conceptualization, Methodology, Investigation, Resources, Data curation, Writing - review & editing, Supervision, Funding acquisition, Project administration. : .

Declaration of Competing Interest

The authors declare that they have no known competing financial interests or personal relationships that could have appeared to influence the work reported in this paper.

Acknowledgements

The authors thank patients, their relatives and healthy controls for their participation in the research. This work was supported by Spanish Ministry of Science and Innovation-Instituto de Salud Carlos III and Fondo Europeo de Desarrollo Regional (FEDER), Unión Europea, "Una manera de hacer Europa" [PI19/00449 to Dr. Lladó (AL)] and CERCA Programme/Generalitat de Catalunya. AL also received funding from Departament de Salut - Generalitat de Catalunya (PERIS 2016-2020 SLT008/18/00061). Oscar Ramos received funding from a PFIS grant (FI18/00121), Sergi Borrego from a Rio Hortega grant. (CM18/00028).

Data collection and sharing for this project was funded by the Alzheimer's Disease Neuroimaging Initiative (ADNI) (National Institutes of Health Grant U01 AG024904) and DOD ADNI (Department of Defense award number W81XWH-12-2-0012). ADNI is funded by the National Institute on Aging, the National Institute of Biomedical Imaging and Bioengineering, and through generous contributions from the following: AbbVie, Alzheimer's Association; Alzheimer's Drug Discovery Foundation; Araclon Biotech; BioClinica, Inc.; Biogen; Bristol-Myers Squibb Company; CereSpir, Inc.; Cogstate; Eisai Inc.; Elan Pharmaceuticals, Inc.; Eli Lilly and Company; EuroImmun; F. Hoffmann-La Roche Ltd and its affiliated company Genentech, Inc.; Fujirebio; GE Healthcare; IXICO Ltd.; Janssen Alzheimer Immunotherapy Research & Development, LLC.; Johnson & Johnson Pharmaceutical Research & Development LLC.; Lumosity; Lundbeck; Merck & Co., Inc.; Meso Scale Diagnostics, LLC.; NeuroRx Research; Neurotrack Technologies; Novartis Pharmaceuticals Corporation; Pfizer Inc.; Piramal Imaging; Servier; Takeda Pharmaceutical Company; and Transition Therapeutics. The Canadian Institutes of Health Research is providing funds to support ADNI clinical sites in Canada. Private sector contributions are facilitated by the Foundation for the National Institutes of Health (www.fnih.org). The grantee organization is the Northern California Institute for Research and Education, and the study is coordinated by the Alzheimer's Therapeutic Research Institute at the University of Southern California. ADNI data are disseminated by the Laboratory for Neuro Imaging at the University of Southern California.

Appendix A. Supplementary data

Supplementary data to this article can be found online at https://doi.org/10.1016/j.nicl.2021.102804.

References

Albert, M.S., DeKosky, S.T., Dickson, D., Dubois, B., Feldman, H.H., Fox, N.C., Gamst, A., Holtzman, D.M., Jagust, W.J., Petersen, R.C., Snyder, P.J., Carrillo, M.C., Thies, B., Phelps, C.H., 2011. The diagnosis of mild cognitive impairment due to Alzheimer's disease: Recommendations from the National Institute on Aging-Alzheimer's Association workgroups on diagnostic guidelines for Alzheimer's disease. Alzheimer's & Dementia 7 (3), 270–279.

Antonell, A., Tort-Merino, A., Ríos, J., Balasa, M., Borrego-Écija, S., Auge, J.M., Muñoz-García, C., Bosch, B., Falgàs, N., Rami, L., Ramos-Campoy, O., Blennow, K., Zetterberg, H., Molinuevo, J.L., Lladó, A., Sánchez-Valle, R., 2020. Synaptic, axonal damage and inflammatory cerebrospinal fluid biomarkers in neurodegenerative dementias. Alzheimer's & Dementia 16 (2), 262–272.

Aziz, A.-L., Giusiano, B., Joubert, S., Duprat, L., Didic, M., Gueriot, C., Koric, L., Boucraut, J., Felician, O., Ranjeva, J.-P., Guedj, E., Ceccaldi, M., 2017. Difference in imaging biomarkers of neurodegeneration between early and late-onset amnestic Alzheimer's disease. Neurobiol. Aging 54, 22–30. https://doi.org/10.1016/j.neurobiolaging.2017.02.010.

Boerwinkle, A.H., Wisch, J.K., Chen, C.D., Gordon, B.A., Butt, O.H., Schindler, S.E., Sutphen, C., Flores, S., Dincer, A., Benzinger, T.L.S., Fagan, A.M., Morris, J.C., Ances, B.M., 2021. Temporal Correlation of CSF and Neuroimaging in the Amyloid-Tau-Neurodegeneration Model of Alzheimer Disease. Neurology 97 (1), e76–e87. https://doi.org/10.1212/wnl.0000000000012123.

Braak, H., Braak, E., 1991. Neuropathological stageing of Alzheimer-related changes. Acta Neuropathol 82 (4), 239–259. https://doi.org/10.1007/BF00308809.

Cavedo, E., Pievani, M., Boccardi, M., Galluzzi, S., Bocchetta, M., Bonetti, M., Thompson, P.M., Frisoni, G.B., 2014. Medial temporal atrophy in early and late-onset Alzheimer's disease. Neurobiol. Aging 35 (9), 2004–2012. https://doi.org/10.1016/j.neurobiolaging.2014.03.009.

Cho, H., Jeon, S., Kang, S.J., Lee, J.-M., Lee, J.-H., Kim, G.H., Shin, J.S., Kim, C.H., Noh, Y., Im, K., Kim, S.T., Chin, J., Seo, S.W., Na, D.L., 2013a. Longitudinal changes of cortical thickness in early- versus late-onset Alzheimer's disease. Neurobiol. Aging 34 (7), 1921.e9–1921.e15. https://doi.org/10.1016/j.neurobiolaging.2013.01.004.

Cho, H., Seo, S.W., Kim, J.-H., Kim, C., Ye, B.S., Kim, G.H., Noh, Y., Kim, H.J., Yoon, C. W., Seong, J.-K., Kim, C.-H., Kang, S.J., Chin, J., Kim, S.T., Lee, K.-H., Na, D.L., 2013b. Changes in subcortical structures in early- versus late-onset Alzheimer's disease. Neurobiol. Aging 34 (7), 1740–1747. https://doi.org/10.1016/j.neurobiolaging.2013.01.001.

Desikan, R.S., Ségonne, F., Fischl, B., Quinn, B.T., Dickerson, B.C., Blacker, D., Buckner, R.L., Dale, A.M., Maguire, R.P., Hyman, B.T., Albert, M.S., Killiany, R.J., 2006. An automated labeling system for subdividing the human cerebral cortex on MRI scans into gyral based regions of interest. NeuroImage 31 (3), 968–980. https://doi.org/10.1016/j.neuroimage.2006.01.021.

Falgàs, N., Ruiz-Peris, M., Pérez-Millan, A., Sala-Llonch, R., Antonell, A., Balasa, M., Borrego-Écija, S., Ramos-Campoy, O., Augé, J.M., Castellví, M., Tort-Merino, A., Olives, J., Fernández-Villullas, G., Blennow, K., Zetterberg, H., Bargalló, N., Lladó, A., Sánchez-Valle, R., 2020. Contribution of CSF biomarkers to early-onset Alzheimer's disease and frontotemporal dementia neuroimaging signatures. Hum. Brain Mapp. 41 (8), 2004–2013. https://doi.org/10.1002/hbm.24925.

Falgàs, N., Tort-Merino, A., Balasa, M., Borrego-Écija, S., Castellví, M., Olives, J., Bosch, B., Fernandez-Villullas, G., Antonell, A., Augé, J.M., Lomeña, F., Perissinotti, A., Bargalló, N., Sánchez-Valle, R., Lladó, A., 2019. Clinical applicability of diagnostic biomarkers in early-onset cognitive impairment. Eur. J. Neurol. 26 (8), 1098–1104. https://doi.org/10.1111/ene.13945.

Fan, Z., Brooks, D.J., Okello, A., Edison, P., 2017. An early and late peak in microglial activation in Alzheimer's disease trajectory. Brain 140, 792–803. https://doi.org/10.1093/brain/aww349.

Feczko, E., Augustinack, J.C., Fischl, B., Dickerson, B.C., 2009. An MRI-based method for measuring volume, thickness and surface area of entorhinal, perirhinal, and posterior parahippocampal cortex. Neurobiol. Aging 30 (3), 420–431. https://doi.org/10.1016/j.neurobiolaging.2007.07.023.

Femminella, G.D., Ninan, S., Atkinson, R., Fan, Z., Brooks, D.J., Edison, P., 2016. Does Microglial Activation Influence Hippocampal Volume and Neuronal Function in Alzheimer's Disease and Parkinson's Disease Dementia? JAD 51 (4), 1275–1289. https://doi.org/10.3233/JAD-150827.

Fiford, C.M., Ridgway, G.R., Cash, D.M., Modat, M., Nicholas, J., Manning, E.N., Malone, I.B., Biessels, G.J., Ourselin, S., Carmichael, O.T., Cardoso, M.J., Barnes, J., 2018. Patterns of progressive atrophy vary with age in Alzheimer's disease patients. Neurobiol. Aging 63, 22–32. https://doi.org/10.1016/j.neurobiolaging.2017.11.002.

Fjell, A.M., Walhovd, K.B., Fennema-Notestine, C., McEvoy, L.K., Hagler, D.J., Holland, D., Brewer, J.B., Dale, A.M., 2010. CSF Biomarkers in Prediction of Cerebral and Clinical Change in Mild Cognitive Impairment and Alzheimer's Disease. J. Neurosci. 30 (6), 2088–2101. https://doi.org/10.1523/JNEUROSCI.3785-09.2010.

Fortea, J., Sala-Llonch, R., Bartrés-Faz, D., Lladó, A., Solé-Padullés, C., Bosch, B., Antonell, A., Olives, J., Sanchez-Valle, R., Molinuevo, J.L., Rami, L., 2011. Cognitively Preserved Subjects with Transitional Cerebrospinal Fluid ß-Amyloid 1-42 Values Have Thicker Cortex in Alzheimer's Disease Vulnerable Areas. Biol. Psychiatry 70 (2), 183–190. https://doi.org/10.1016/j.biopsych.2011.02.017.

Hamelin, L., Bertoux, M., Bottlaender, M., Corne, H., Lagarde, J., Hahn, V., Mangin, J.-F., Dubois, B., Chupin, M., de Souza, L.C., Colliot, O., Sarazin, M., 2015. Sulcal morphology as a new imaging marker for the diagnosis of early onset Alzheimer's disease. Neurobiol. Aging 36 (11), 2932–2939. https://doi.org/10.1016/j.neurobiolaging.2015.04.019.

Harper, L., Bouwman, F., Burton, E.J., Barkhof, F., Scheltens, P., O'Brien, J.T., Fox, N.C., Ridgway, G.R., Schott, J.M., 2017. Patterns of atrophy in pathologically confirmed dementias: a voxelwise analysis. J. Neurol. Neurosurg. Psychiatry 88 (11), 908–916. https://doi.org/10.1136/jnnp-2016-314978.

Hyman, B.T., Phelps, C.H., Beach, T.G., Bigio, E.H., Cairns, N.J., Carrillo, M.C., Dickson, D.W., Duyckaerts, C., Frosch, M.P., Masliah, E., Mirra, S.S., Nelson, P.T., Schneider, J.A., Thal, D.R., Thies, B., Trojanowski, J.Q., Vinters, H.V., Montine, T.J., 2012. National Institute on Aging-Alzheimer's Association guidelines for the neuropathologic assessment of Alzheimer's disease. Alzheimer's & Dementia 8 (1), 1–13. https://doi.org/10.1016/j.jalz.2011.10.007.

Insel, P.S., Mattsson, N., Mackin, R.S., Schöll, M., Nosheny, R.L., Tosun, D., Donohue, M. C., Aisen, P.S., Jagust, W.J., Weiner, M.W., 2016. Accelerating rates of cognitive decline and imaging markers associated with β-amyloid pathology. Neurology 86 (20), 1887–1896. https://doi.org/10.1212/WNL.0000000000002683.

Jack Jr., C.R., Bennett, D.A., Blennow, K., Carrillo, M.C., Dunn, B., Haeberlein, S.B., Holtzman, D.M., Jagust, W., Jessen, F., Karlawish, J., Liu, E., Molinuevo, J.L., Montine, T., Phelps, C., Rankin, K.P., Rowe, C.C., Scheltens, P., Siemers, E., Snyder, H.M., Sperling, R., Elliott, C., Masliah, E., Ryan, L., Silverberg, N., 2018. NIA-AA Research Framework: Toward a biological definition of Alzheimer's disease. Alzheimer's & Dementia 14 (4), 535–562. https://doi.org/10.1016/j.jalz.2018.02.018.

Jack, C.R., Bernstein, M.A., Fox, N.C., Thompson, P., Alexander, G., Harvey, D., Borowski, B., Britson, P.J., L. Whitwell, J., Ward, C., Dale, A.M., Felmlee, J.P., Gunter, J.L., Hill, D.L.G., Killiany, R., Schuff, N., Fox-Bosetti, S., Lin, C.,

Studholme, C., DeCarli, C.S., Gunnar Krueger, Ward, H.A., Metzger, G.J., Scott, K.T., Mallozzi, R., Blezek, D., Levy, J., Debbins, J.P., Fleisher, A.S., Albert, M., Green, R., Bartzokis, G., Glover, G., Mugler, J., Weiner, M.W., 2008. The Alzheimer's disease neuroimaging initiative (ADNI): MRI methods. J. Magn. Reson. Imaging 27 (4), 685–691. https://doi.org/10.1002/jmri.21049.

La Joie, R., Visani, A.V., Baker, S.L., Brown, J.A., Bourakova, V., Cha, J., Chaudhary, K., Edwards, L., Iaccarino, L., Janabi, M., Lesman-Segev, O.H., Miller, Z.A., Perry, D.C., O'Neil, J.P., Pham, J., Rojas, J.C., Rosen, H.J., Seeley, W.W., Tsai, R.M., Miller, B.L., Jagust, W.J., Rabinovici, G.D., 2020. Prospective longitudinal atrophy in Alzheimer's disease correlates with the intensity and topography of baseline tau-PET. Sci. Transl. Med. 12 (524), eaau5732. https://doi.org/10.1126/scitranslmed.aau5732.

Kaur, G., Poljak, A., Braidy, N., Crawford, J.D., Lo, J., Sachdev, P.S., 2020. Fluid Biomarkers and APOE Status of Early Onset Alzheimer's Disease Variants: A Systematic Review and Meta-Analysis. JAD 75 (3), 827–843. https://doi.org/10.3233/JAD-200052.

Koedam, E.L.G.E., Lauffer, V., van der Vlies, A.E., van der Flier, W.M., Scheltens, P., Pijnenburg, Y.A.L., 2010. Early-Versus Late-Onset Alzheimer's Disease: More than Age Alone. JAD 19 (4), 1401–1408. https://doi.org/10.3233/JAD-2010-1337.

Kreisl, W.C., Lyoo, C.H., McGwier, M., Snow, J., Jenko, K.J., Kimura, N., Corona, W., Morse, C.L., Zoghbi, S.S., Pike, V.W., McMahon, F.J., Turner, R.S., Innis, R.B., 2013. In vivo radioligand binding to translocator protein correlates with severity of Alzheimer's disease. Brain 136, 2228–2238. https://doi.org/10.1093/brain/awt145.

Landau, S.M., Breault, C., Joshi, A.D., Pontecorvo, M., Mathis, C.A., Jagust, W.J., Mintun, M.A., 2013. Amyloid-β Imaging with Pittsburgh Compound B and Florbetapir: Comparing Radiotracers and Quantification Methods and Initiative for the Alzheimer's Disease Neuroimaging. Soc. Nucl. Med. 54, 70–77. https://doi.org/10.2967/jnumed.112.109009.Amyloid-.

Lee, E.C., Kang, J.M., Seo, S., Seo, H.E., Lee, S.Y., Park, K.H., Na, D.L., Noh, Y., Seong, J. K., 2020. Association of Subcortical Structural Shapes With Tau, Amyloid, and Cortical Atrophy in Early-Onset and Late-Onset Alzheimer's Disease. Front. Aging Neurosci. 12, 1–11. https://doi.org/10.3389/fnagi.2020.563559.

Marshall, G.A., Fairbanks, L.A., Tekin, S., Vinters, H.V., Cummings, J.L., 2007. Early-Onset Alzheimer's Disease Is Associated With Greater Pathologic Burden. J. Geriatr. Psychiatry Neurol. 20 (1), 29–33. https://doi.org/10.1177/0891988706297086.

Mattsson, N., Ossenkoppele, R., Smith, R., Strandberg, O., Ohlsson, T., Jögi, J., Palmqvist, S., Stomrud, E., Hansson, O., 2018. Greater tau load and reduced cortical thickness in APOE ε4-negative Alzheimer's disease: a cohort study. Alzheimer's Res. Ther. 10, 1–12. https://doi.org/10.1186/s13195-018-0403-x.

McKhann, G.M., Knopman, D.S., Chertkow, H., Hyman, B.T., Jack Jr., C.R., Kawas, C.H., Klunk, W.E., Koroshetz, W.J., Manly, J.J., Mayeux, R., Mohs, R.C., Morris, J.C., Rossor, M.N., Scheltens, P., Carrillo, M.C., Thies, B., Weintraub, S., Phelps, C.H., 2011. The diagnosis of dementia due to Alzheimer's disease: Recommendations from the National Institute on Aging-Alzheimer's Association workgroups on diagnostic guidelines for Alzheimer's disease. Alzheimer's & Dementia 7 (3), 263–269. https://doi.org/10.1016/j.jalz.2011.03.005.

Mendez, M.F., 2012. Early-onset Alzheimer's Disease: Nonamnestic Subtypes and Type 2 AD. Arch. Med. Res. 43 (8), 677–685. https://doi.org/10.1016/j.arcmed.2012.11.009.

Migliaccio, R., Agosta, F., Possin, K.L., Canu, E., Filippi, M., Rabinovici, G.D., Rosen, H. J., Miller, B.L., Gorno-Tempini, M.L., Galimberti, D., 2015. Mapping the Progression of Atrophy in Early- and Late-Onset Alzheimer's Disease. JAD 46 (2), 351–364. https://doi.org/10.3233/JAD-142292.

Möller, C., Vrenken, H., Jiskoot, L., Versteeg, A., Barkhof, F., Scheltens, P., van der Flier, W.M., 2013. Different patterns of gray matter atrophy in early- and late-onset Alzheimer's disease. Neurobiol. Aging 34 (8), 2014–2022. https://doi.org/10.1016/j.neurobiolaging.2013.02.013.

Murray, M.E., Graff-Radford, N.R., Ross, O.A., Petersen, R.C., Duara, R., Dickson, D.W., 2011. Neuropathologically defined subtypes of Alzheimer's disease with distinct clinical characteristics: a retrospective study. Lancet Neurology 10 (9), 785–796. https://doi.org/10.1016/S1474-4422(11)70156-9.

Ossenkoppele, R., Cohn-Sheehy, B.I., La Joie, R., Vogel, J.W., Möller, C., Lehmann, M., van Berckel, B.N.M., Seeley, W.W., Pijnenburg, Y.A., Gorno-Tempini, M.L., Kramer, J.H., Barkhof, F., Rosen, H.J., van der Flier, W.M., Jagust, W.J., Miller, B.L., Scheltens, P., Rabinovici, G.D., 2015a. Atrophy patterns in early clinical stages across distinct phenotypes of Alzheimer's disease: Origin and Spread of Atrophy in AD Variants. Hum. Brain Mapp. 36 (11), 4421–4437. https://doi.org/10.1002/hbm.22927.

Ossenkoppele, R., Mattsson, N., Teunissen, C.E., Barkhof, F., Pijnenburg, Y., Scheltens, P., van der Flier, W.M., Rabinovici, G.D., 2015b. Cerebrospinal fluid biomarkers and cerebral atrophy in distinct clinical variants of probable Alzheimer's disease. Neurobiol. Aging 36 (8), 2340–2347. https://doi.org/10.1016/j.neurobiolaging.2015.04.011.

Ossenkoppele, R., Zwan, M.D., Tolboom, N., van Assema, D.M.E., Adriaanse, S.F., Kloet, R.W., Boellaard, R., Windhorst, A.D., Barkhof, F., Lammertsma, A.A., Scheltens, P., van der Flier, W.M., van Berckel, B.N.M., 2012. Amyloid burden and metabolic function in early-onset Alzheimer's disease: parietal lobe involvement. Brain 135 (7), 2115–2125. https://doi.org/10.1093/brain/aws113.

Palmqvist, S., Schöll, M., Strandberg, O., Mattsson, N., Stomrud, E., Zetterberg, H., Blennow, K., Landau, S., Jagust, W., Hansson, O., 2017. Earliest accumulation of β-amyloid occurs within the default-mode network and concurrently affects brain connectivity. Nat Commun 8 (1). https://doi.org/10.1038/s41467-017-01150-x.

Parbo, P., Ismail, R., Sommerauer, M., Stokholm, M.G., Hansen, A.K., Hansen, K.V., Amidi, A., Schaldemose, J.L., Gottrup, H., Brændgaard, H., Eskildsen, S.F., Borghammer, P., Hinz, R., Aanerud, J., Brooks, D.J., 2018. Does inflammation precede tau aggregation in early Alzheimer's disease? A PET study. Neurobiol. Disease 117, 211–216. https://doi.org/10.1016/j.nbd.2018.06.004.

Pegueroles, J., Vilaplana, E., Montal, V., Sampedro, F., Alcolea, D., Carmona-Iragui, M., Clarimon, J., Blesa, R., Lleó, A., Fortea, J., 2017. Longitudinal brain structural changes in preclinical Alzheimer's disease. Alzheimer's & Dementia 13 (5), 499–509. https://doi.org/10.1016/j.jalz.2016.08.010.

Pillai, J.A., Larvie, M., Chen, J., Crawford, A., Cummings, J.L., Jones, S.E., 2020. Spatial patterns of correlation between cortical amyloid and cortical thickness in a tertiary clinical population with memory deficit. Sci. Rep. 10, 1–13. https://doi.org/10.1038/s41598-020-77503-2.

Reuter, M., Schmansky, N.J., Rosas, H.D., Fischl, B., 2012. Within-subject template estimation for unbiased longitudinal image analysis. NeuroImage 61 (4), 1402–1418. https://doi.org/10.1016/j.neuroimage.2012.02.084.

Risacher, S.L., Shen, L.i., West, J.D., Kim, S., McDonald, B.C., Beckett, L.A., Harvey, D.J., Jack Jr., C.R., Weiner, M.W., Saykin, A.J., 2010. Longitudinal MRI atrophy biomarkers: Relationship to conversion in the ADNI cohort. Neurobiol. Aging 31 (8), 1401–1418. https://doi.org/10.1016/j.neurobiolaging.2010.04.029.

Savva, G.M., Wharton, S.B., Ince, P.G., Forster, G., Matthews, F.E., Brayne, C., 2009. Age, Neuropathology, and Dementia. N Engl J Med 360 (22), 2302–2309. https://doi.org/10.1056/NEJMoa0806142.

Schöll, M., Ossenkoppele, R., Strandberg, O., Palmqvist, S., Jögi, J., Ohlsson, T., Smith, R., Hansson, O., 2017. Distinct 18F-AV-1451 tau PET retention patterns in early- and late-onset Alzheimer's disease. Brain 140, 2286–2294. https://doi.org/10.1093/brain/awx171.

Seidman, L.J., Faraone, S.V., Goldstein, J.M., Goodman, J.M., Kremen, W.S., Matsuda, G., Hoge, E.A., Kennedy, D., Makris, N., Caviness, V.S., Tsuang, M.T., 1997. Reduced subcortical brain volumes in nonpsychotic siblings of schizophrenic patients: A pilot magnetic resonance imaging study. Am. J. Med. Genet. - Neuropsychiatr. Genet. 74, 507–514. https://doi.org/10.1002/(SICI)1096-8628(19970919)74:5<507::AID-AJMG11>3.0.CO;2-G.

Shaw, L.M., Vanderstichele, H., Knapik-Czajka, M., Clark, C.M., Aisen, P.S., Petersen, R. C., Blennow, K., Soares, H., Simon, A., Lewczuk, P., Dean, R., Siemers, E., Potter, W., Lee, V.-Y., Trojanowski, J.Q., 2009. Cerebrospinal fluid biomarker signature in Alzheimer's disease neuroimaging initiative subjects. Ann Neurol. 65 (4), 403–413. https://doi.org/10.1002/ana.21610.

Tarawneh, R., Head, D., Allison, S., Buckles, V., Fagan, A.M., Ladenson, J.H., Morris, J.C., Holtzman, D.M., 2015. Cerebrospinal Fluid Markers of Neurodegeneration and Rates of Brain Atrophy in Early Alzheimer Disease. JAMA Neurol. 72 (6), 656. https://doi.org/10.1001/jamaneurol.2015.0202.

Thijssen, E.H., La Joie, R., Wolf, A., Strom, A., Wang, P., Iaccarino, L., Bourakova, V., Cobigo, Y., Heuer, H., Spina, S., VandeVrede, L., Chai, X., Proctor, N.K., Airey, D.C., Shcherbinin, S., Duggan Evans, C., Sims, J.R., Zetterberg, H., Blennow, K., Karydas, A.M., Teunissen, C.E., Kramer, J.H., Grinberg, L.T., Seeley, W.W., Rosen, H., Boeve, B.F., Miller, B.L., Rabinovici, G.D., Dage, J.L., Rojas, J.C., Boxer, A. L., 2020. Diagnostic value of plasma phosphorylated tau181 in Alzheimer's disease and frontotemporal lobar degeneration. Nat. Med. 26 (3), 387–397. https://doi.org/10.1038/s41591-020-0762-2.

van de Pol, L.A., Hensel, A., Barkhof, F., Gertz, H.J., Scheltens, P., van der Flier, W.M., 2006. Hippocampal atrophy in Alzheimer disease: Age matters. Neurology 66 (2), 236–238. https://doi.org/10.1212/01.wnl.0000194240.47892.4d.

Wattmo, C., Wallin, Å.K., 2017. Early- versus late-onset Alzheimer's disease in clinical practice: cognitive and global outcomes over 3 years. Alzheimers. Res. Ther. 9, 70. https://doi.org/10.1186/s13195-017-0294-2.

Whitwell, J.L., Dickson, D.W., Murray, M.E., Weigand, S.D., Tosakulwong, N., Senjem, M.L., Knopman, D.S., Boeve, B.F., Parisi, J.E., Petersen, R.C., Jack Jr, C.R., Josephs, K.A., 2012. Neuroimaging correlates of pathologically defined subtypes of Alzheimer's disease: a case-control study. Lancet Neurology 11 (10), 868–877. https://doi.org/10.1016/S1474-4422(12)70200-4.

Whitwell, J.L., Graff-Radford, J., Tosakulwong, N., Weigand, S.D., Machulda, M.M., Senjem, M.L., Spychalla, A.J., Vemuri, P., Jones, D.T., Drubach, D.A., Knopman, D. S., Boeve, B.F., Ertekin-Taner, N., Petersen, R.C., Lowe, V.J., Jack Jr., C.R., Josephs, K.A., 2018. Imaging correlations of tau, amyloid, metabolism, and atrophy in typical and atypical Alzheimer's disease. Alzheimer's & Dementia 14 (8), 1005–1014. https://doi.org/10.1016/j.jalz.2018.02.020.

Zetterberg, H., Skillbäck, T., Mattsson, N., Trojanowski, J.Q., Portelius, E., Shaw, L.M., Weiner, M.W., Blennow, K., 2016. Association of Cerebrospinal Fluid Neurofilament Light Concentration With Alzheimer Disease Progression. JAMA Neurol 73 (1), 60. https://doi.org/10.1001/jamaneurol.2015.3037.

Supplementary material:

Table 1. Cortical thickness measurements at baseline

Region	LEFT HEMISPHERE					RIGHT HEMISPHERE				
	EOAD-HCB		HC		p value	EOAD-HCB		HC		p value
	CTh (mm)	SD	CTh (mm)	SD		CTh (mm)	SD	CTh (mm)	SD	
Bankssts	2.38	0.19	2.56	0.19	0.0093	2.40	0.19	2.63	0.14	0.0010
Caudal anterior cingulate	2.73	0.20	2.67	0.21	0.7547	2.56	0.15	2.53	0.20	0.8270
Caudal middle frontal	2.52	0.11	2.65	0.10	0.0027	2.51	0.13	2.62	0.12	0.0234
Cuneus	1.94	0.12	1.88	0.12	0.8901	1.99	0.12	1.96	0.12	0.8901
Entorhinal	3.05	0.38	3.49	0.35	0.0021	3.36	0.30	3.62	0.22	0.0090
Fusiform	2.61	0.17	2.78	0.14	0.0037	2.68	0.19	2.81	0.12	0.0202
Inferior parietal	2.27	0.21	2.53	0.12	0.0003	2.30	0.22	2.55	0.10	0.0007
Inferior temporal	2.63	0.17	2.86	0.15	0.0003	2.73	0.17	2.86	0.12	0.0135
Insula	2.93	0.14	2.96	0.15	0.2947	2.86	0.19	2.97	0.14	0.0694
Isthmus cingulate	2.17	0.18	2.31	0.19	0.0217	2.33	0.21	2.36	0.22	0.5081
Latera occipital	2.22	0.22	2.35	0.16	0.0667	2.28	0.22	2.38	0.15	0.1730
Lateral orbitofrontal	2.64	0.15	2.66	0.07	0.4596	2.70	0.15	2.72	0.16	0.3823
Lingual	2.02	0.12	2.00	0.13	0.6177	2.10	0.12	2.06	0.11	0.8470
Medial orbitofrontal	2.34	0.16	2.47	0.09	0.0150	2.45	0.14	2.44	0.11	0.5397
Middle temporal	2.66	0.17	2.93	0.14	0.0001	2.71	0.19	2.96	0.11	0.0001
Parahippocampal	2.65	0.29	2.78	0.27	0.1099	2.74	0.26	2.80	0.16	0.1436
Para central	2.49	0.12	2.48	0.13	0.6329	2.52	0.16	2.55	0.13	0.3132
Pars opercularis	2.58	0.09	2.59	0.10	0.5713	2.55	0.13	2.60	0.13	0.1807
Pars orbitalis	2.69	0.18	2.71	0.19	0.3882	2.77	0.21	2.76	0.15	0.5484
Pars triangularis	2.47	0.15	2.48	0.10	0.3374	2.47	0.14	2.47	0.12	0.5556
Pericalcarine	1.75	0.14	1.69	0.16	0.8633	1.80	0.14	1.76	0.19	0.6771
Postcentral	2.16	0.13	2.24	0.11	0.0524	2.13	0.12	2.21	0.10	0.0322
Posterior cingulate	2.46	0.10	2.48	0.13	0.2517	2.52	0.11	2.46	0.15	0.9063
Precentral	2.62	0.15	2.66	0.12	0.3229	2.55	0.15	2.61	0.14	0.1412
Precuneus	2.26	0.14	2.48	0.12	0.0001	2.30	0.15	2.49	0.12	0.0007
Rostral anterior cingulate	2.74	0.16	2.80	0.14	0.1916	2.95	0.20	2.85	0.15	0.9240
Rostral middle frontal	2.39	0.11	2.46	0.09	0.0265	2.39	0.09	2.42	0.10	0.2205
Superior frontal	2.69	0.08	2.75	0.08	0.0283	2.73	0.09	2.73	0.08	0.4596
Superior parietal	2.20	0.21	2.36	0.12	0.0114	2.14	0.23	2.32	0.11	0.0079
Superior temporal	2.67	0.10	2.80	0.14	0.0060	2.74	0.15	2.85	0.14	0.0293
Supramarginal	2.46	0.12	2.63	0.09	0.0001	2.43	0.15	2.62	0.12	0.0012
Frontal pole	2.69	0.21	2.86	0.29	0.0482	2.73	0.22	2.76	0.17	0.2582
Temporal pole	3.45	0.32	3.79	0.30	0.0021	3.63	0.26	3.88	0.30	0.0098
Transverse temporal	2.43	0.16	2.40	0.20	0.7483	2.51	0.11	2.50	0.19	0.5323
Mean thickness	2.44	0.07	2.55	0.09	0.0007	2.46	0.09	2.55	0.09	0.0042

Abbreviations: CTh, cortical thickness; EOAD, early-onset AD; HCB, Hospital Clinic; HC, healthy controls; bankssts, banks of the superior temporal sulcus; SD, standard deviation.

Table 2. Subcortical gray matter volume measurements at baseline

Region	EOAD-HCB		HC		p value
	Vol (mm^3)	SD	Vol (mm^3)	SD	
Left Hippocampus	3285.5	476.7	3955.4	549.8	0.00071
Left Amygdala	1131.2	169.1	1487.9	199.5	0.00001
Left Thalamus	6681.4	820.1	6890.6	702.3	0.35216
Left Caudate	3271.8	725.8	3381.7	383.9	0.47613
Left Putamen	4420.4	607.2	4425.7	586.8	0.39761
Left Pallidum	1912.8	197.9	1830.0	222.5	0.91150
Left Accumbens area	301.7	111.2	399.1	83.5	0.01272
Left Cerebellum white matter	16165.5	2185.8	15195.8	1797.0	0.91792
Left Cerebellum cortex	50878.4	8162.6	49087.5	4847.2	0.50796
Left lateral ventricle	14495.3	9877.6	11418.9	7765.1	0.14365
Left inferior lateral ventricle	849.1	514.3	388.3	280.1	0.00099
Right Hippocampus	3425.4	481.5	4020.1	510.6	0.00116
Right Amygdala	1398.5	173.1	1721.4	216.2	0.00004
Right Thalamus	6723.7	748.6	6927.0	781.5	0.26765
Right Caudate	3523.4	556.8	3525.7	405.0	0.52387
Right Putamen	4406.2	502.3	4472.6	595.8	0.20578
Right Pallidum	1814.7	214.8	1727.2	162.6	0.94021
Right Accumbens area	459.6	74.8	526.3	97.0	0.03219
Right Cerebellum white matter	15002.1	2418.8	15051.9	2493.9	0.53975
Right Cerebellum cortex	51667.4	8560.7	49923.8	4295.5	0.42871
Right lateral ventricle	12424.5	6479.2	9973.5	6080.8	0.08850
Right inferior lateral ventricle	812.0	733.6	328.4	167.2	0.00116
Brain stem	20002.9	2904.5	19580.9	2023.9	0.73235

Abbreviations: Vol, volume; EOAD, early-onset AD; HCB, Hospital Clinic; HC, healthy controls; SD, standard deviation.

Table 3. Cortical thickness symmetrized percent change (%) at two years

Region	LEFT HEMISPHERE					RIGHT HEMISPHERE				
	EOAD-HCB		HC		p value	EOAD-HCB		HC		p value
	spc (%)	SD	spc (%)	SD		spc (%)	SD	spc (%)	SD	
Bankssts	-8	4.6	-0.4	1.7	0.00000021	-4.5	9	-0.3	2.9	0.00900153
Caudal anterior cingulate	-1.2	3.3	-0.2	2.5	0.30867791	-2.1	5.6	-0.1	2.1	0.12600864
Caudal middle frontal	-5	4.4	0.1	1.8	0.00001426	-3.3	3.6	-0.4	1.7	0.00624418
Cuneus	-2.7	3.4	0.6	3.1	0.00624418	-3	3.6	0.8	2.6	0.00050682
Entorhinal	-12.1	5.3	-0.6	1.9	0.00000003	-12.5	4.3	-0.4	2.9	0.00000005
Fusiform	-7.4	4.9	0.2	1.4	0.00000047	-8.9	4.7	-0.1	1.8	0.00000009
Inferior parietal	-7.3	4.4	-0.4	1.4	0.00000264	-6.2	4.9	0.1	1.4	0.00019260
Inferior temporal	-7.6	4.1	-0.2	1.3	0.00000013	-6	3.9	0.6	1.6	0.00000193
Insula	-4.8	2.1	0.1	2.1	0.00000098	-4.4	4.7	0.4	2.5	0.00029643
Isthmus cingulate	-7.3	4.8	-0.4	2.4	0.00000480	-7.6	5	-0.7	1.2	0.00000264
Latera occipital	-4.4	3.7	0.5	1.8	0.00001837	-4	4.4	1	2.3	0.00050682
Lateral orbitofrontal	-2.9	5.3	0.5	1.4	0.01272157	-3.5	4	-0.3	1.7	0.00706989
Lingual	-3.3	2.1	1	3.4	0.00011211	-5	4.5	0.2	2.9	0.00009107
Medial orbitofrontal	-2.1	8	-0.8	3.5	0.20577542	-2.8	4.5	-0.1	1.9	0.04633203
Middle temporal	-7.9	3.9	0	1.2	0.00000480	-6.4	3.7	-0.2	1.1	0.00000358
Parahippocampal	-8.2	4.2	0	2.5	0.00000480	-8.5	6.4	0.1	1.8	0.00001100
Para central	-2.4	4.1	0.3	4	0.02925895	-2.3	6.2	1.4	3.2	0.03219154
Pars opercularis	-3.8	3.9	0.4	1	0.00002350	-1.3	3	0	2	0.13463717
Pars orbitalis	-2.6	5	-0.5	2.2	0.03535338	-3.2	4.3	0.4	2	0.00157417
Pars triangularis	-2.1	3.5	-0.3	1.9	0.08849631	-0.8	2.6	0.2	1.6	0.22947857
Pericalcarine	-2.5	5.1	1.1	5.5	0.03875665	-3.6	7.1	0.2	4.9	0.07601140
Postcentral	-3.6	2.6	0.4	1.3	0.00000840	-1.7	3.1	0.3	1.9	0.02925895
Posterior cingulate	-3.8	3.8	-0.3	2	0.00323799	-3.3	4.2	0.1	1.4	0.00244638
Precentral	-2	3.1	1	1.9	0.00135140	-0.7	4.4	0.5	2.1	0.08208077
Precuneus	-8.6	4.5	-0.7	2.2	0.00000032	-6.5	4.4	-0.1	1.6	0.00002350
Rostral anterior cingulate	-2.5	4.3	-0.9	3.4	0.07027853	-3.7	3	-1.7	2.2	0.05500848
Rostral middle frontal	-3.4	4.2	-0.3	1.6	0.00135140	-3	4.7	0.2	1.5	0.02925895
Superior frontal	-2.9	3.4	0.1	2	0.00115662	-3.4	3.4	0	1.2	0.00024608
Superior parietal	-6	4.3	-0.2	1.5	0.00001100	-5.7	3.8	-0.2	1.3	0.00005925
Superior temporal	-6.8	3.6	0.1	0.9	0.00000138	-4.3	3.3	-0.3	0.9	0.00001837
Supramarginal	-6.5	3.4	-0.3	1.2	0.00000098	-3.5	5.8	-0.2	1.3	0.02403716
Frontal pole	-1.8	4.2	0.2	3.6	0.13463717	-1.2	8.4	-1.4	3.2	0.60239318
Temporal pole	-6.9	5.1	-0.1	2.8	0.00000193	-7.1	5.9	-0.7	3	0.00001426
Transverse temporal	-4.5	4.8	0.6	3.6	0.00060167	-2.1	4.9	-0.2	2.6	0.02403716
Mean thickness	-4.7	2.4	0.1	0.9	0.00000009	-4.1	1.9	0.1	1	0.00000032

Abbreviations: EOAD, early-onset AD; HCB, Hospital Clinic; HC, healthy controls; bankssts, banks of the superior temporal sulcus; SD, standard deviation; spc, symmetrized percent change

Table 4. Cortical thickness rate of change (%) at two years

Region	LEFT HEMISPHERE					RIGHT HEMISPHERE				
	EOAD-HCB		HC		P value	EOAD-HCB		HC		P value
	roc (%)	SD	roc (%)	SD		roc (%)	SD	roc (%)	SD	
Bankssts	-0.09	0.05	0.00	0.02	0.00000032	-0.05	0.10	-0.01	0.04	0.01136049
Caudal anterior cingulate	-0.02	0.04	0.00	0.03	0.30867791	-0.03	0.07	0.00	0.03	0.08208077
Caudal middle frontal	-0.06	0.05	0.00	0.02	0.00001426	-0.04	0.04	-0.01	0.02	0.00624418
Cuneus	-0.03	0.03	0.01	0.03	0.00371067	-0.03	0.04	0.01	0.02	0.00042537
Entorhinal	-0.17	0.06	-0.01	0.03	0.00000005	-0.20	0.06	0.00	0.05	0.00000005
Fusiform	-0.09	0.06	0.00	0.02	0.00000069	-0.11	0.05	0.00	0.03	0.00000009
Inferior parietal	-0.08	0.05	0.00	0.02	0.00000638	-0.07	0.05	0.00	0.02	0.00026131
Inferior temporal	-0.10	0.05	0.00	0.02	0.00000013	-0.08	0.05	0.01	0.02	0.00000193
Insula	-0.07	0.03	0.00	0.03	0.00000193	-0.06	0.06	0.01	0.05	0.00024608
Isthmus cingulate	-0.08	0.06	0.00	0.03	0.00000638	-0.09	0.06	-0.01	0.01	0.00000264
Latera occipital	-0.05	0.04	0.00	0.02	0.00002988	-0.04	0.05	0.01	0.03	0.00042537
Lateral orbitofrontal	-0.03	0.06	0.01	0.02	0.01012329	-0.05	0.05	0.00	0.02	0.00798629
Lingual	-0.03	0.02	0.01	0.03	0.00013732	-0.05	0.05	0.00	0.03	0.00009107
Medial orbitofrontal	-0.02	0.09	-0.01	0.04	0.19447303	-0.03	0.05	0.00	0.02	0.04633203
Middle temporal	-0.10	0.05	0.00	0.02	0.00000480	-0.09	0.05	0.00	0.02	0.00000480
Parahippocampal	-0.10	0.05	0.00	0.04	0.00000358	-0.11	0.09	0.00	0.03	0.00000840
Para central	-0.03	0.05	0.01	0.05	0.01959784	-0.03	0.08	0.02	0.04	0.01421629
Pars opercularis	-0.05	0.04	0.01	0.01	0.00001837	-0.02	0.04	0.00	0.03	0.14364877
Pars orbitalis	-0.03	0.06	-0.01	0.03	0.02172539	-0.04	0.06	0.00	0.03	0.00157417
Pars triangularis	-0.02	0.04	0.00	0.02	0.07601140	-0.01	0.03	0.00	0.02	0.25459007
Pericalcarine	-0.02	0.05	0.01	0.05	0.04241212	-0.03	0.07	0.00	0.04	0.08208077
Postcentral	-0.04	0.03	0.00	0.01	0.00000358	-0.02	0.03	0.00	0.02	0.02654484
Posterior cingulate	-0.04	0.04	0.00	0.02	0.00211786	-0.04	0.05	0.00	0.02	0.00244638
Precentral	-0.03	0.04	0.01	0.02	0.00083957	-0.01	0.06	0.01	0.03	0.07027853
Precuneus	-0.09	0.04	-0.01	0.03	0.00000047	-0.07	0.05	0.00	0.02	0.00002350
Rostral anterior cingulate	-0.03	0.05	-0.01	0.05	0.06487399	-0.05	0.04	-0.02	0.03	0.04241212
Rostral middle frontal	-0.04	0.04	0.00	0.02	0.00240957	-0.03	0.05	0.00	0.02	0.02403716
Superior frontal	-0.04	0.04	0.00	0.03	0.00115662	-0.04	0.05	0.00	0.02	0.00020343
Superior parietal	-0.06	0.05	0.00	0.02	0.00001426	-0.06	0.04	0.00	0.01	0.00005925
Superior temporal	-0.09	0.04	0.00	0.01	0.00000138	-0.06	0.04	0.00	0.01	0.00002988
Supramarginal	-0.08	0.04	0.00	0.02	0.00000138	-0.04	0.06	0.00	0.02	0.02925895
Frontal pole	-0.02	0.05	0.00	0.05	0.13463717	-0.01	0.11	-0.02	0.04	0.58690608
Temporal pole	-0.11	0.06	0.00	0.05	0.00000358	-0.12	0.09	-0.01	0.06	0.00003774
Transverse temporal	-0.05	0.05	0.01	0.04	0.00050682	-0.03	0.06	0.00	0.03	0.03535338
Mean thickness	-0.06	0.03	0.00	0.01	0.00000013	-0.05	0.02	0.00	0.01	0.00000032

Abbreviations: EOAD, early-onset AD; HCB, Hospital Clinic; HC, healthy controls; bankssts, banks of the superior temporal sulcus; SD, standard deviation; roc, rate of change

Table 5. Subcortical gray matter volume symmetrized percent change (%) at two years

Region	EOAD-HCB		HC		p value
	spc %	SD	spc %	SD	
Left Hippocampus	-10.4	6.3	-1.0	1.7	0.0000084
Left Amygdala	-12.3	7.3	-0.5	3.8	0.0000002
Left Thalamus	-7.3	3.9	-1.2	1.7	0.0000084
Left Caudate	-8.9	8.8	-1.2	1.6	0.0002964
Left Putamen	-6.5	5.7	-1.0	2.1	0.0021179
Left Pallidum	2.7	3.3	0.1	2.8	0.9872784
Left Accumbens area	-24.5	37.0	-4.0	10.6	0.0195978
Left Cerebellum white matter	0.8	6.4	0.6	2.9	0.4130939
Left Cerebellum cortex	-3.8	3.1	-1.0	2.0	0.0013514
Left lateral ventricle	34.3	15.0	4.8	8.5	0.0000001
Left inferior lateral ventricle	48.8	18.6	6.9	15.1	0.0000001
Right Hippocampus	-14.0	5.9	-1.5	3.7	0.0000010
Right Amygdala	-10.4	5.8	-2.2	6.0	0.0000184
Right Thalamus	-7.3	3.9	-1.3	1.3	0.0000064
Right Caudate	-7.2	8.3	-2.2	2.5	0.0424121
Right Putamen	-7.4	7.3	-2.4	2.7	0.0217254
Right Pallidum	2.6	8.9	0.2	5.8	0.7189750
Right Accumbens area	-5.7	10.1	-2.8	5.3	0.2174468
Right Cerebellum white matter	-1.1	7.8	-2.0	3.3	0.6023932
Right Cerebellum cortex	-4.8	4.4	-1.2	3.7	0.0009870
Right lateral ventricle	29.8	13.9	4.8	8.9	0.0000019
Right inferior lateral ventricle	43.2	19.3	0.3	14.8	0.0000002
Brain stem	-2.8	2.0	-0.9	1.8	0.0079863

Abbreviations: EOAD, early-onset AD; HCB, Hospital Clinic; HC, healthy controls; SD, standard deviation; spc, symmetrized percent change.

Table 6. Subcortical gray matter volume rate of change (%) at two years

Region	EOAD-HCB		HC		p value
	roc %	SD	roc %	SD	
Left Hippocampus	-162.0	90.1	-19.4	32.4	0.00000840
Left Amygdala	-61.3	27.0	-4.3	28.2	0.00000264
Left Thalamus	-236.4	123.7	-40.7	59.8	0.00001100
Left Caudate	-117.3	84.3	-17.9	22.3	0.00029643
Left Putamen	-135.7	114.7	-20.5	43.8	0.00244638
Left Pallidum	24.8	31.8	2.6	28.8	0.98727843
Left Accumbens area	-16.5	26.0	-5.4	19.3	0.06487399
Left Cerebellum white matter	53.5	523.8	66.1	222.4	0.38227532
Left Cerebellum cortex	-987.1	872.8	-230.4	409.2	0.00135140
Left lateral ventricle	2834.0	1887.3	208.4	669.3	0.00000021
Left inferior lateral ventricle	255.5	134.4	14.2	29.7	0.00000001
Right Hippocampus	-225.4	103.1	-28.6	63.4	0.00000069
Right Amygdala	-67.0	32.8	-16.7	42.4	0.00002988
Right Thalamus	-236.7	123.5	-47.5	47.3	0.00002350
Right Caudate	-113.8	109.8	-39.5	41.3	0.03535338
Right Putamen	-151.4	142.8	-49.6	56.1	0.02654484
Right Pallidum	22.5	76.4	2.4	50.6	0.70529305
Right Accumbens area	-11.0	22.0	-6.4	15.1	0.26764856
Right Cerebellum white matter	-129.7	598.0	-138.5	261.0	0.61772468
Right Cerebellum cortex	-1214.4	1114.7	-257.3	831.4	0.00071194
Right lateral ventricle	2184.3	1501.3	191.8	609.8	0.00000138
Right inferior lateral ventricle	247.6	275.8	2.6	26.3	0.00000005
Brain stem	-272.0	194.2	-87.9	170.9	0.00424182

Abbreviations: EOAD, early-onset AD; HCB, Hospital Clinic; HC, healthy controls; SD, standard deviation; roc, rate of change.

Table 7. Correlation between longitudinal cortical loss and initial cerebrospinal fluid biomarkers using the full sample of EOAD-HCB and HC subjects

Region	Aβ42 ρ	p value	t-tau ρ	p value	p-tau ρ	p value	NfL ρ	p value
Left bankssts	0.52	0.00332	-0.74	0.00000496	-0.69	0.00003	-0.73	0.00000817
Left caudal middle frontal	0.58	0.0007	-0.58	0.000874	-0.46	0.00978	-0.65	0.000158
Left entorhinal	0.68	0.0000422	-0.78	0.00000127	-0.74	0.00000511	-0.82	0.00000102
Left fusiform	0.63	0.000225	-0.65	0.000118	-0.61	0.000314	-0.67	0.0000765
Left inferior parietal	0.59	0.000535	-0.62	0.000259	-0.5	0.00468	-0.71	0.0000215
Left inferior temporal	0.64	0.000131	-0.7	0.0000167	-0.64	0.000157	-0.72	0.000012
Left insula	0.65	0.00011	-0.68	0.0000433	-0.54	0.00192	-0.72	0.0000145
Left Isthmus cingulate	0.62	0.000265	-0.58	0.000883	-0.56	0.00113	-0.58	0.000895
Left lateral occipital	0.56	0.00125	-0.58	0.000775	-0.57	0.0011	-0.63	0.000297
Left lingual	0.52	0.00326	-0.57	0.00111	-0.56	0.00142	-0.58	0.000976
Left middle temporal	0.59	0.000552	-0.62	0.000262	-0.53	0.00246	-0.68	0.0000528
Left para hippocampal	0.56	0.00122	-0.65	0.000117	-0.61	0.000347	-0.65	0.000142
Left pars opercularis	0.65	0.000126	-0.52	0.00329	-0.46	0.0103	-0.59	0.000768
Left postcentral	0.53	0.0025	-0.74	0.00000404	-0.62	0.000262	-0.65	0.000148
Left precuneus	0.64	0.00015	-0.64	0.000155	-0.51	0.00373	-0.64	0.000214
Left superior parietal	0.45	0.0126	-0.65	0.000104	-0.55	0.00175	-0.71	0.0000202
Left superior temporal	0.68	0.0000416	-0.6	0.000427	-0.51	0.0037	-0.73	0.0000105
Left supramarginal	0.56	0.00136	-0.67	0.000067	-0.6	0.000409	-0.73	0.00001
Left temporal pole	0.76	0.00000261	-0.55	0.00153	-0.54	0.00192	-0.65	0.000162
Left transverse temporal	0.41	0.0222	-0.56	0.00126	-0.53	0.00259	-0.54	0.00231
Left Mean Thickness	0.63	0.000212	-0.68	0.0000356	-0.59	0.00057	-0.74	0.00000726
Right cuneus	0.34	0.0613	-0.65	0.00011	-0.63	0.000207	-0.54	0.00221
Right entorhinal	0.7	0.0000218	-0.71	0.0000125	-0.57	0.001	-0.76	0.00000357
Right fusiform	0.67	0.0000653	-0.8	0.00000106	-0.61	0.000379	-0.71	0.0000183
Right inferior parietal	0.55	0.00141	-0.54	0.00165	-0.45	0.0103	-0.59	0.000675
Right inferior temporal	0.54	0.00188	-0.72	0.0000106	-0.62	0.000256	-0.73	0.00000845
Right insula	0.46	0.0095	-0.62	0.00028	-0.53	0.00266	-0.55	0.00192
Right Isthmus cingulate	0.59	0.000632	-0.63	0.000198	-0.54	0.00206	-0.63	0.000276
Right lateral occipital	0.36	0.0465	-0.62	0.0003	-0.52	0.00321	-0.58	0.000895
Right lingual	0.48	0.00676	-0.64	0.000133	-0.46	0.0104	-0.71	0.0000226
Right middle temporal	0.6	0.000518	-0.66	0.0000716	-0.56	0.00124	-0.7	0.0000283
Right para hippocampal	0.54	0.00197	-0.66	0.0000775	-0.57	0.00101	-0.72	0.000015
Right precuneus	0.48	0.00645	-0.6	0.000476	-0.53	0.0024	-0.67	0.0000846
Right superior frontal	0.46	0.0095	-0.5	0.00483	-0.38	0.0336	-0.74	0.00000575
Right superior parietal	0.49	0.00607	-0.58	0.000783	-0.49	0.0054	-0.66	0.0000935
Right superior temporal	0.71	0.0000164	-0.53	0.00233	-0.43	0.0159	-0.52	0.00382
Right temporal pole	0.64	0.000173	-0.65	0.000128	-0.55	0.00166	-0.73	0.0000109
Right Mean Thickness	0.62	0.00029	-0.71	0.0000137	-0.56	0.00123	-0.76	0.00000308

Abbreviations: Aβ42, amyloid β42; p-tau, phosphorylated tau; t-tau, total tau; NfL, neurofilament light chain, ρ, Spearman's rank correlation coefficient.

Table 8. Correlation between longitudinal subcortical atrophy and initial cerebrospinal fluid biomarkers using the full sample of EOAD-HCB and HC subjects

Region	Aβ42 ρ	p value	t-tau ρ	p value	p-tau ρ	p value	NfL ρ	p value
Left Hippocampus	0.55	0.00151	-0.65	0.000102	-0.53	0.00237	-0.63	0.000246
Left Amygdala	0.55	0.00144	-0.76	0.00000214	-0.67	0.0000586	-0.68	0.0000651
Left Thalamus	0.59	0.000652	-0.52	0.00292	-0.51	0.00358	-0.63	0.000286
Left Putamen	0.31	0.0865	-0.54	0.00217	-0.48	0.00751	-0.48	0.0079
Left Pallidum	-0.24	0.199	0.4	0.0269	0.36	0.0458	0.27	0.144
Left Cerebellum Cortex	0.51	0.00379	-0.42	0.0185	-0.27	0.136	-0.39	0.0323
Left Lateral Ventricle	-0.66	0.0000707	0.66	0.0000745	0.54	0.00182	0.76	0.000003
Right Hippocampus	0.55	0.0017	-0.71	0.0000119	-0.62	0.00025	-0.71	0.0000189
Right Amygdala	0.61	0.000317	-0.64	0.000136	-0.51	0.00398	-0.6	0.000593
Right Thalamus	0.55	0.00151	-0.57	0.000994	-0.51	0.00418	-0.68	0.0000595
Right Cerebellum Cortex	0.38	0.0367	-0.54	0.0021	-0.37	0.0409	-0.55	0.00178
Right Lateral Ventricle	-0.64	0.000159	0.62	0.0003	0.48	0.00626	0.68	0.0000595

Abbreviations: Aβ42, amyloid β42; p-tau, phosphorylated tau; t-tau, total tau; NfL, neurofilament light chain, ρ, Spearman's rank correlation coefficient.

Table 9. Florbetapir-PET SUVR in the regions analyzed in EOAD-ADNI

	Right precuneus	Right superior parietal	Global composite	Parietal lobe
SUVR (SD)	1.68 (0.20)	1.44 (0.22)	1.54 (0.20)	1.56 (0.21)

Abbreviations: SUVR, Standardized Uptake Value Ratio; SD, standard deviation.

Figure 1. Correlation between the different CSF biomarkers at baseline in EOAD-HCB

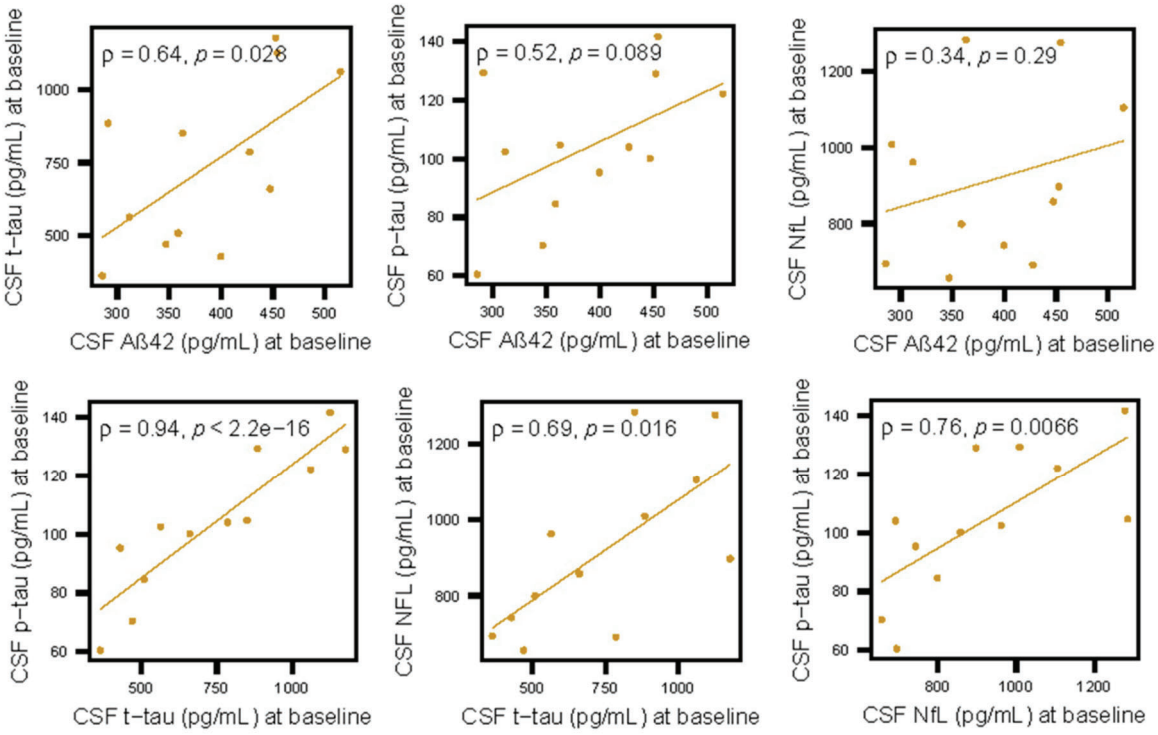

Figure 2. Correlation between the different CSF biomarkers at baseline in EOAD-ADNI and LOAD-ADNI

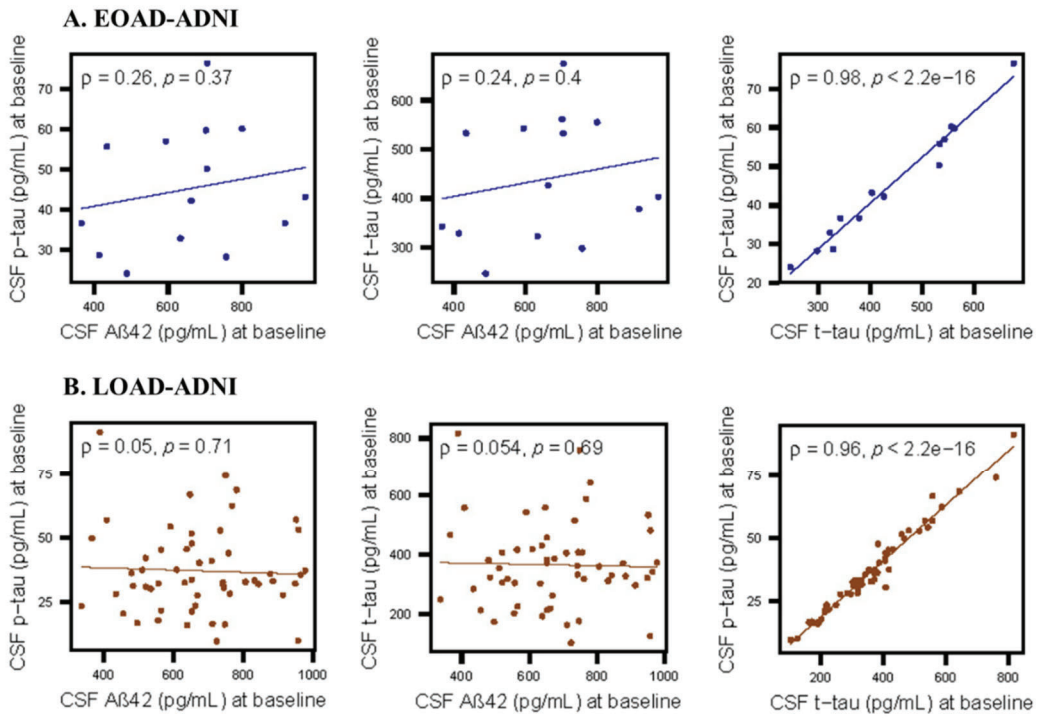

Figure 3 Correlation between initial CSF biomarkers levels and baseline atrophy in EOAD-HCB

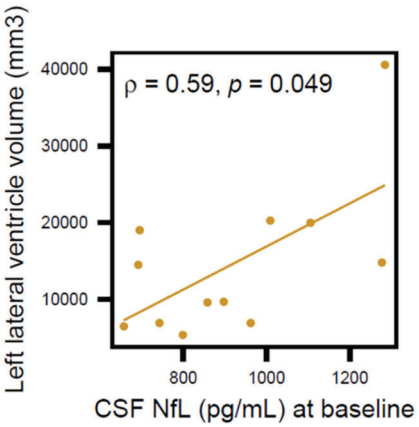

OBJETIVO 3

Estudiar la capacidad para predecir los cambios cognitivos longitudinales de las alteraciones en grosor cortical y volumen subcortical en RM craneal que presentan en el momento del diagnóstico los sujetos con EAIP confirmada biológicamente en comparación con sujetos control.

Título del trabajo:

"Baseline MRI atrophy predicts 2-year cognitive outcomes in early-onset Alzheimer's disease."

Autores: Contador, José; Pérez-Millan, Agnès; Guillen, Nuria; Tort-Merino, Adrià; Balasa, Mircea; Falgás, Neus; Olives, Jaume; Castellví, Magdalena; Borrego-Écija, Sergi; Bosch, Beatriz; Fernández-Villullas, Guadalupe; Ramos-Campoy, Oscar; Antonell, Anna; Bargalló, Nuria; Sanchez-Valle, Raquel; Sala-Llonch, Roser; Lladó, Albert

Journal of Neurology 2022;269(5):2573-2583.
doi: 10.1007/s00415-021-10851-9
IF: 4.849. Q1, Clinical neurology

Journal of Neurology (2022) 269:2573–2583
https://doi.org/10.1007/s00415-021-10851-9

ORIGINAL COMMUNICATION

Baseline MRI atrophy predicts 2-year cognitive outcomes in early-onset Alzheimer's disease

José Contador[1] · Agnès Pérez-Millan[1,2] · Nuria Guillen[1] · Adrià Tort-Merino[1] · Mircea Balasa[1,3] · Neus Falgàs[1,4,5] · Jaume Olives[1] · Magdalena Castellví[1] · Sergi Borrego-Écija[6] · Beatriz Bosch[1] · Guadalupe Fernández-Villullas[1] · Oscar Ramos-Campoy[1] · Anna Antonell[1] · Nuria Bargalló[7] · Raquel Sanchez-Valle[1,8] · Roser Sala-Llonch[2,9] · Albert Lladó[1,8]

Received: 20 September 2021 / Revised: 12 October 2021 / Accepted: 13 October 2021 / Published online: 19 October 2021

Abstract

Background MRI atrophy predicts cognitive status in AD. However, this relationship has not been investigated in early-onset AD (EOAD, < 65 years) patients with a biomarker-based diagnosis.

Methods Forty eight EOAD (MMSE ≥ 15; A + T + N +) and forty two age-matched healthy controls (HC; A − T − N −) from a prospective cohort underwent full neuropsychological assessment, 3T-MRI scan and lumbar puncture at baseline. Participants repeated the cognitive assessment annually. We used linear mixed models to investigate whether baseline cortical thickness (CTh) or subcortical volume predicts two-year cognitive outcomes in the EOAD group.

Results In EOAD, hemispheric CTh and ventricular volume at baseline were associated with global cognition, language and attentional/executive functioning 2 years later ($p < 0.0028$). Regional CTh was related to most cognitive outcomes ($p < 0.0028$), except verbal/visual memory subtests. Amygdalar volume was associated with letter fluency test ($p < 0.0028$). Hippocampal volume did not show significant associations.

Conclusion Baseline hemispheric/regional CTh, ventricular and amygdalar volume, but not the hippocampus, predict two-year cognitive outcomes in EOAD.

Keywords Early-onset Alzheimer's disease · Magnetic resonance imaging (MRI) · Biomarkers · Longitudinal · Progression · Neuropsychological evaluation · Cognition · Prediction biomarkers

Abbreviations

AD	Alzheimer's disease
Aβ	Amyloid-β

Roser Sala-Llonch and Albert Lladó have contributed equally to this work.

✉ Albert Lladó
allado@clinic.cat

[1] Alzheimer's Disease and Other Cognitive Disorders Unit, Neurology Service, Hospital Clínic de Barcelona, Institut d'Investigacions Biomèdiques August Pi i Sunyer (IDIBAPS), Universitat de Barcelona, Barcelona, Spain

[2] Institute of Neurosciences. Department of Biomedicine, Faculty of Medicine, Institut d'Investigacions Biomèdiques August Pi i Sunyer (IDIBAPS), University of Barcelona, Barcelona, Spain

[3] Atlantic Fellow for Equity in Brain Health, Global Brain Heath Institute, Trinity College Institute of Neuroscience, Dublin, Ireland

[4] Atlantic Fellow for Equity in Brain Health, Global Brain Heath Institute, Department of Neurology, University of California, San Francisco, CA, USA

[5] Department of Neurology, Memory & Aging Center, Weill Institute for Neurosciences, University of California, San Francisco, CA, USA

[6] Department of Neurology, Fundació Sanitària Mollet, Mollet del Vallés, Barcelona, Spain

[7] Image Diagnostic Centre Radiology Department, Hospital Clínic de Barcelona, Magnetic Resonance Image Core facility Institut d'Investigacions Biomèdiques August Pi i Sunyer (IDIBAPS), Barcelona, Spain

[8] Centro de Investigación Biomédica en Red de Enfermedades Neurodegenerativas, CIBERNED, Spain

[9] Biomedical Imaging Group, Biomedical Research Networking Center in Bioengineering, Biomaterials and Nanomedicine (CIBER-BBN), Barcelona, Spain

bankssts	Banks of the superior temporal sulcus
BDAE	The Boston Diagnostic Aphasia Examination
BNT	Boston Naming Test
CERAD	Consortium to Establish a Registry for Alzheimer's disease
CSF	Cerebrospinal fluid
CTh	Cortical thickness
DFR	Delayed free recall
Digits-B	Digits span backwards
Digits-F	Digits span forwards
DTR	Delayed total recall
EOAD	Early-onset AD
LFT	Letter fluency test
FCSRT	Free and Cued Selective Reminding Test
FDG-PET	Fluorodeoxyglucose positron emission tomography
FL	Free learning
GC	Global composite
HC	Healthy controls
HCB	Hospital Clínic de Barcelona
LM	Linear model
LME	Linear mixed-effects model
LOAD	Late-onset AD
MMSE	Mini-Mental State Examination
MRI	Magnetic resonance imaging
MTL	Medial temporal lobe
NIA-AA	National Institute on Aging-Alzheimer's Association
SF	Semantic fluency test
TL	Total learning
TMT-A	Trail Making Test-A
VOSP	Visual object and space perception battery
WAB	Western Aphasia Battery
WAIS	Wechsler Adult Intelligence Scale
YOE	Years of education

Introduction

Alzheimer's disease (AD) is classified into early-onset (EOAD, age at onset < 65 years) and late-onset (LOAD, > 65 years) presentations. Both entities feature the progressive deposition of amyloid-β (Aβ) and tau proteins that leads to synaptic and neuronal loss and the subsequent cognitive impairment [1]. However, compared to LOAD, EOAD subjects present a greater pathological burden in neocortical regions and less hippocampal involvement [2, 3]. In addition, EOAD tends to present a pattern of widespread neocortical atrophy, as seen in magnetic resonance imaging (MRI) studies [4–6], and the medial temporal lobe (MTL) atrophy, an established neurodegeneration biomarker in AD, has shown limited utility in this population [7]. On the other hand, EOAD shows a higher frequency of non-amnestic symptoms and faster cognitive decline than LOAD [8, 9].

The National Institute on Aging-Alzheimer's Association (NIA-AA) provides a framework for in vivo evidence of Aβ plaques and Tau deposit (A/T biomarkers), as well as for neurodegeneration (N) [10], with the A + T + N + and A + T + N − subtypes showing the highest rates of progression from preclinical stages to AD's dementia. However, the links between the ATN system and the cognitive status are modest and there is still a clinical need to identify patients at the greatest risk for cognitive decline. In this sense, brain atrophy in MRI, especially in the MTL structures, has yielded satisfactory results in tracking neurodegeneration [11] and predicting clinical progression [12–14]. In EOAD, cross-sectional MRI studies have shown an association between the cognitive profile and the pattern of brain atrophy [15, 16]. However, literature describing how baseline MRI atrophy may predict cognitive status in EOAD is lacking. Moreover, whether the outcomes emphasizing memory and hippocampus should be applied to this subgroup remains an unanswered question.

Here, we include sporadic EOAD subjects (A + T + N +) and healthy controls (HC; A − T − N −) who underwent a baseline 3T-MRI and lumbar puncture for analysis of cerebrospinal fluid (CSF) biomarkers (Aβ42, p-tau and t-tau). First, we compare the longitudinal changes in a comprehensive neuropsychological evaluation, as well as the baseline pattern of atrophy in MRI, between EOAD and HC. Then, in the EOAD group, we investigated the relationship between baseline MRI measures reflecting global atrophy (i.e. hemispheric cortical thickness (CTh) and lateral ventricles (LVs) volume) and cognitive outcomes up to two years. We hypothesized that global atrophy would predict the cognitive status in non-amnestic domains rather than in memory measures. Finally, we used the measures of regional cortical thinning and subcortical volume loss in EOAD to investigate region-specific associations with the future cognitive status. We hypothesized that measures of neocortical regions, rather than the MTL structures, would be predictors of the cognitive outcomes in EOAD.

Material and methods

Study participants

We included 48 EOAD patients (Mini-Mental State Examination (MMSE) score ≥ 15) and 42 age-matched HC from a prospective cohort recruited at the "Alzheimer's disease and Other Cognitive Disorders Unit", Hospital Clínic de Barcelona (HCB). At baseline, all participants underwent a comprehensive neuropsychological testing, a 3T-MRI scan and a lumbar puncture to analyze AD CSF biomarkers. During the

follow-up, the neuropsychological evaluation was repeated annually over 2 years (namely visit 1 and visit 2), except for those enrolled in clinical trials, who were unable to perform the battery or withdrew their consent.

All the EOAD patients presented CSF levels of AD biomarkers in the range suggesting AD neuropathology (A + T +) with neurodegeneration (N +) according to the NIA-AA Research Framework 2018 [10]. EOAD subjects also fulfilled diagnostic criteria for mild cognitive impairment due to AD, or AD mild dementia [17, 18]. HC presented normal cognition and normal CSF levels of core biomarkers (A − T − N −). We excluded participants with previous psychiatric or neurological conditions, autosomal dominant pattern of AD inheritance, poor MRI quality or gross brain pathology (i.e., stroke, tumor). HC were obtained from different research projects. They were a combination of patients' relatives recruited from our outpatient's clinic and volunteers who came to our center to participate in research.

The study was approved by Hospital Clínic Ethics Committee and all the individuals gave written informed consent for their clinical data to be used for research purposes.

Laboratory testing

Commercially available single-analyte enzyme-linked immunosorbent assay (ELISA) was used to determine levels of CSF Aβ42, p-tau and t-tau (INNOTEST, Fujirebio Europe N.V., Gent, Belgium). The CSF Aβ42 (A), p-tau (T) and t-tau (N) levels were used to determine the ATN status according to cut-off values determined by our laboratory [19]. *APOE* genotyping was performed through the analysis of rs429358 and rs7412 polymorphisms, either using TaqMan genotyping (Thermo Fisher Scientific, Waltham, MA, USA) or Sanger sequencing. Individuals were classified according to the presence of at least one *APOE* ε4 allele (carriers) or the absence of *APOE* ε4 alleles (non-carriers).

Cognitive assessment

All subjects completed an initial comprehensive neuropsychological battery administered by a trained neuropsychologist, including sixteen cognitive performances (five cognitive domains) and the MMSE as a measure of global cognition [20]. The same cognitive battery was performed annually.

The Free and Cued Selective Reminding Test (FCSRT) [21] was used to assess verbal learning [free learning (FL) and total learning (TL) scores] and memory function [delayed free recall (DFR) and delayed total recall (DTR) scores]. Delayed visual memory was measured using the Landscape test (LT) [22]. Language evaluation comprised the Boston Naming Test (BNT) [23], a semantic fluency test (SF) [24] and the auditory comprehension subtest of the Boston Diagnostic Aphasia Examination (BDAE) [25]. The ideomotor praxis subtest of the Western Aphasia Battery (WAB) [26] and the constructional praxis subtest included in the Consortium to Establish a Registry for Alzheimer's Disease (CERAD) battery [27] were used to assess the praxis domain. Visual-spatial perception was measured by the incomplete letters and number location subtests of the Visual Object and Space Perception battery (VOSP-letters/VOSP-numbers, respectively) [28]. Attention and executive functions evaluation consisted in the Trail Making Test-A (TMT-A) [29], a letter fluency test (LFT) [30] and the digit span forwards (attention span, Digits-F) and backwards (working memory, Digits-B) subtests of the Wechsler Adult Intelligence Scale (WAIS) [31].

All scores were z-normalized using the mean and standard deviation of HC at baseline. In the case of TMT-A, we reversed the score sign to maintain an interpretation of worsening performance, lower score. For each subject, we created a global composite (GC) using the mean z-score for all tests except MMSE (16 cognitive tests). Not available values were omitted.

MRI acquisition and processing

A high-resolution 3D structural data set (T1-weighted, MP-RAGE, repetition time = 2.300 ms, echo time = 2.98 ms, 240 slices, field-of-view = 256 mm, voxel size = 1 × 1 × 1 mm) was acquired for each individual at baseline in a 3T Magnetom Trio Tim scanner (Siemens Medical Systems, Germany) at HCB. In addition, 3 EOAD subjects were scanned in a 3T Prisma scanner (Siemens Medical Systems, Germany) at HCB using the same protocol.

We used the processing stream available in FreeSurfer version 6.0 (http://surfer.nmr.mgh.harvard.edu/) to perform cortical reconstruction and volumetric segmentation of the T1-weighted acquisitions. FreeSurfer preprocessing steps are fully reported elsewhere [32, 33]. FreeSurfer allowed us to generate automated CTh maps and segmentation of the subcortical structures. We obtained global measures of mean CTh and volume of the LVs of the left and right hemispheres (lh, rh). In addition, for studying regional effects, we used the summary measures of mean CTh in 68 cortical parcellations and gray matter volumes of 17 subcortical structures, all derived from atlases available in FreeSurfer [34, 35]. Subcortical volumes were normalized by the estimated intracranial volume and scaled with a factor of 100. All the images were visually inspected and manually corrected if needed.

Statistical analysis

Demographics, genetics and CSF biomarker levels

At baseline, EOAD and HC were compared using t Student tests for continuous variables and χ^2 tests for the sex, *APOE*

and laterality distributions. Due to sample size reductions at Visit 1 and Visit 2, between-group differences in the successive visits were analyzed using the Mann–Whitney *U* tests for continuous variables and Fisher's exact tests for categorical data. A p value < 0.05 was considered statistically significant. All statistical analyses in this study were conducted using R 4.0.2 (http://www.R-project.org).

Neuropsychological scores

We studied group differences in neuropsychological scores to evaluate which domains were affected at baseline and at 2 years point. At baseline, we used linear models (LM) to calculate between-group differences in neuropsychological z-scores, with age at neuropsychological testing (age), sex, years of education (YOE) and *APOE* status as predictors. Prior to analyses, all dichotomous variables (e.g., sex) were dummy-coded to make them usable in regression models.

We performed linear mixed-effects models (LME) to examine differences in cognitive trajectories between EOAD and HC at 2 years. The z-scores of the tests at visit 2 were used as the variable to be predicted. Participants were modeled as random effects and the diagnostic group, the visit (baseline, visit 1, visit 2) and their interaction (group × visit) were introduced as fixed effects. In addition, baseline z-scores, age, sex, YOE and *APOE* status were also introduced as fixed effects. The group × visit 2 interaction was selected as the main contrast of interest. After Bonferroni correction (initial p level = 0.05, number of tests = 18), a p value < 0.0028 was considered statistically significant.

Structural differences at baseline

Similarly, we evaluated the differences of baseline MRI between EOAD and HC to obtain the patterns of atrophy as well as their MRI-derived summary measures. We calculated differences between groups in CTh and volume measures using LM. Age at MRI scan, sex and *APOE* status were introduced as covariates of no interest. After Bonferroni correction for multiple comparisons (initial p level = 0.05, number of tests = 89), only p values < 0.0006 were considered statistically significant. As we had slightly different acquisitions in a subset of participants, we repeated the analysis with the scan as a predictor to discard any effect of scan change.

MRI prediction of 2-years cognitive outcomes

We performed LMEs in EOAD to investigate whether baseline atrophy predicts cognition at 2 years. Cognitive z-scores were introduced as dependent variables. Participants were modeled as random effects, while fixed effects were: visit (baseline, visit 1, visit 2)), the brain structural measures (introduced individually), and the interaction between brain measurements and visit (MRI x visit). In addition, baseline z-score for each cognitive measure, age, sex, YOE and *APOE* status were also introduced as fixed effects, to be used as covariates of no interest. We performed the analysis for each of the MRI measures that resulted significant in the baseline analysis of group differences, as well as for global measures. MRI × visit 2 interaction was selected as the main contrast of interest. A p value < 0.0028 was considered statistically significant.

Results

Demographics, genetics and CSF biomarker levels

EOAD and HC characteristics at baseline are summarized in Table 1. Compared to HC, EOAD presented lower Aβ42 and higher p-tau and t-tau levels and a higher proportion of *APOE* ε4 carriers (all $p < 0.05$). We found no differences in age, YOE, time between visits, time between the neuropsychological assessments and MRI scan/lumbar puncture, sex or laterality. 23 EOAD and 29 HC subjects continued at visit 1 whereas 15 EOAD and 28 HC did at visit 2 (Supplementary Table 1 and 2).

Neuropsychological scores

At baseline, compared to HC, EOAD patients scored lower in all tests of the neuropsychological battery ($p < 0.05$, Bonferroni corrected, Fig. 1).

At 2 years, EOAD declined faster in all the cognitive scores than HC ($p < 0.05$, Bonferroni corrected, Table 2), except for Digits-B.

MRI atrophy at baseline

At baseline, lh and rh CTh was lower in EOAD than HC and LVs volumes were higher ($p < 0.05$, Bonferroni corrected; Fig. 2a). When comparing the lateralization effects in global measures of atrophy in EOAD, no hemispheric asymmetries were found in CTh ($p = 0.6$) or LVs volume ($p = 0.4$).

Regarding the regional pattern of atrophy in EOAD, we found lower CTh bilaterally in superior frontal, caudal middle frontal, rostral middle frontal, fusiform, supramarginal, precuneus, superior and inferior parietal; banks of the superior temporal sulcus (bankssts), superior, middle and inferior temporal; posterior and isthmus cingulate and lateral occipital regions. In addition, lower CTh was found in EOAD in the right entorhinal, insula and parahippocampal areas ($p < 0.05$, Bonferroni corrected; Fig. 2b). Finally, we found reduced subcortical volume in EOAD in the bilateral amygdala and hippocampus ($p < 0.05$, Bonferroni

Table 1 Demographics, clinical characteristics and CSF biomarker levels of the study groups

	EOAD ($n=48$)			HC ($n=42$)			p value
	N	Mean	SD	*N*	Mean	SD	
Age at onset (years)	48	56.46	4.24	N/A	N/A	N/A	N/A
CSF Aβ42 (pg/ml)	48	422.26	133.64	42	826.70	205.61	1^{-16}*
CSF p-Tau (pg/ml)	48	98.96	36.17	42	51.19	12.67	1^{-11}*
CSF Tau (pg/ml)	48	696.92	435.06	42	219.53	71.35	1^{-9}*
Age at MRI scan (years)	48	59.23	4.38	42	57.51	5.22	0.10
Age at NPS (years)	48	59.17	4.37	42	57.49	5.23	0.11
MMSE score	48	22.77	3.57	42	28.76	1.61	2^{-15}*
Time MRI-LP (years)	48	0.13	0.20	42	0.11	0.12	0.52
Time NPS-MRI (years)	48	0.09	0.11	42	0.10	0.12	0.66
Time NPS-LP (years)	48	0.11	0.22	42	0.15	0.15	0.31
Years of education	48	12.33	4.65	42	12.14	4.45	0.84
Sex (Female)	27	N/A	N/A	32	N/A	N/A	0.08
Laterality (Right)	47	N/A	N/A	40	N/A	N/A	0.91
APOE4 (Carriers)	21	N/A	N/A	8	N/A	N/A	0.02*
Time Visit 0-Visit 1 (years)	23	1.07	0.14	29	1.11	0.13	0.2
Time Visit 0-Visit 2 (years)	15	2.06	0.18	28	2.13	0.23	0.1

EOAD and HC characteristics were compared using *t* Student test for continuous variables, linear mixed-effect model for the MMSE and the 2 test for the sex, *APOE* ε4 and laterality distributions

EOAD early-onset AD; *HC* healthy controls; *NPS* Neuropsychological assessment; *N/A* not applicable; *MRI* Magnetic resonance imaging; *CSF* cerebrospinal fluid; *MMSE* Mini-Mental State Examination; *Aβ42* amyloid β42; *p-tau* phosphorylated tau; *t-tau* total tau; *LP* Lumbar Puncture; *SD* standard deviation

*Significant differences at p value <0.05

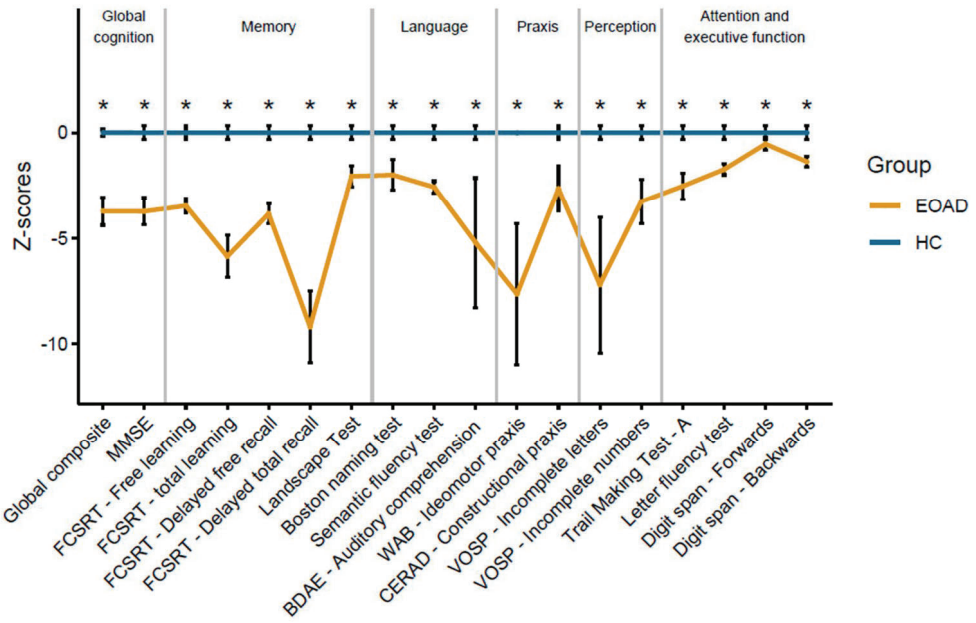

Fig. 1 Baseline neuropsychological scores and error bars across the study groups (*$p<0.05$, Bonferroni corrected). Key: *EOAD* early-onset AD; *HC* healthy controls; *BDAE* Boston Diagnostic Aphasia Examination; *CERAD* Consortium to Establish a Registry for Alzheimer's disease; *FCSRT* Free and Cued Selective Reminding Test; *MMSE* Mini-Mental State Examination; *VOSP* Visual Object and Space Perception; *WAB* Western Aphasia Battery

corrected; Fig. 2c). After using the type of MRI scan as a covariate, results did not change ($p<0.05$, Bonferroni corrected), except for lh rostral middle frontal ($p=0.05$, Bonferroni corrected).

Global brain measures at baseline predict 2-year cognitive outcomes

At 2 years point, the hemispheric CTh and the volume of

Table 2 Between-group differences in two-year cognitive outcomes

Test	Std. β	SD	Raw *p* value
Global composite	− 4.11	0.38	5^{-20}*
MMSE	− 4.13	0.37	3^{-21}*
FCSRT—free learning	− 1.2	0.22	1^{-7}*
FCSRT—total learning	− 2.88	0.36	4^{-13}*
FCSRT—delayed free recall	− 1.32	0.25	6^{-7}*
FCSRT—delayed total recall	− 4.11	0.75	2^{-7}*
Landscape test	− 2.5	0.41	8^{-9}*
Boston naming test	− 3.73	0.37	2^{-18}*
Semantic fluency test	− 0.94	0.24	2^{-4}*
BDAE—auditory comprehension	− 16.99	2.67	3^{-9}*
CERAD—constructional praxis	− 2.93	0.49	3^{-8}*
VOSP—incomplete letters	− 8.08	1.12	5^{-11}*
VOSP—incomplete numbers	− 2.66	0.56	6^{-6}*
WAB—ideomotor praxis	− 9.72	1.82	4^{-7}*
Trail Making Test—A	− 1.79	0.36	2^{-6}*
Letter fluency test	− 0.91	0.20	2^{-5}*
Digits span—Forwards	− 1.13	0.25	1^{-5}*
Digits span—Backwards	− 0.53	0.35	2^{-2}

Linear mixed-effects models for between group differences in cognitive outcomes at 2 years

SD standard deviation; *BDAE* Boston Diagnostic Aphasia Examination; *CERAD* Consortium to Establish a Registry for Alzheimer's Disease; *FCSRT* Free and Cued Selective Reminding Test; *MMSE* Mini-Mental State Examination; *VOSP* Visual Object and Space Perception; *WAB* Western Aphasia Battery; *Std β* standardized β coefficients

*Cognitive scores with a significant group × visit 2 interaction (adjusted *p* value < 0.05 after Bonferroni correction)

the LVs in EOAD at baseline were associated with the cognitive outcomes in 7 out of 18 neuropsychological scores. Lower lh CTh at baseline was associated with lower z-scores in MMSE at 2 years, in addition to SF and LFT tests. In contrast, lower rh CTh at baseline was related to lower TMT-A z-scores at 2 years. On the other hand, a higher lh/rh LV volume was associated with lower z-scores in GC and MMSE. In addition, higher lh/rh LV was associated with lower BDAE cognitive outcomes, whereas higher rh LV volume was related to worse Digits-F performance at 2 years ($p < 0.0028$, Fig. 3).

Regional pattern of atrophy in EOAD predicts 2-year cognitive outcomes

In EOAD, multiple regions that presented atrophy at baseline were associated with the cognitive status at 2 years, including all cognitive scores except for DTR and LT ($p < 0.0028$; Fig. 4). In the vast majority of studied regions, we found a positive association between the initial atrophy and the cognitive outcomes at 2 years (i.e. higher regional CTh or volume at baseline in EOAD predicted better z-scores at visit 2). The cortical and subcortical regions at baseline that were related to the cognitive status at visit 2 included: GC: lh amygdala, bankssts, fusiform, inferior parietal, lateral occipital, middle temporal, precuneus, superior parietal and supramarginal regions and rh parahippocampal, precuneus and supramarginal regions; MMSE: lh inferior temporal, middle temporal, superior frontal and supramarginal and rh inferior temporal, insula and supramarginal; FL: lh caudal middle frontal and superior temporal and rh rostral middle frontal; DFR: rh rostral middle frontal; BNT: lh/rh supramarginal, rh parahippocampal; BDAE: lh middle temporal and supramarginal and rh parahippocampal; SF: lh middle temporal, inferior temporal and superior frontal; CERAD: lh/rh bankssts and posterior cingulate, lh fusiform and supramarginal and rh precuneus and supramarginal; WAB: lh fusiform and superior parietal and rh parahippocampal; VOSP-letters: rh posterior cingulate and supramarginal; VOSP-numbers: lh posterior cingulate and precuneus; LFT: lh amygdala, bankssts and supramarginal and rh parahippocampal; TMT-A: lh/rh bankssts, inferior parietal and superior frontal, lh rostral middle frontal and supramarginal and rh fusiform, superior temporal, middle temporal and inferior temporal; Digits-B: rh parahippocampal and superior temporal ($p < 0.0028$).

On the other hand, higher CTh in lh superior parietal and lateral occipital regions at baseline was associated with lower scores in TL. Higher CTh in rh entorhinal was related to lower scores in Digits-F ($p < 0.0028$).

Discussion

In this prospective study, we investigated the relationship between initial atrophy in EOAD patients (A + T + N +) and the subsequent cognitive status 2 years later. We found that greater hemispheric CTh loss or LV enlargement at baseline predicted worse cognitive outcomes in global cognition and in non-amnestic domains. Furthermore, CTh measures of the neocortex in EOAD, rather than those of MTL structures, predicted neuropsychological scores at 2 years, except for the delayed verbal and visual memory scores.

EOAD's cognitive impairment at baseline involved amnestic and non-amnestic domains. These results support the clinical heterogeneity previously observed in EOAD patients, and they contrast with the predominance of memory alterations reported in LOAD [9, 36, 37]. We describe a pattern of widespread cortical atrophy, with relative preservation of the MTL cortex, which is in consonance with previous investigations reporting that the associative cortices are more vulnerable to atrophy than the MTL in EOAD [4–6]. Similarly, this pattern of extensive cortical reduction in EOAD has been related to

Journal of Neurology (2022) 269:2573–2583

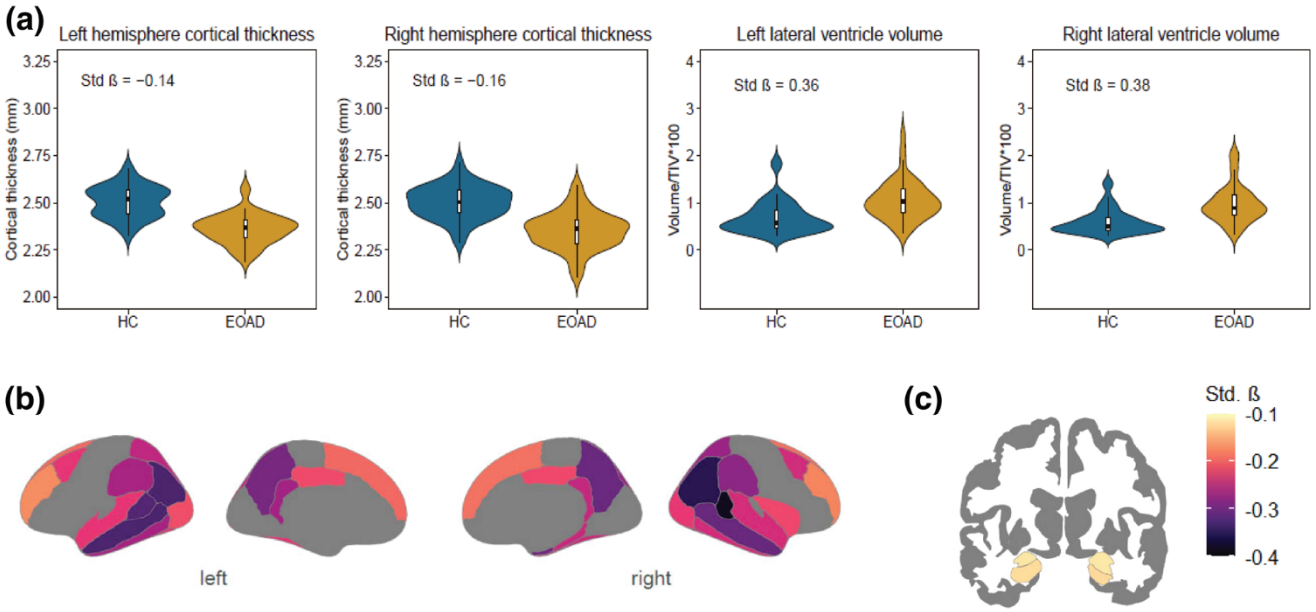

Fig. 2 EOAD and HC MRI significant differences in: **a** global structural measures, **b** regional cortical thickness and **c** subcortical gray matter volume. We show standardized β coefficients $p < 0.05$ (Bonferroni corrected) from linear models used to explore between-group differences in MRI measures at baseline. Key: *EOAD* early-onset AD; *HC* healthy control; *Std. β*, standardized β coefficients

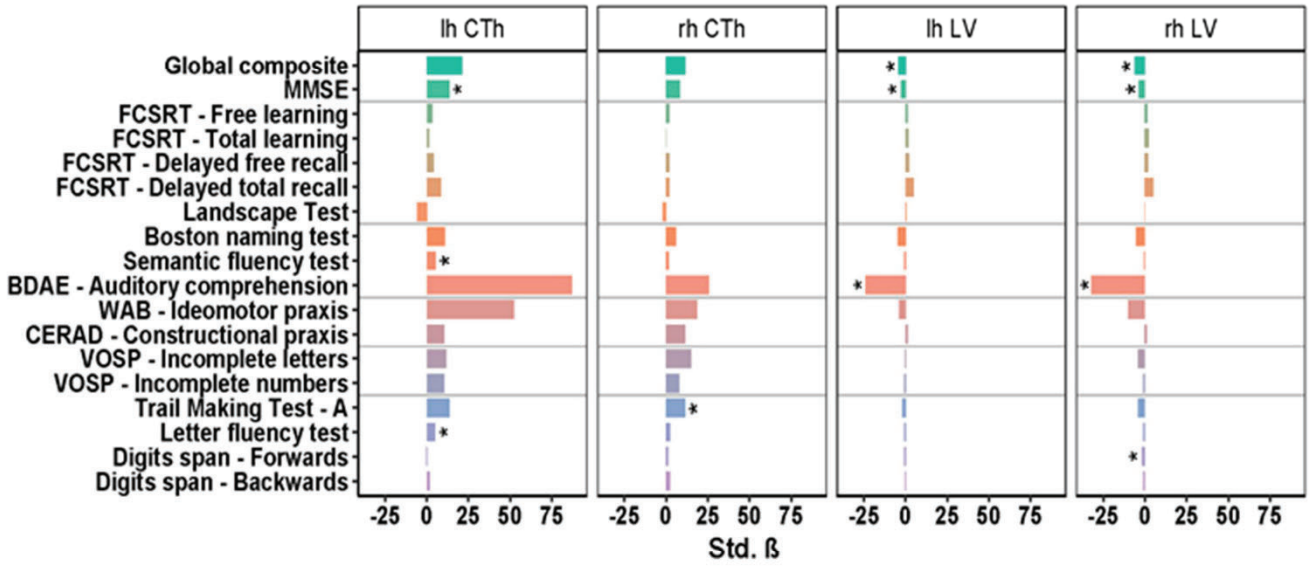

Fig. 3 Interaction between baseline structural measures in MRI and two-year cognitive outcomes in EOAD. We highlighted MRI measures that exhibited a significant MRI x Visit 2 interaction in linear mixed-effects models ($*p < 0.0028$). Key: *BDAE* Boston Diagnostic Aphasia Examination; *CERAD* Consortium to Establish a Registry for Alzheimer's disease; *CTh* cortical thickness; *FCSRT* Free and Cued Selective Reminding Test; *lh* left hemisphere; *LV* lateral ventricle; *MMSE* Mini-Mental State Examination; *rh* right hemisphere; *VOSP* visual object and space perception; *WAB* Western Aphasia Battery; *Std. β* standardized β coefficients

multidomain cognitive impairment [15], even suggesting that these patients have a more aggressive form of AD [3]. Furthermore, the observed decline in all the cognitive domains explored in our cohort aligns with the idea of a faster deterioration beyond the memory domain in EOAD patients without a biomarker-based diagnosis [38].

We showed that greater global atrophy in EOAD at baseline was associated with worse cognitive status in global

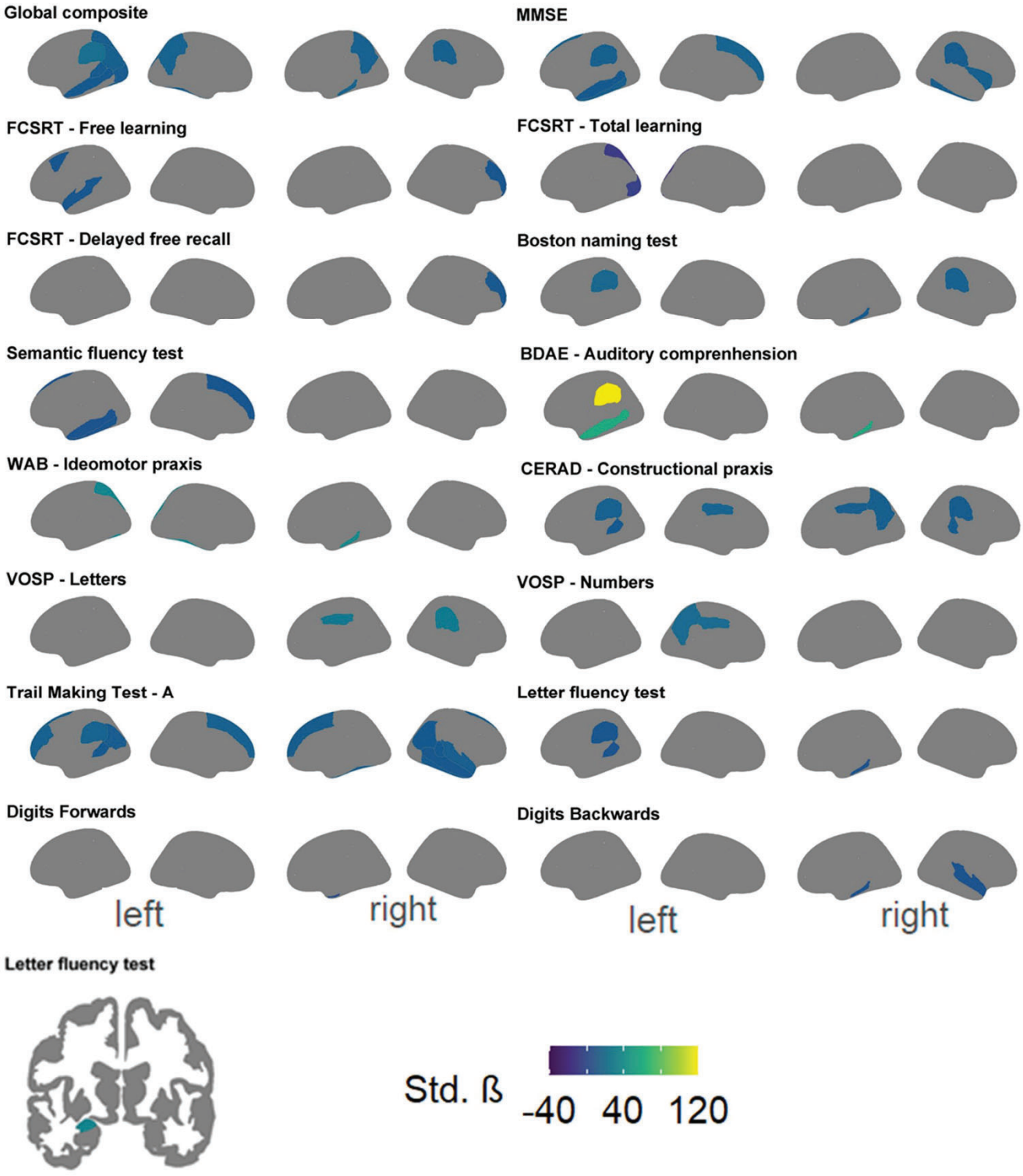

Fig. 4 Maps of cortical and subcortical regions that predicted cognitive outcomes at 2 years in EOAD ($p < 0.0028$). Abbreviations: *BDAE* auditory comprehension subtest from the Boston Diagnostic Aphasia Examination; *CERAD* Constructional praxis subtest from the Consortium to Establish a Registry for Alzheimer's disease battery; *MMSE* Mini-Mental State Examination; *WAB* Praxis Ideomotor praxis subtest from the Western Aphasia Battery; *Std β* standardized β coefficients

cognition, language and attentional/executive functioning. Previously, in cross-sectional studies, atrophy in EOAD has been related to global cognition and attentional/executive performance, whereas memory has been associated with atrophy in LOAD subjects. Moreover, cognitive impairment could be more related to atrophy in EOAD than in LOAD [16], in which other brain pathologies than AD contribute to the cognitive profile [39, 40].

Memory outcomes have been linked to AD atrophy, especially to the MTL [41]. However, our results suggest that global or MTL atrophy is not the best indicator of future memory performance in EOAD. We found that MRI measures of neocortical regions correlated with non-amnestic outcomes in EOAD. In addition, measures of the frontal and lateral-temporal regions were associated with memory outcomes (free learning and delayed free recall). Still, no brain region was associated with the future scores in delayed total recall or landscape test. We also observed that a relative conservation of right parietal and occipital regions was associated with worse learning outcomes, suggesting that EOAD patients with lesser posterior atrophy might show faster decline in this domain [15].

In our study, we did not find a relationship between the cognitive status at 2 years in EOAD and baseline hippocampal volume. In contrast, entorhinal CTh and amygdala volume predicted scores in the attention/executive domain. We are aware that neuropsychological constructs explore divergent aspects of cognition, and pathological changes might exert effect before atrophy appears [42]. However, our aim here was not to find atrophy correlates of the cognitive phenomenology in EOAD, but to provide structural information that might be useful for prediction models of disease evolution in EOAD patients. We have shown that baseline neocortical atrophy in EOAD might better predict the subsequent cognitive decline than the hippocampus, which might also be insensitive for EOAD diagnosis [7]. Our findings support the notion that atrophy beyond the MTL is associated with younger age and extensive cognitive decline, including non-amnestic domains [2, 43, 44], and different brain networks may be affected according to age at onset [45, 46]. According to our results, global cognition and domain-specific scores at 2 years in EOAD are mostly attributed to baseline atrophy in parietal and lateral temporal regions. These regions, rather than the MTL structures, might be useful for identifying patients with a faster clinical progression of the disease.

The strengths of our study are the use of CSF biomarkers for the characterization of all participants. In addition, we used global and regional measures of atrophy, including CTh and subcortical gray matter volume, to predict cognitive performance in a comprehensive neuropsychological evaluation, including 16 cognitive test (five cognitive domains) and global cognition measures. The main limitation is the relatively small sample size and the loss of patients longitudinally, especially at 2 years. In this sense, we tried to minimize longitudinal biases by using a LME approach to our data. On the other hand, we examined the effect of a single brain region on future cognitive status, while a multivariate analysis including multiple brain areas as predictors might estimate the importance of each MRI measure to the cognitive outcomes and the interdependencies between different regions. Another limitation of our work is the lack of a LOAD sample to compare our results with. However, LOAD was outside the scope of our research cohort, which is based uniquely in EOAD. Although there are previous studies in LOAD subjects or that do not take into account the age of the participants, we believe that the comparison of our findings to those in LOAD would be useful to better understand the differences between AD patients according to the age at onset. Furthermore, fluorodeoxyglucose positron emission tomography (FDG-PET) data is not available in our study and we are aware that the association of the FDG-PET uptake with the neuropsychological scores, and the comparison of these findings with the MRI results, would help to better understand the relationship between neurodegeneration and clinical progression. Nevertheless, to our knowledge, this is the first prospective study to investigate the relationship between the initial brain atrophy and the short-term cognitive outcomes in EOAD subjects with a biomarker-based diagnosis. Our study provides data for future hypothesis testing, narrowing the field of brain MRI measurements that could predict the evolution of the disease in EOAD. The demonstration of the efficacy of disease-modifying therapies is obtained through biomarkers and clinical assessments. A better understanding of the disease according to the age at onset could provide specific biomarkers of clinical progression for each individual in clinical trial designs, selecting those individuals with a higher risk of clinical decline and increasing the chance of observing a positive response to drugs.

In conclusion, global atrophy in EOAD at baseline was related to outcomes in global cognition, language and attentional/executive functioning at 2 years. However, memory, praxis or visuospatial outcomes were not related to global atrophy in EOAD. On the other hand, baseline atrophy in neocortical regions in EOAD was associated with the future cognitive status in all domains and global cognition. However, the hippocampus was insensitive to predict cognitive changes over time. Whether cognitive performance in EOAD can be predicted by an age-specific pattern of atrophy must be assessed in larger cohorts.

Supplementary Information The online version contains supplementary material available at https://doi.org/10.1007/s00415-021-10851-9.

Acknowledgements The authors thank patients, their relatives and healthy controls for their participation in the research. We acknowledge support for the project provided by Spanish Ministry of Science and Innovation-Instituto de Salud Carlos III, Fondo Europeo de Desarrollo Regional (FEDER), Unión Europea, "Una manera de hacer Europa", CERCA Programme/Generalitat de Catalunya and Departament de Salut—Generalitat de Catalunya (PERIS 2016-2020). We also are indebted to the Magnetic Resonance Image core facility of the Institut d'Investigacions Biomèdiques August Pi i Sunyer (IDIBAPS) for the technical help.

Funding This work was supported by Spanish Ministry of Science and Innovation-Instituto de Salud Carlos III and Fondo Europeo de Desarrollo Regional (FEDER), Unión Europea, "Una manera de hacer Europa" [PI19/00449 to Dr. Lladó (AL)] and CERCA Programme/Generalitat de Catalunya. AL also received funding from Departament de Salut—Generalitat de Catalunya (PERIS 2016–2020 SLT008/18/00061). Roser Sala-Llonch received funding from the Biomedical Imaging Group, Biomedical Research Networking Center in Bioengineering, Biomaterials and Nanomedicine (CIBER-BBN), Barcelona, Spain. Nuria Guillén received funding from a PFIS grant (FI20/00076). Oscar Ramos received funding from a PFIS grant (FI18/00121). This work has been partially performed thanks to the 3T Equipment of Magnetic Resonance at IDIBAPS (project IBPS15-EE-3688 co funded by MCIU and by ERDF).

Data availability The summary tables that support the findings of this study are available on request from the corresponding author, AL.

Code availability Code used in this study is available on request from the corresponding author, AL.

Declarations

Conflicts of interest On behalf of all authors, the corresponding author states that there is no conflict of interest.

Ethical approval Approval was obtained from Hospital Clínic Ethics Committee. The procedures used in this study adhere to the tenets of the Declaration of Helsinki.

Consent to participate/Consent for publication Informed consent was obtained from all individual participants included in the study.

References

1. Jack CR, Knopman DS, Jagust WJ et al (2013) Tracking pathophysiological processes in Alzheimer's disease: an updated hypothetical model of dynamic biomarkers. Lancet Neurol 12:207–216. https://doi.org/10.1016/S1474-4422(12)70291-0
2. Murray ME, Graff-Radford NR, Ross OA et al (2011) Neuropathologically defined subtypes of Alzheimer's disease with distinct clinical characteristics: a retrospective study. Lancet Neurol 10:785–796. https://doi.org/10.1016/S1474-4422(11)70156-9
3. Mendez MF (2012) Early-onset Alzheimer's disease: nonamnestic subtypes and type 2 AD. Arch Med Res 43:677–685. https://doi.org/10.1016/j.arcmed.2012.11.009
4. Ossenkoppele R, Cohn-Sheehy BI, La Joie R et al (2015) Atrophy patterns in early clinical stages across distinct phenotypes of Alzheimer's disease. Hum Brain Mapp 36:4421–4437. https://doi.org/10.1002/hbm.22927
5. Aziz AL, Giusiano B, Joubert S et al (2017) Difference in imaging biomarkers of neurodegeneration between early and late-onset amnestic Alzheimer's disease. Neurobiol Aging 54:22–30. https://doi.org/10.1016/j.neurobiolaging.2017.02.010
6. Harper L, Bouwman F, Burton EJ et al (2017) Patterns of atrophy in pathologically confirmed dementias: a voxelwise analysis. J Neurol Neurosurg Psychiatry 88:908–916. https://doi.org/10.1136/jnnp-2016-314978
7. Falgàs N, Sánchez-Valle R, Bargalló N et al (2019) Hippocampal atrophy has limited usefulness as a diagnostic biomarker on the early onset Alzheimer's disease patients: a comparison between visual and quantitative assessment. NeuroImage Clin 23:101927. https://doi.org/10.1016/j.nicl.2019.101927
8. Koedam ELGE, Lauffer V, Van Der Vlies AE et al (2010) Early-versus late-onset Alzheimer's disease: more than age alone. J Alzheimer's Dis 19:1401–1408. https://doi.org/10.3233/JAD-2010-1337
9. Balasa M, Gelpi E, Antonell A et al (2011) Clinical features and APOE genotype of pathologically proven early-onset Alzheimer disease. Neurology 76:1720–1725. https://doi.org/10.1212/WNL.0b013e31821a44dd
10. Jack CR, Bennett DA, Blennow K et al (2018) NIA-AA research framework: toward a biological definition of Alzheimer's disease. Alzheimer's Dement 14:535–562. https://doi.org/10.1016/j.jalz.2018.02.018
11. Schuff N, Woerner N, Boreta L et al (2009) MRI of hippocampal volume loss in early Alzheimers disease in relation to ApoE genotype and biomarkers. Brain 132:1067–1077. https://doi.org/10.1093/brain/awp007
12. Van Rossum IA, Vos SJB, Burns L et al (2012) Injury markers predict time to dementia in subjects with MCI and amyloid pathology. Neurology 79:1809–1816. https://doi.org/10.1212/WNL.0b013e3182704056
13. Marizzoni M, Ferrari C, Jovicich J et al (2019) Predicting and tracking short term disease progression in amnestic mild cognitive impairment patients with prodromal Alzheimer's disease: structural brain biomarkers. J Alzheimer's Dis 69:3–14. https://doi.org/10.3233/JAD-180152
14. Tabatabaei-Jafari H, Shaw ME, Walsh E, Cherbuin N (2019) Regional brain atrophy predicts time to conversion to Alzheimer's disease, dependent on baseline volume. Neurobiol Aging 83:86–94. https://doi.org/10.1016/j.neurobiolaging.2019.08.033
15. Phillips ML, Stage EC, Lane KA et al (2019) Neurodegenerative patterns of cognitive clusters of early-onset Alzheimer's disease subjects: evidence for disease heterogeneity. Dement Geriatr Cogn Disord 46202:1–12. https://doi.org/10.1159/000504341
16. Van Der Vlies AE, Staekenborg SS, Admiraal-Behloul F et al (2013) Associations between magnetic resonance imaging measures and neuropsychological impairment in early and late onset Alzheimer's disease. J Alzheimer's Dis 35:169–178. https://doi.org/10.3233/JAD-121291
17. McKhann GM, Knopman DS, Chertkow H et al (2011) The diagnosis of dementia due to Alzheimer's disease: recommendations from the National Institute on Aging-Alzheimer's Association workgroups on diagnostic guidelines for Alzheimer's disease. Alzheimer's Dement 7:263–269. https://doi.org/10.1016/j.jalz.2011.03.005
18. Albert MS, DeKosky ST, Dickson D et al (2011) The diagnosis of mild cognitive impairment due to Alzheimer's disease: recommendations from the National Institute on Aging-Alzheimer's Association workgroups on diagnostic guidelines for Alzheimer's disease. Alzheimer's Dement 7:270–279. https://doi.org/10.1016/j.jalz.2011.03.008
19. Antonell A, Tort-Merino A, Ríos J et al (2020) Synaptic, axonal damage and inflammatory cerebrospinal fluid biomarkers in

neurodegenerative dementias. Alzheimer's Dement 16:262–272. https://doi.org/10.1016/j.jalz.2019.09.001
20. Folstein MF, Folstein SE, McHugh PR (1975) "Mini-mental state". A practical method for grading the cognitive state of patients for the clinician. J Psychiatr Res. https://doi.org/10.1016/0022-3956(75)90026-6
21. Grober E, Buschke H, Korey SR (1987) Genuine memory deficits in dementia. Dev Neuropsychol 3:13–36. https://doi.org/10.1080/87565648709540361
22. Valls Pedret C, Olives Cladera J, Bosch Capdevila B et al (2011) Test de paisajes para la valoración de la memoria visual en la enfermedad de Alzheimer. Rev Neurol 53:1. https://doi.org/10.33588/rn.5301.2011238
23. Kaplan E, Goodglass HWS (1983) The Boston Naming Test. Philadelphia Lea Febiger
24. Roth C (2011) Boston Diagnostic Aphasia Examination. In: Jeffrey SK, John D, Bruce C (eds) Encyclopedia of Clinical Neuropsychology. Springer, New York
25. Goodglass H, Kaplan E, Barresi B (2001) The Assessment of Aphasia and Related Disorders. Lippincott Williams & Wilkins
26. Kertesz A (2007) Western Aphasia Battery: Revised. Pearson
27. Morris JC, Heyman A, Mohs RC et al (1989) The consortium to establish a registry for Alzheimer's disease (CERAD). Part I. Clinical and neuropsychological assessment of Alzheimer's disease. Neurology. https://doi.org/10.1212/wnl.39.9.1159
28. Warrington EK, James M (1991) The visual object and space perception battery
29. Reitan RM, Wolfson D (1985) The Halstead-Reitan Neuropsychological Test Battery: theory and clinical interpretation. Neuropsychology Press, USA
30. Newcombe F (1969) Missile Wounds of the Brain: a Study of Psychological Deficits. Oxford U.P.
31. Wechsler D (2008) WAIS-IV : Wechsler adult intelligence scale. TX Psychol Corp, San Antonio
32. Fischl B, Dale AM (2000) Measuring the thickness of the human cerebral cortex from magnetic resonance images. Proc Natl Acad Sci USA 97:11050–11055. https://doi.org/10.1073/pnas.200033797
33. Fischl B, van der Kouwe A, Destrieux C et al (2004) Automatically parcellating the human cerebral cortex. Cereb Cortex 14:11–22. https://doi.org/10.1093/cercor/bhg087
34. Desikan RS, Ségonne F, Fischl B et al (2006) An automated labeling system for subdividing the human cerebral cortex on MRI scans into gyral based regions of interest. Neuroimage 31:968–980. https://doi.org/10.1016/j.neuroimage.2006.01.021
35. Seidman LJ, Faraone SV, Goldstein JM et al (1997) Reduced subcortical brain volumes in nonpsychotic siblings of schizophrenic patients: a pilot magnetic resonance imaging study. Am J Med Genet Neuropsychiatr Genet 74:507–514. https://doi.org/10.1002/(SICI)1096-8628(19970919)74:5%3c507::AID-AJMG11%3e3.0.CO;2-G
36. Palasí A, Gutiérrez-Iglesias B, Alegret M et al (2015) Differentiated clinical presentation of early and late-onset Alzheimer's disease: is 65 years of age providing a reliable threshold? J Neurol 262:1238–1246. https://doi.org/10.1007/s00415-015-7698-3
37. Smits LL, Pijnenburg YAL, Koedam ELGE et al (2012) Early onset Alzheimer's disease is associated with a distinct neuropsychological profile. J Alzheimer's Dis 30:101–108. https://doi.org/10.3233/JAD-2012-111934
38. Wattmo C, Wallin ÅK (2017) Early- versus late-onset Alzheimer disease: long-term functional outcomes, nursing home placement, and risk factors for rate of progression. Dement Geriatr Cogn Dis Extra 7:172–187. https://doi.org/10.1159/000455943
39. Pontecorvo MJ, Devous MD, Navitsky M et al (2017) Relationships between flortaucipir PET tau binding and amyloid burden, clinical diagnosis, age and cognition. Brain 140:748–763. https://doi.org/10.1093/brain/aww334
40. Koychev I, Gunn RN, Firouzian A et al (2017) PET tau and amyloid-β burden in mild Alzheimer's disease: divergent relationship with age, cognition, and cerebrospinal fluid biomarkers. J Alzheimer's Dis 60:283–293. https://doi.org/10.3233/JAD-170129
41. Quenon L, Dricot L, Woodard JL et al (2016) Prediction of free and cued selective reminding test performance using volumetric and amyloid-based biomarkers of Alzheimer's disease. J Int Neuropsychol Soc 22:991–1004. https://doi.org/10.1017/S1355617716000813
42. Ossenkoppele R, Smith R, Ohlsson T et al (2019) Associations between tau, Aβ, and cortical thickness with cognition in Alzheimer disease. Neurology 92:e601–e612. https://doi.org/10.1212/WNL.0000000000006875
43. Whitwell JL, Dickson DW, Murray ME et al (2012) Neuroimaging correlates of pathologically defined subtypes of Alzheimer's disease: a case-control study. Lancet Neurol 11:868–877. https://doi.org/10.1016/S1474-4422(12)70200-4
44. Risacher SL, Anderson WH, Charil A et al (2017) Alzheimer disease brain atrophy subtypes are associated with cognition and rate of decline. Neurology 89:2176–2186. https://doi.org/10.1212/WNL.0000000000004670
45. Park KH, Noh Y, Choi EJ et al (2017) Functional connectivity of the hippocampus in early- and vs. late-onset alzheimer's disease. J Clin Neurol 13:387–393. https://doi.org/10.3988/jcn.2017.13.4.387
46. Dickerson BC, Brickhouse M, McGinnis S, Wolk DA (2017) Alzheimer's disease: The influence of age on clinical heterogeneity through the human brain connectome. Alzheimer's Dement Diagnosis. Assess Dis Monit 6:122–135. https://doi.org/10.1016/j.dadm.2016.12.007

Supplementary material:

Supplementary Table 1
Demographics, clinical characteristics, and CSF biomarker levels for participants at visit 1

	EOAD (n=23)			HC (n=29)			
	N	Mean	SD	N	Mean	SD	p value
Age at onset (years)	23	55.87	4.60	N/A	N/A	N/A	N/A
CSF Aβ42 (pg/ml)	23	396.91	119.47	29	857.49	230.82	2^{-12}*
CSF p-tau (pg/ml)	23	101.66	33.11	29	51.44	11.79	7^{-08}*
CSF t-tau (pg/ml)	23	692.59	330.51	29	225.94	70.66	1^{-09}*
Time baseline-Visit 1 (years)	23	1.07	0.14	29	1.11	0.13	0.2
Age at NPS (years)	23	59.71	4.65	29	59.51	4.36	1
MMSE score (baseline)	23	22.30	3.18	29	28.72	1.49	5^{-09}*
MMSE score (Visit 1)	22	20.64	5.25	29	28.90	1.21	4^{-08}*
Time Visit 1 - MRI (years)	23	1	0.14	29	1.09	0.19	0.16
Time Visit 2 - LP (years)	23	1.11	0.19	29	1.13	0.24	0.57
Years of education	23	11.78	4.49	29	12.07	4.17	0.80
Sex (Female)	14	N/A	N/A	22	N/A	N/A	0.37
Laterality (Right)	22	N/A	N/A	27	N/A	N/A	1
APOE4 (Carriers)	8	N/A	N/A	3	N/A	N/A	0.04*

EOAD and HC characteristics at Visit 1. Asterisks indicate significant differences at $p<0.05$.
Key: EOAD, early-onset AD; HC, healthy controls; NPS, Neuropsychological assessment; N/A, not applicable; MRI, Magnetic resonance imaging; CSF, cerebrospinal fluid; MMSE, Mini-Mental State Examination; Aβ42, amyloid β42; p-tau, phosphorylated tau; t-tau, total tau; LP, Lumbar Puncture; SD, standard deviation

Supplementary Table 2
Demographics, clinical characteristics and CSF biomarker levels for participants at visit 2

	EOAD (n=15)			HC (n=28)			
	N	Mean	SD	N	Mean	SD	p value
Age at onset (years)	15	57.60	4.63	-	-	-	-
CSF Aβ42 (pg/ml)	15	413.57	112.25	28	870.12	228.06	9^{-10}*
CSF p-tau (pg/ml)	15	94.01	31.38	28	55.16	13.14	7^{-05}*
CSF t-tau (pg/ml)	15	654.24	288.42	28	238.60	72.56	1^{-08}*
Time baseline-Visit 2	15	2.03	0.12	28	2.11	0.17	0.13
Age at Visit 2(years)	15	62.11	4.86	28	58.86	4.07	0.03*
MMSE score (baseline)	15	21.80	3.19	28	28.93	1.54	1^{-07}*
MMSE score (Visit 2)	15	15.27	5.06	27	29.00	1.07	6^{-08}*
Time Visit 2- MRI (years)	15	1.98	0.12	28	2.10	0.19	0.03*
Time Visit 2 - LP (years)	15	2.06	0.18	28	2.13	0.23	0.10
Years of education	15	11.13	4.53	28	12.39	4.10	0.27
Sex (Female)	9	N/A	N/A	22	N/A	N/A	0.29
Laterality (Right)	14	N/A	N/A	26	N/A	N/A	1
APOE4 (Carriers)	5	N/A	N/A	6	N/A	N/A	0.47

EOAD and HC characteristics at visit 2. Asterisks indicate significant differences at $p<0.05$. Key: EOAD, early-onset AD; HC, healthy controls; NPS, Neuropsychological assessment; N/A, not applicable; MRI, Magnetic resonance imaging; CSF, cerebrospinal fluid; MMSE, Mini-Mental State Examination; Aβ42, amyloid β42; p-tau, phosphorylated tau; t-tau, total tau; LP, Lumbar Puncture; SD, standard deviation Examination.

VII. DISCUSION

VII. DISCUSION

En los trabajos que conforman la presente tesis doctoral se han investigado las alteraciones transversales y los cambios longitudinales en RM craneal estructural en sujetos con EAIP confirmada biológicamente, además de la variabilidad existente en la enfermedad en base al sexo de los sujetos. Por otro lado, los trabajos incluidos también han evaluado la capacidad de la RM craneal estructural para predecir la evolución cognitiva de los sujetos con EAIP, así como la relación entre los niveles de biomarcadores en LCR en el momento del diagnóstico y la progresión de la atrofia, ampliando el conocimiento sobre el valor pronóstico de los biomarcadores en la EAIP. Si bien algunos trabajos previos han estudiado los cambios patológicos en la EAIP, son pocos los estudios que incluyen exclusivamente sujetos con confirmación de la enfermedad mediante el uso de biomarcadores en LCR y un perfil A+T+N+ según los últimos criterios de investigación de la NIA-AA de 2018 (28).

El primer trabajo presentado investiga de forma transversal las diferencias en grosor cortical, volumen hipocampal y sus subcampos, deterioro cognitivo y niveles de biomarcadores de LCR entre mujeres y hombres con EAIP en fase de DCL o demencia leve. Aunque trabajos previos han evaluado diferencias en diferentes biomarcadores entre sexos en la EA (ver Ferretti et al., 2018 para una revisión (53)), este es el primer trabajo exclusivamente centrado en la EAIP. Los resultados de este trabajo indican que existen diferencias en la propagación y susceptibilidad a la enfermedad entre sexos en la EAIP. Aunque puedan ser sutiles, los hallazgos añaden nueva información para crear grupos biológicamente más homogéneos en futuras investigaciones, necesarios ya sea para entender la fisiopatología de la enfermedad o probar la eficacia de tratamientos modificadores de la enfermedad (103). Según los resultados de este primer trabajo, la extensión de la atrofia, la magnitud de los síntomas cognitivos y su relación con la atrofia cerebral, o los niveles de tau en LCR, podrían variar según el sexo de los sujetos con EAIP, añadiendo heterogeneidad a los estudios si no se tuviera en cuenta este factor en su planificación.

Por un lado, cuando se comparan directamente hombres y mujeres con EAIP, los hombres parecen mostrar una mayor pérdida cortical en el LTM, concretamente en la región parahipocampal. Sin embargo, al comparar mujeres y hombres con sus respectivos controles, el patrón de pérdida cortical es más extenso en las mujeres en el momento del diagnóstico, afectando a regiones parietotemporales de ambos hemisferios y no a la corteza del LTM, mientras que en los hombres la pérdida cortical está más limitada al hemisferio izquierdo y afecta a la corteza del LTM. Acorde con la

pérdida cortical, las mujeres muestran afectación de ambos hipocampos y la mayoría de los subcampos hipocampales, mientras que la afectación de los subcampos es más limitada en hombres, y únicamente el hipocampo izquierdo muestra diferencias con los controles del mismo sexo. Los patrones de pérdida cortical en el neocórtex observados en ambos sexos son congruentes con los hallazgos de estudios en la EAIP que no han tenido en cuenta la influencia del sexo (67–71), y van en la línea de los hallazgos de los siguientes trabajos presentados en esta tesis doctoral. Sin embargo, en cuanto al hipocampo, estudios previos han descrito una pérdida de volumen generalizada en los subcampos del hipocampo en la EAIP (75), que van más en consonancia con los hallazgos encontrados en las mujeres. Llama la atención que la región Cuerno de Amón 1 (CA1) del hipocampo no mostró diferencias frente a controles en hombres, cuando ha sido descrita como una de las regiones iniciales de depósito de neurofibrilar en la EA (104). No obstante, se ha descrito un fenotipo de EA con escasa afectación hipocampal que es más frecuente en hombres (105). Además, la evidencia previa en la EA apunta a que las mujeres presentan una mayor carga de patología tau en la corteza y el hipocampo, tanto en estudios de PET (93,106) como anatomopatológicos (59,60). Otros estudios anatomopatológicos analizando sujetos con EAIP también han encontrado un mayor grado de patología tau en mujeres, incluyendo los subcampos del hipocampo CA1 y subiculum, y sin que existan diferencias en el número de diagnósticos patológicos concomitantes entre sexos (18). Por otro lado, aun siendo aquí la frecuencia de portadores del alelo ε4 de *APOE* similar entre sexos en EAIP, el alelo ε4 podría condicionar una mayor atrofia hipocampal en mujeres que en hombres con EA (107). También la mayor frecuencia del genotipo de *APOE ε4* en mujeres con EAIP que en sus respectivos controles podría verse reflejada en una mayor afectación hipocampal en mujeres con la enfermedad. Sin embargo, para evitar precisamente la influencia de este factor, nuestros resultados han sido ajustados por la presencia o no del alelo ε4 de *APOE*.

Acorde con nuestros hallazgos, cuando se usen medidas de RM craneal para evaluar la progresión de la EAIP, no sólo la edad de inicio puede influir, sino también el sexo de los sujetos. En este sentido, la utilización de regiones como el precuneus podría asegurar que se están evaluando cambios en el grosor cortical en ambos sexos en la EAIP, mientras que la corteza del LTM o el hipocampo parecen mostrar dimorfismo sexual. Las diferencias en cuanto a cómo se organizan los cambios patológicos en el cerebro de hombres y mujeres podrían estar en relación con vías anatómicas y funcionales, y conexiones asociadas, específicas para cada uno de los sexos. Así, algunos trabajos han mostrado una mayor densidad de redes neuronales y conexiones regionales en relación con una mayor

carga de tau en todo el cerebro en mujeres con EA (108). En este sentido, los sujetos con EAIP también parecen mostrar un patrón de redes neuronales que se diferencia de la EAIT, con menos cambios funcionales en regiones conectadas con el hipocampo (109). Nuevos estudios en el futuro centrados en la EAIP tendrán que analizar las diferencias en redes neuronales entre sexos y su relación con la neurodegeneración.

Por otro lado, en este primer trabajo y en línea con la evidencia actual, no encontramos diferencias entre sexos en los niveles de Aβ42 en LCR (32). Por contra, las mujeres con EAIP presentaron niveles más altos de p-tau y t-tau en LCR que los hombres. Sin embargo, no encontramos una relación con el genotipo de *APOE* como trabajos previos, en los que niveles más altos de tau en mujeres se asociaron a la presencia del alelo ε4 de *APOE* (65,110). Por otro lado, otros estudios han encontrado niveles más altos de tau tanto en mujeres portadoras de *APOE* ε4 como en no portadoras dependiendo del estadio clínico de la enfermedad (111). Si bien la asociación entre el depósito cerebral de tau y los niveles de p-tau o t-tau en LCR es modesta en sujetos con EA amiloide positivos (112), en nuestro trabajo se podría hipotetizar que los niveles más altos de t-tau o p-tau en mujeres podrían estar en relación con la mayor extensión de la neurodegeneración observada en ellas o un supuesto mayor depósito de ovillos neurofibrilares de tau. Además, existe evidencia de que la disminución de los niveles de estradiol en mujeres posmenopáusicas parece aumentar la actividad de las enzimas involucradas en la fosforilación de tau, conduciendo a niveles más altos de p-tau. Por otro lado, la caída de los niveles de estrógenos provocarían un mayor estrés oxidativo y disfunción mitocondrial, que a través de mecanismos de apoptosis podría provocar aumentos en las concentraciones de t-tau (113). Niveles más altos de testosterona también podrían ser un factor protector frente al aumento de tau (114). Teniendo en cuenta estos hallazgos, sería necesario investigar más en profundidad si los puntos de corte han de ser diferentes para cada sexo, buscando que sean lo más sensibles y específicos posible para mujeres u hombres. En este trabajo se ha visto también que las concentraciones de NfL en LCR, biomarcador de neurodegeneración como t-tau, no mostraron diferencias entre hombres y mujeres, en contra de la evidencia previa que muestra niveles más altos en hombres (64). Si bien t-tau y NfL son biomarcadores de neurodegeneración, proporcionan en parte información independiente sobre la integridad neuronal. Los NfL en LCR son una medida de daño axonal inespecífico mientras que t-tau, aunque también se elevaría en otras condiciones, podría reflejar un daño neuronal más indicativo de EA (115), y además sus niveles están estrechamente relacionados con los niveles de p-tau. Los niveles de NfL parecen aumentar con la edad, se relacionan con la presencia de factores de riesgo cardiovasculares y

aumentan en otras enfermedades neurológicas. Hasta qué punto la edad u otros factores juegan un papel en los niveles de NfL en cada sexo tendrá que ser evaluado en futuros estudios.

Por último, acorde con la mayor extensión en mujeres de pérdida de grosor cortical y volumen hipocampal en ambos hemisferios, este primer trabajo también muestra como el sexo femenino parece presentar deterioro en más dominios cognitivos que los hombres cuando se compara con controles de su mismo sexo. Estos hallazgos son congruentes con la evidencia previa, sobre todo en EAIT, que apunta a una mayor afectación cognitiva en mujeres (58,116,117). Así mismo, que las mujeres presenten mayores diferencias cognitivas frente a controles de su mismo sexo podría tener que ver con la mayor ventaja cognitiva de las mujeres sanas, principalmente en memoria verbal (118), ventaja que parece desaparecer o incluso invertirse con la enfermedad. Por el contrario, los hombres parecen preservar las habilidades visoperceptivas/visoespaciales y motoras (119). Además, no sólo el patrón de atrofia y el deterioro cognitivo es más extenso en mujeres, sino que la relación entre ambos podría ser más estrecha. En este trabajo, menor grosor cortical en regiones parietotemporales o menor volumen hipocampal se correlacionó con peores puntuaciones cognitivas exclusivamente en el sexo femenino. Trabajos previos también han encontrado una mayor relación entre el depósito de tau y las puntuaciones cognitivas en mujeres (120), y sería interesante examinar en el futuro si otros procesos patológicos se relacionan con el deterioro cognitivo. Hay que tener presente que habitualmente se usan medidas cognitivas para definir y monitorizar la enfermedad, y aquí se han utilizado medidas cognitivas similares para mujeres y hombres, mientras que sería importante analizar el uso de evaluaciones más específicas para cada sexo, medidas que podrían presentar una mejor relación con la atrofia dependiendo del sexo y reflejar la evolución de la enfermedad más estrechamente. Por otro lado, medidas de atrofia en RM que sean comunes para mujeres y hombres también servirían para capturar adecuadamente los cambios de la enfermedad.

Una de las grandes limitaciones de este estudio es que no se han tenido en cuenta los cambios vasculares u hormonales de los sujetos. Existe evidencia de que la enfermedad cerebrovascular contribuye al deterioro cognitivo en la EA (121), y el sexo masculino parece que presenta más cambios vasculares relacionados con la edad (122). Además, el papel de las hormonas sexuales es un importante objeto de estudio en el dimorfismo sexual del deterioro cognitivo (123). Futuros estudios tendrán que analizar la influencia de estos factores en las diferencias entre sexos en la EAIP.

Tras añadir información a la evidencia disponible de estudios transversales de RM craneal en la EAIP, el segundo trabajo de esta tesis se ha centrado

en evaluar la capacidad de la RM craneal de describir los cambios longitudinales en grosor cortical y volumen subcortical en sujetos con EAIP con un perfil A+T+N+ en LCR. Aunque algunos estudios han evaluado con anterioridad la evolución de la atrofia en la EAIP, las conclusiones hacía un patrón de atrofia longitudinal característico no son del todo concluyentes, ya que la mayoría de estos trabajos han incluido sujetos sin confirmación biológica de la enfermedad mediante biomarcadores (72–74) y/o han evaluado el efecto de la edad como covariable en los análisis estadísticos (78,86,124,125). Por otro lado, el uso frecuente de medidas de volumen sin añadir medidas de grosor cortical han podido limitar también los resultados previos, pues las últimas parecen estar menos influenciadas por otras patologías o la edad (126).

Los hallazgos de este segundo trabajo muestran que la pérdida de grosor cortical y volumen subcortical en el momento del diagnóstico involucra regiones parietales, temporales laterales y occipitales, además del hipocampo y la amígdala, mientras que la corteza entorrinal y parahipocampal no muestran diferencias respecto a controles. Posteriormente, en un tiempo de dos años, la atrofia se extiende por el neocórtex, incluyendo el LTM, y afectando a estructuras subcorticales más allá del hipocampo o la amígdala. Este trabajo muestra que la EAIP A+T+N+ presenta una afectación progresiva y nada desdeñable de estructuras neocorticales diferente de la afectación más focalizada en el LTM de la EAIT (74), con un gradiente de atrofia que va desde regiones posteriores a anteriores (86,125). Además, la afectación de estructuras subcorticales más allá del hipocampo y la amígdala va en la línea las descripciones previas en EAIP (72,125), no estando tampoco limitada la afectación subcortical al LTM. Según la clasificación anatomopatológica actual de la enfermedad, el estadio de acúmulo de ovillos neurofibrilares de tau en el LTM precedería a su aparición neocortical (11,12), sin embargo ésta no sería la única forma en que la patología se extiende por el cerebro. Estudios anatomopatológicos que han tenido en cuenta la edad de inicio (16,17,127) muestran menor afectación del LTM y mayor carga patológica fuera de él en sujetos jóvenes con la enfermedad, congruente con el patrón que hemos observado. También los estudios de PET-tau, tanto de corte transversal (86,88,89) como longitudinal (87,128), han encontrado mayor depósito de patología tau fuera del LTM en sujetos jóvenes. Por otro lado, la captación de flortaucipir en el LTM se ha visto que aumenta con la edad independientemente de la positividad de amiloide (90), por lo que la afectación por la patología tau independiente de amiloide en el LTM en jóvenes no sería tan prominente. Nuestro estudio muestra, al menos a nivel de atrofia, una extensa afectación en regiones neocorticales antes que en la corteza del LTM, apoyando que existe una secuencia diferente de progresión de la atrofia a lo esperado en la

EAIT, y que podría traducir diferencias en el depósito de tau dependiendo de la edad de inicio. Por otro lado, las alteraciones mnésicas en la EA tradicionalmente han sido ligadas a la pérdida neuronal en estructuras del LTM. Sin embargo, este segundo trabajo, compuesto mayormente por sujetos con un inicio amnésico, apoyaría la hipótesis de que los síntomas de la enfermedad podrían estar en relación con la disrupción de otras redes anatómicas más allá de la red funcional por defecto (129–131). Así una mayor afectación del fascículo fronto-occipital o cíngulo en la EAIP (132), facilitarían la propagación de la patología tau de forma más rápida. Esto explicaría en parte la morfología específica de la extensión de la patología tau en la EAIP frente a la EAIT.

Debido al tamaño limitado de la muestra de este trabajo, no se ha realizado un análisis estratificado por sexos, si bien cabría preguntarse, al tratarse de participantes de la misma cohorte y en vista de los hallazgos del primer trabajo, si el hecho de que no existan diferencias respecto a controles en la corteza del LTM no estará influenciado por la mayor proporción de mujeres en este estudio (2:1). Además, al ser el genotipo *APOE* un factor que confiere patrones de vulnerabilidad a la enfermedad específicos en el cerebro, la baja proporción de sujetos portadores de *APOE* ε4 también podría contribuir a la mayor atrofia en regiones posteriores observada, mientras que una mayor edad y el alelo ε4 se asociarían a un patrón de atrofia más centrado en el LTM (81). El hecho de que, como hemos visto, exista menor afectación del LTM en fases de DCL o demencia leve y además muestre dimorfismo sexual, apoya que no es una región con gran aplicabilidad clínica en la EAIP (66). En vista de los hallazgos, se podría hipotetizar que es preferible usar regiones corticales parietales o temporales laterales, que se encuentran afectadas desde fases iniciales y en ambos sexos.

Estudios previos han analizado de forma transversal la asociación de los niveles de biomarcadores en LCR con la pérdida cerebral en la EAIP (62,70). Sin embargo, todavía no existen biomarcadores que permitan detectar qué sujetos con EA presentarán un curso clínico más agresivo. Dado que los biomarcadores en LCR preceden a la atrofia en RM, este segundo trabajo también ha evaluado la capacidad de los niveles de biomarcadores en LCR en el momento del diagnóstico de detectar qué sujetos presentarán mayor atrofia cerebral en los 2 años posteriores. Los resultados muestran que niveles iniciales más altos de Aβ42 en LCR, siempre dentro del rango patológico, se relacionaron con mayor pérdida cortical en regiones parietales, mientras que niveles más altos de t-tau se relacionaron con una mayor pérdida progresiva de volumen en la amígdala. A priori, la relación entre niveles de Aβ42 más cerca del punto de corte de la normalidad con una mayor pérdida de grosor cortical puede parecer contraintuitiva. Sin

embargo, estudios previos ya han puesto de manifiesto que podría existir una aceleración de la atrofia en sujetos cognitivamente sanos con niveles de amiloide en rango de la normalidad pero próximos al punto de corte patológico, quizás reflejando la susceptibilidad que pueden tener algunos sujetos a pequeños acúmulos de amiloide (133). Otros trabajos han propuesto una relación en U invertida entre los niveles de amiloide y el grosor cortical en regiones característicamente afectadas en la EA. Según esta relación cuadrática, los sujetos con niveles de amiloide en el tercil medio, es decir, niveles transicionales entre lo normal y patológico, presentarían un engrosamiento cortical comparado con sujetos en el tercil con niveles dentro del rango de normalidad (134). Este incremento de grosor cortical que precedería al adelgazamiento cortical podría verse reflejado en una aceleración de la atrofia posteriormente en sujetos con niveles patológicos de amiloide cerca del punto de corte, y se ha relacionado con una hipertrofia neuronal previa a la atrofia y el inicio de los síntomas (135). También se ha sugerido que el aumento de grosor cortical podría tener que ver con una mayor inflamación secundaria al depósito amiloide en estas regiones, y algunos autores proponen dos picos de activación de la microglia en la EA, uno protector contra el acúmulo de amiloide seguido de otro proinflamatorio (136), el cual provocaría una aceleración de la neurodegeneración en un segundo tiempo. Dado el tamaño limitado de la muestra, con el objetivo de confirmar nuestros hallazgos y evaluar su especificidad en EAIP, se analizaron sujetos con EAIP y EAIT de la cohorte “Alzheimer's Disease Neuroimaging Initiative” (ADNI). En esta muestra independiente, se replicó la asociación de los niveles de Aβ42 con una pérdida acelerada de grosor cortical parietal en los sujetos con EAIP, no así en sujetos con EAIT, sugiriendo que la asociación podría ser más específica de sujetos con un inicio precoz, quizás al presentar mayor inflamación que las presentaciones tardías (137).

Hemos visto también que mayor concentración de t-tau basal se asoció únicamente a una pérdida más rápida de volumen en la amígdala. Los niveles de t-tau han sido relacionados con la pérdida de volumen progresiva en distintas regiones en la EA (98) y, como marcador de daño axonal, podrían estar más relacionados con la pérdida de volumen que con el grosor cortical (138). Además, su relación con la pérdida de volumen sería independiente de la edad, al observarse también la misma relación en sujetos con EAIT de la cohorte ADNI. Como ya ha sido descrito, los niveles de NfL, como marcador también de daño axonal y relacionado con la pérdida de sustancia blanca, mostraron una asociación positiva con el aumento ventricular en el momento del diagnóstico, sin mostrar, a diferencia de estudios previos, una asociación con la velocidad de la atrofia cerebral (99,139). En conjunto, estos hallazgos ponen de manifiesto la compleja

relación entre los biomarcadores de LCR y la pérdida neuronal. Si bien, podrían ser útiles para predecir cambios estructurales transversales o longitudinales y ayudar a seleccionar sujetos con rápida progresión o monitorizar el efecto de tratamientos modificadores de la enfermedad.

Aunque con el cambio conceptual de la enfermedad a una entidad biológica cada vez más se están intentando implementar medidas que usen biomarcadores para monitorizar la enfermedad o demostrar el efecto de tratamientos modificadores, en la actualidad es todavía habitual el uso de medidas cognitivas en este sentido. Dado que, según el modelo actual de la EA, la atrofia en RM precede y se encuentra en estrecha relación con la aparición de los síntomas cognitivos, el tercer trabajo de esta tesis ha querido analizar la capacidad de las medidas basales de grosor cortical y volumen subcortical para predecir los cambios longitudinales de una batería neuropsicológica completa. Por un lado, los resultados de este último trabajo reafirman en una cohorte de sujetos con EAIP A+T+N+ que, a pesar de presentarse mayoritariamente con un perfil amnésico de la enfermedad, la pérdida cognitiva en la EAIP es amplia y heterogénea, involucrando otros dominios cognitivos en el momento del diagnóstico (22,55,140). Además, la pérdida cognitiva en dos años involucra los cinco dominios explorados, asociándose la EAIP con un declinar más agresivo cuando se compara con la EAIT (20), y apoyando la idea de que la EAIP no es una enfermedad tan centrada en el LTM como en la EAIT, dónde existe una afectación predominante de la memoria. Por otro lado, el patrón de atrofia en RM craneal que hemos observado va en consonancia con los resultados descritos previamente en esta tesis, con relativo respeto de la corteza del LTM, y un patrón similar se ha asociado con los síntomas cognitivos en trabajos previos de corte transversal en EAIP (141,142).

En los resultados de este trabajo se puede ver que una mayor afectación en el momento del diagnóstico en medidas de atrofia global, como son la disminución del grosor cortical hemisférico o el aumento del volumen ventricular, predicen un mayor declinar cognitivo global y en puntuaciones de lenguaje y funciones ejecutivas. Las futuras puntuaciones de memoria no se asociaron a ninguna medida de RM, quizás porque a pesar de ser un dominio afectado podría guardar poca relación con la atrofia no tan centrada en el LTM como también hemos visto en el segundo trabajo, donde sujetos mayoritariamente con un inicio amnésico no mostraron afectación del LTM. Además, en este tercer trabajo se ha visto que la atrofia de regiones neocorticales en la EAIP y no tanto la atrofia observada en el LTM es capaz de predecir la pérdida cognitiva durante los dos años posteriores, tanto en medidas globales de cognición como en medidas de dominios amnésicos y no amnésicos. Llama la atención que el hipocampo, tan ligado a la pérdida de memoria en la EA (143,144), no mostró ningún resultado significativo a la

hora de predecir las futuras puntuaciones. Sin embargo, al no realizar un análisis estratificado por sexos, cabría preguntarse si existe dimorfismo sexual en la relación entre las puntuaciones cognitivas y el hipocampo, como hemos visto en el primer trabajo, donde sí que existe una asociación transversal entre el hipocampo y las puntuaciones de memoria en mujeres. Por otro lado, vemos que son las regiones parietales y temporales laterales en el momento del diagnóstico las que parecen ser más útiles en identificar qué sujetos con EAIP presentarán un declinar cognitivo acelerado en los dos años siguientes. De nuevo, estos hallazgos ponen de manifiesto como estas regiones, más que el hipocampo o la corteza del LTM, serían más características de la afectación que produce la EAIP, y además guardan una relación más estrecha con la progresión clínica, siendo útiles para detectar qué sujetos con EAIP tienen más probabilidad de empeorar más rápidamente, y en los que existiría más probabilidad de observar el efecto de un fármaco modificador de la enfermedad a corto plazo.

En este trabajo, las futuras puntuaciones de memoria se relacionaron con el grosor cortical de regiones frontales y temporo-laterales en el momento del diagnóstico, y ninguna región cerebral mostró asociación con la afectación en el recuerdo diferido característico de la EA. Así, las evaluaciones centradas en memoria podrían no ser un buen indicador de la pérdida neuronal en la EAIP y quizás distintas variables como el sexo de los sujetos podrían influir en la relación entre la atrofia y el deterioro cognitivo y han de tenerse en cuenta en modelos multivariados. En esta línea, estudios transversales previos han mostrado que la atrofia en la EAIP se relaciona con síntomas ejecutivos/atencionales mientras que la atrofia en la EAIT está más ligada a síntomas de memoria (141). También, es interesante ver en este trabajo como una relativa preservación de regiones posteriores se relacionó con peores puntuaciones en aprendizaje, quizá apuntando a diferentes subtipos de patrones de atrofia (142). De todas maneras, es evidente que la relación que existe entre los cambios producidos por la enfermedad y los síntomas observados es compleja, y no sólo los cambios estructurales en RM parecen contribuir a la pérdida cognitiva, pues otros cambios patológicos que aquí no han sido estudiados, como podría ser la disfunción sináptica secundaria al depósito de tau, también podrían contribuir al deterioro cognitivo (145).

Para finalizar, además de las limitaciones expuestas en cada uno de los trabajos, el reducido tamaño de la muestra estudiada ha podido influir en algunas conclusiones. A las dificultades que presentan en general los estudios longitudinales, especialmente en EA, en la que el empeoramiento progresivo de los sujetos obstaculiza el seguimiento, se suman los inconvenientes ocasionados por la pandemia de COVID-19. El confinamiento, el estrés emocional, las restricciones hospitalarias y la

reticencia legítima a participar en investigación, tratándose además de un colectivo tan vulnerable a la infección, han podido determinar las evaluaciones longitudinales que se han podido realizar.

VIII. CONCLUSIONES

VIII. CONCLUSIONES

1. La progresión de la atrofia cerebral en sujetos con EAIP se puede monitorizar mediante RM craneal estructural de 3T y seguiría un patrón diferente al descrito en presentaciones tardías de la enfermedad. En el momento del diagnóstico, la atrofia cerebral en la EAIP involucra regiones neocorticales, hipocampo y amígdala, con menor afectación de la corteza del lóbulo temporal medial de lo que sucede en EAIT. Además, existen diferencias entre sexos en la distribución espacial de la atrofia. A los dos años, la atrofia cerebral en la EAIP sigue un gradiente que va desde regiones corticales posteriores a anteriores y se observa una pérdida de volumen más allá de las estructuras subcorticales inicialmente afectadas.
2. El sexo de los sujetos podría influir en el grado de deterioro cognitivo en el momento del diagnóstico de la EAIP, así como en la relación entre los síntomas cognitivos y la atrofia cerebral. Las medidas de atrofia global o de regiones neocorticales obtenidas con RM en el momento del diagnóstico predicen mejor que la atrofia de las estructuras temporales mediales la evolución cognitiva a los dos años de los sujetos con EAIP.
3. Los biomarcadores en líquido cefalorraquídeo de patología amiloide (Aβ42) y neurodegeneración (t-tau) en el momento del diagnóstico de la EAIP podrían ser útiles para predecir qué sujetos presentarán mayor atrofia cerebral a los dos años.

IX. BIBLIOGRAFIA

IX. BIBLIOGRAFIA

1. Maurer K, Volk S, Gerbaldo H. Auguste D and Alzheimer's disease. Lancet. 1997;349(9064):1546–9.
2. Nichols E, Steinmetz JD, Vollset SE, Fukutaki K, Chalek J, Abd-Allah F, et al. Estimation of the global prevalence of dementia in 2019 and forecasted prevalence in 2050: an analysis for the Global Burden of Disease Study 2019. Lancet Public Health. 2022;7(2):e105–25.
3. Garre-Olmo J. Epidemiología de la enfermedad de Alzheimer y otras demencias. 2018;66(11):377–86.
4. 2021 Alzheimer's disease facts and figures. Alzheimers Dement [Internet]. 2021;17(3):327–406. Available from: https://alz-journals.onlinelibrary.wiley.com/doi/abs/10.1002/alz.12328
5. Zhu XC, Tan L, Wang HF, Jiang T, Cao L, Wang C, et al. Rate of early onset Alzheimer's disease: A systematic review and meta-analysis. Ann Transl Med. 2015;3(3):38.
6. Reitz C, Rogaeva E, Beecham GW. Late-onset vs nonmendelian early-onset Alzheimer disease: A distinction without a difference? Neurol Genet. 2020;6(5):e512.
7. Hendriks S, Peetoom K, Bakker C, van der Flier WM, Papma JM, Koopmans R, et al. Global Prevalence of Young-Onset Dementia: A Systematic Review and Meta-analysis. JAMA Neurol [Internet]. 2021;78(9):1080-90. Available from: https://jamanetwork.com/journals/jamaneurology/fullarticle/2781919
8. Contador J, Tort-Merino A, Balasa M, Falgàs N, Olives J, Castellví M, et al. Four years' experience in an early-onset dementia clinic in Barcelona. In: 2020 Alzheimer's Association International Conference [Internet]; 2020 Jul 27-31; Online conference. Alzheimers Dement, 2020. 16(S7):e037911. Available from: https://alz-journals.onlinelibrary.wiley.com/doi/full/10.1002/alz.037911
9. Graff-Radford J, Yong KXX, Apostolova LG, Bouwman FH, Carrillo M, Dickerson BC, et al. New insights into atypical Alzheimer's disease in the era of biomarkers. Lancet Neurol [Internet]. 2021;20(3):222–34. Available from: http://dx.doi.org/10.1016/S1474-4422(20)30440-3
10. Apostolova LG, Aisen P, Eloyan A, Fagan A, Fargo KN, Foroud T, et al. The Longitudinal Early-onset Alzheimer's Disease Study (LEADS): Framework and methodology. Alzheimers Dement. 2021;17(12):2043–55.
11. Hyman BT, Phelps CH, Beach TG, Bigio EH, Cairns NJ, Carrillo MC, et al. National Institute on Aging-Alzheimer's Association guidelines for the neuropathologic assessment of Alzheimer's disease. Alzheimers Dement. 2012;8(1):1–13.

12. Braak H, Braak E. Neuropathological stageing of Alzheimer-related changes. Acta Neuropathol [Internet]. 1991 Sep;82(4):239–59. Available from: http://link.springer.com/10.1007/BF00308809

13. Serrano-Pozo A, Frosch MP, Masliah E, Hyman BT. Neuropathological alterations in Alzheimer disease. Cold Spring Harb Perspect Med. 2011;1(1):a006189.

14. Sperling RA, Aisen PS, Beckett LA, Bennett DA, Craft S, Fagan AM, et al. Toward defining the preclinical stages of alzheimer's disease: Recommendations from the national institute on aging. Alzheimers Dement. 2011;7(3):280–92.

15. Mendez MF. Early-onset Alzheimer's Disease: Nonamnestic Subtypes and Type 2 AD. Arch Med Res [Internet]. 2012;43(8):677–85. Available from: https://www.ncbi.nlm.nih.gov/pmc/articles/PMC3624763/pdf/nihms412728.pdf

16. Marshall GA, Fairbanks LA, Tekin S, Vinters H V., Cummings JL. Early-onset Alzheimer's disease is associated with greater pathologic burden. J Geriatr Psychiatry Neurol. 2007;20(1):29–33.

17. Murray ME, Graff-Radford NR, Ross OA, Petersen RC, Duara R, Dickson DW. Neuropathologically defined subtypes of Alzheimer's disease with distinct clinical characteristics: a retrospective study. Lancet Neurol [Internet]. 2011;10(9):785–96. Available from: https://linkinghub.elsevier.com/retrieve/pii/S1474442211701569

18. Spina S, La Joie R, Petersen C, Nolan AL, Cuevas D, Cosme C, et al. Comorbid neuropathological diagnoses in early versus late-onset Alzheimer's disease. Brain. 2021;144(7):2186-98.

19. Kunkle BW, Vardarajan BN, Naj AC, Whitehead PL, Rolati S, Slifer S, et al. Early-onset Alzheimer disease and candidate risk genes involved in endolysosomal transport. JAMA Neurol. 2017;74(9):1113–22.

20. Wattmo C, Wallin ÅK. Early- versus late-onset Alzheimer's disease in clinical practice: cognitive and global outcomes over 3 years. Alzheimers Res Ther [Internet]. 2017;9(1):70. Available from: http://alzres.biomedcentral.com/articles/10.1186/s13195-017-0294-2

21. van der Flier WM, Pijnenburg YAL, Fox NC, Scheltens P. Early-onset versus late-onset Alzheimer's disease: The case of the missing APOE ε4 allele. Lancet Neurol [Internet]. 2011;10(3):280–8. Available from: http://dx.doi.org/10.1016/S1474-4422(10)70306-9

22. Balasa M, Gelpi E, Antonell A, Rey MJ, Sánchez-Valle R, Molinuevo JL, et al. Clinical features and APOE genotype of pathologically proven early-onset Alzheimer disease. Neurology. 2011;76(20):1720–5.

23. McKhann G, Drachman D, Folstein M, Katzman R, Price D, Stadlan EM. Clinical diagnosis of alzheimer's disease: Report of the NINCDS-ADRDA Work Group under the auspices of Department of Health and

Human Services Task Force on Alzheimer's Disease. Neurology. 1984;34(7):939–44.

24. Beach TG, Monsell SE, Phillips LE, Kukull W. Accuracy of the clinical diagnosis of Alzheimer disease at National Institute on Aging Alzheimer Disease Centers, 2005-2010. J Neuropathol Exp Neurol. 2012;71(4):266–73.

25. Nelson PT, Head E, Schmitt FA, Davis PR, Neltner JH, Jicha GA, et al. Alzheimer's disease is not "brain aging": Neuropathological, genetic, and epidemiological human studies. Acta Neuropathol. 2011;121(5):571–87.

26. McKhann GM, Knopman DS, Chertkow H, Hyman BT, Jack CR, Kawas CH, et al. The diagnosis of dementia due to Alzheimer's disease: Recommendations from the National Institute on Aging-Alzheimer's Association workgroups on diagnostic guidelines for Alzheimer's disease. Alzheimers Dement [Internet]. 2011;7(3):263–9. Available from: http://doi.wiley.com/10.1016/j.jalz.2011.03.005

27. Albert MS, DeKosky ST, Dickson D, Dubois B, Feldman HH, Fox NC, et al. The diagnosis of mild cognitive impairment due to Alzheimer's disease: Recommendations from the National Institute on Aging-Alzheimer's Association workgroups on diagnostic guidelines for Alzheimer's disease. Alzheimers Dement [Internet]. 2011;7(3):270–9. Available from: http://doi.wiley.com/10.1016/j.jalz.2011.03.008

28. Jack CR, Bennett DA, Blennow K, Carrillo MC, Dunn B, Haeberlein SB, et al. NIA-AA Research Framework: Toward a biological definition of Alzheimer's disease. Alzheimers Dement [Internet]. 2018;14(4):535–62. Available from: https://linkinghub.elsevier.com/retrieve/pii/S1552526018300724

29. Kovacs GG, Milenkovic I, Wöhrer A, Höftberger R, Gelpi E, Haberler C, et al. Non-Alzheimer neurodegenerative pathologies and their combinations are more frequent than commonly believed in the elderly brain: A community-based autopsy series. Acta Neuropathol. 2013;126(3):365–84.

30. Dubois B, Villain N, Frisoni GB, Rabinovici GD, Sabbagh M, Cappa S, et al. Clinical diagnosis of Alzheimer's disease: recommendations of the International Working Group. Lancet Neurol. 2021;20(6):484–96.

31. Seppala TT, Nerg O, Koivisto AM, Rummukainen J, Puli L, Zetterberg H, et al. CSF biomarkers for Alzheimer disease correlate with cortical brain biopsy findings. Neurology [Internet]. 2012;78(20):1568–75. Available from: https://www.neurology.org/lookup/doi/10.1212/WNL.0b013e3182563bd0

32. Mattsson N, Lönneborg A, Boccardi M, Blennow K, Hansson O, Geneva Task Force for the Roadmap of Alzheimer's Biomarkers. Clinical validity of cerebrospinal fluid Aβ42, tau, and phospho-tau as

biomarkers for Alzheimer's disease in the context of a structured 5-phase development framework. Neurobiol Aging. 2017;52:196–213.

33. Mattsson-Carlgren N, Andersson E, Janelidze S, Ossenkoppele R, Insel P, Strandberg O, et al. Aβ deposition is associated with increases in soluble and phosphorylated tau that precede a positive Tau PET in Alzheimer's disease. Sci Adv. 2020;6(16):eaaz2387.

34. Engelborghs S, Niemantsverdriet E, Struyfs H, Blennow K, Brouns R, Comabella M, et al. Consensus guidelines for lumbar puncture in patients with neurological diseases. Alzheimers Dement (Amst). 2017;8:111–26.

35. Falgàs N, Tort-Merino A, Balasa M, Borrego-Écija S, Castellví M, Olives J, et al. Clinical applicability of diagnostic biomarkers in early-onset cognitive impairment. Eur J Neurol. 2019;26(8):1098–104.

36. Palmqvist S, Janelidze S, Quiroz YT, Zetterberg H, Lopera F, Stomrud E, et al. Discriminative Accuracy of Plasma Phospho-tau217 for Alzheimer Disease vs Other Neurodegenerative Disorders. JAMA. 2020;324(8):772–81.

37. Li Y, Schindler SE, Bollinger JG, Ovod V, Mawuenyega KG, Weiner MW, et al. Validation of Plasma Amyloid-β 42/40 for Detecting Alzheimer Disease Amyloid Plaques. Neurology. 2022;98(7):e688–99.

38. Chow N, Hwang KS, Hurtz S, Green AE, Somme JH, Thompson PM et al. Comparing 3T and 1.5T MRI for mapping hippocampal atrophy in the Alzheimer's disease neuroimaging initiative. AJNR Am J Neuroradiol [Internet]. 2015;36(4):653–60. Available from: http://www.embase.com/search/results?subaction=viewrecord&from=export&id=L603721870%0Ahttp://dx.doi.org/10.3174/ajnr.A4228

39. Jack CR, Holtzman DM. Biomarker modeling of alzheimer's disease. Neuron. 2013;80(6):1347–58.

40. Dallaire-Théroux C, Callahan BL, Potvin O, Saikali S, Duchesne S. Radiological-Pathological Correlation in Alzheimer's Disease: Systematic Review of Antemortem Magnetic Resonance Imaging Findings. J Alzheimers Dis. 2017;57(2):575–601.

41. Frisoni GB, Fox NC, Jack CR, Scheltens P, Thompson PM. The clinical use of structural MRI in Alzheimer disease. Nat Rev Neurol [Internet]. 2010;6(2):67–77. Available from: http://dx.doi.org/10.1038/nrneurol.2009.215

42. Cardinale F, Chinnici G, Bramerio M, Mai R, Sartori I, Cossu M, et al. Validation of FreeSurfer-Estimated Brain Cortical Thickness: Comparison with Histologic Measurements. Neuroinformatics. 2014;12(4):535–42.

43. Dickerson BC, Bakkour A, Salat DH, Feczko E, Pacheco J, Greve DN, et al. The cortical signature of Alzheimer's disease: Regionally specific cortical thinning relates to symptom severity in very mild to mild AD

dementia and is detectable in asymptomatic amyloid-positive individuals. Cereb Cortex. 2009;19(3):497–510.

44. Bakkour A, Morris JC, Dickerson BC. The cortical signature of prodromal AD: Regional thinning predicts mild AD dementia. Neurology. 2009;72(12):1048–55.

45. Konijnenberg E, Fereshtehnejad SM, Ten Kate M, Eriksdotter M, Scheltens P, Johannsen P, et al. Early-Onset Dementia: Frequency, Diagnostic Procedures, and Quality Indicators in Three European Tertiary Referral Centers. Alzheimer Dis Assoc Disord. 2017;31(2):146–51.

46. Lombardi G, Crescioli G, Cavedo E, Lucenteforte E, Casazza G, Bellatorre AG, et al. Structural magnetic resonance imaging for the early diagnosis of dementia due to Alzheimer's disease in people with mild cognitive impairment. Cochrane Database Syst Rev [Internet]. 2020;3(3):CD009628. Available from: http://doi.wiley.com/10.1002/14651858.CD009628.pub2

47. Lo Buono V, Palmeri R, Corallo F, Allone C, Pria D, Bramanti P, et al. Diffusion tensor imaging of white matter degeneration in early stage of Alzheimer's disease: a review. Int J Neurosci [Internet]. 2020;130(3):243–50. Available from: https://doi.org/10.1080/00207454.2019.1667798

48. Gusnard DA, Raichle ME. Searching for a baseline: Functional imaging and the resting human brain. Nat Rev Neurosci [Internet]. 2001;2(10):685–94. Available from: http://www.jneurosci.org/cgi/content/abstract/26/41/10376%5Cn

49. Barkhof F, Haller S, Rombouts SARB. Resting-state functional MR imaging: A new window to the brain. Radiology. 2014;272(1):29–49.

50. Landau SM, Harvey D, Madison CM, Koeppe RA, Reiman EM, Foster NL, et al. Associations between cognitive, functional, and FDG-PET measures of decline in AD and MCI. Neurobiol Aging. 2011;32(7):1207–18.

51. Chiotis K, Saint-Aubert L, Boccardi M, Gietl A, Picco A, Varrone A, et al. Clinical validity of increased cortical uptake of amyloid ligands on PET as a biomarker for Alzheimer's disease in the context of a structured 5- phase development framework. Neurobiol Aging. 2017;52(2017):214–27.

52. Lowe VJ, Lundt ES, Albertson SM, Min HK, Fang P, Przybelski SA, et al. Tau-positron emission tomography correlates with neuropathology findings. Alzheimers Dement. 2020;16(3):561–71.

53. Ferretti MT, Iulita MF, Cavedo E, Chiesa PA, Dimech AS, Chadha AS, et al. Sex differences in Alzheimer disease — The gateway to precision medicine. Nat Rev Neurol [Internet]. 2018;14(8):457–69. Available from: http://dx.doi.org/10.1038/s41582-018-0032-9

54. Koedam ELGE, Lauffer V, Van Der Vlies AE, Van Der Flier WM, Scheltens P, Pijnenburg YAL. Early-versus late-onset Alzheimer's disease: More than age alone. J Alzheimer's Dis. 2010;19(4):1401–8.

55. Palasí A, Gutiérrez-Iglesias B, Alegret M, Pujadas F, Olabarrieta M, Liébana D, et al. Differentiated clinical presentation of early and late-onset Alzheimer's disease: is 65 years of age providing a reliable threshold? J Neurol. 2015;262(5):1238–46.

56. Stanley K, Walker Z. Do patients with young onset Alzheimer's disease deteriorate faster than those with late onset Alzheimer's disease? A review of the literature. Int Psychogeriatr. 2014;26(12):1945–53.

57. Panegyres PK, Chen HY. Differences between early and late onset Alzheimer's disease. Am J Neurodegener Dis. 2013;2(4):300–6.

58. Irvine K, Laws KR, Gale TM, Kondel TK. Greater cognitive deterioration in women than men with Alzheimer's disease: A meta analysis. J Clin Exp Neuropsychol. 2012;34(9):989–98.

59. Filon JR, Intorcia AJ, Sue LI, Vazquez Arreola E, Wilson J, Davis KJ, et al. Gender differences in Alzheimer disease: Brain atrophy, histopathology burden, and cognition. J Neuropathol Exp Neurol. 2016;75(8):748–54.

60. Liesinger AM, Graff-Radford NR, Duara R, Carter RE, Hanna Al-Shaikh FS, Koga S, et al. Sex and age interact to determine clinicopathologic differences in Alzheimer's disease. Acta Neuropathol [Internet]. 2018;136(6):873–85. Available from: https://doi.org/10.1007/s00401-018-1908-x

61. Schoonenboom NSM, Pijnenburg YAL, Mulder C, Rosso SM, Van Elk E-J, Van Kamp GJ, et al. Amyloid β(1–42) and phosphorylated tau in CSF as markers for early-onset Alzheimer disease. Neurology [Internet]. 2004;62(9):1580–4. Available from: http://www.neurology.org/lookup/doi/10.1212/01.WNL.0000123249.58898.E0

62. Ossenkoppele R, Mattsson N, Teunissen CE, Barkhof F, Pijnenburg Y, Scheltens P, et al. Cerebrospinal fluid biomarkers and cerebral atrophy in distinct clinical variants of probable Alzheimer's disease. Neurobiol Aging [Internet]. 2015;36(8):2340–7. Available from: http://dx.doi.org/10.1016/j.neurobiolaging.2015.04.011

63. Andreasen N, Hesse C, Davidsson P, Minthon L, Wallin A, Winblad B, et al. Cerebrospinal Fluid β-Amyloid(1-42) in Alzheimer Disease: differences between early- and late-onset Alzheimer disease and stability during the course of disease. Arch Neurol [Internet]. 1999;56(6):673-80. Available from: http://archneur.jamanetwork.com/article.aspx?doi=10.1001/archneur.56.6.673

64. Bridel C, Van Wieringen WN, Zetterberg H, Tijms BM, Teunissen CE, Alvarez-Cermeño JC, et al. Diagnostic Value of Cerebrospinal Fluid Neurofilament Light Protein in Neurology: A Systematic Review and Meta-analysis. JAMA Neurol. 2019;76(9):1035–48.

65. Hohman TJ, Dumitrescu L, Barnes LL, Thambisetty M, Beecham G, Kunkle B, et al. Sex-specific association of apolipoprotein e with cerebrospinal fluid levels of tau. JAMA Neurol. 2018;75(8):989–98.

66. Falgàs N, Sánchez-Valle R, Bargalló N, Balasa M, Fernández-Villullas G, Bosch B, et al. Hippocampal atrophy has limited usefulness as a diagnostic biomarker on the early onset Alzheimer's disease patients: A comparison between visual and quantitative assessment. NeuroImage Clin [Internet]. 2019;23:101927. Available from: https://doi.org/10.1016/j.nicl.2019.101927

67. Möller C, Vrenken H, Jiskoot L, Versteeg A, Barkhof F, Scheltens P, et al. Different patterns of gray matter atrophy in early- and late-onset Alzheimer's disease. Neurobiol Aging [Internet]. 2013;34(8):2014–22. Available from: http://dx.doi.org/10.1016/j.neurobiolaging.2013.02.013

68. Aziz AL, Giusiano B, Joubert S, Duprat L, Didic M, Gueriot C, et al. Difference in imaging biomarkers of neurodegeneration between early and late-onset amnestic Alzheimer's disease. Neurobiol Aging [Internet]. 2017;54:22–30. Available from: http://dx.doi.org/10.1016/j.neurobiolaging.2017.02.010

69. Harper L, Bouwman F, Burton EJ, Barkhof F, Scheltens P, O'Brien JT, et al. Patterns of atrophy in pathologically confirmed dementias: A voxelwise analysis. J Neurol Neurosurg Psychiatry. 2017;88(11):908–16.

70. Falgàs N, Ruiz-Peris M, Pérez-Millan A, Sala-Llonch R, Antonell A, Balasa M, et al. Contribution of CSF biomarkers to early-onset Alzheimer's disease and frontotemporal dementia neuroimaging signatures. Hum Brain Mapp [Internet]. 2020;41(8):2004-13. Available from: https://onlinelibrary.wiley.com/doi/abs/10.1002/hbm.24925

71. Ossenkoppele R, Cohn-Sheehy BI, La Joie R, Vogel JW, Möller C, Lehmann M, et al. Atrophy patterns in early clinical stages across distinct phenotypes of Alzheimer's disease. Hum Brain Mapp. 2015;36(11):4421–37. Available from: https://onlinelibrary.wiley.com/doi/abs/10.1002/hbm.24925

72. Cho H, Seo SW, Kim JH, Kim C, Ye BS, Kim GH, et al. Changes in subcortical structures in early- versus late-onset Alzheimer's disease. Neurobiol Aging [Internet]. 2013;34(7):1740–7. Available from: http://dx.doi.org/10.1016/j.neurobiolaging.2013.01.001

73. Cho H, Jeon S, Kang SJ, Lee JM, Lee JH, Kim GH, et al. Longitudinal changes of cortical thickness in early- versus late-onset Alzheimer's disease. Neurobiol Aging. 2013;34(7):1921.e9-15.

74. Migliaccio R, Agosta F, Possin KL, Canu E, Filippi M, Rabinovici GD, et al. Mapping the progression of atrophy in early- and late-onset alzheimer's disease. J Alzheimers Dis. 2015;46(2):351-64

75. Parker TD, Slattery CF, Yong KXX, Nicholas JM, Paterson RW, Foulkes AJM, et al. Differences in hippocampal subfield volume are seen in phenotypic variants of early onset Alzheimer's disease. NeuroImage Clin [Internet]. 2019;21:101632. Available from: https://doi.org/10.1016/j.nicl.2018.101632

76. Apostolova LG, Dinov ID, Dutton RA, Hayashi KM, Toga AW, Cummings JL, et al. 3D comparison of hippocampal atrophy in amnestic mild cognitive impairment and Alzheimer's disease. Brain [Internet]. 2006;129(11):2867–73. Available from: https://academic.oup.com/brain/article-lookup/doi/10.1093/brain/awl274

77. Sundermann EE, Biegon A, Rubin LH, Lipton RB, Mowrey W, Landau S, et al. Better verbal memory in women than men in MCI despite similar levels of hippocampal atrophy. Neurology [Internet]. 2016;86(15):1368– 76. Available from: https://www.neurology.org/lookup/doi/10.1212/WNL.0000000000002570

78. Hua X, Hibar DP, Lee S, Toga AW, Jack CR, Weiner MW, et al. Sex and age differences in atrophic rates: An ADNI study with n=1368 MRI scans. Neurobiol Aging. 2010;31(8):1463–80.

79. Lee J, Cho H, Jeon S, Kim HJ, Kim YJ, Lee J, et al. Sex-Related Reserve Hypothesis in Alzheimer's Disease: Changes in Cortical Thickness with a Five-Year Longitudinal Follow-Up. J Alzheimers Dis. 2018;65(2):641–9.

80. Skup M, Zhu H, Wang Y, Giovanello KS, Lin J, Shen D, et al. Sex differences in grey matter atrophy patterns among AD and aMCI patients: Results from ADNI. Neuroimage [Internet]. 2011;56(3):890–906. Available from: https://www.ncbi.nlm.nih.gov/pmc/articles/PMC3624763/pdf/nihms412728.pdf

81. La Joie R, Visani A V., Lesman-Segev OH, Baker SL, Edwards L, Iaccarino L, et al. Association of APOE4 and Clinical Variability in Alzheimer Disease With the Pattern of Tau- and Amyloid-PET. Neurology. 2021;96(5):e650-61

82. Whitwell JL, Martin P, Graff-Radford J, Machulda MM, Senjem ML, Schwarz CG, et al. The role of age on tau PET uptake and gray matter atrophy in atypical Alzheimer's disease. Alzheimers Dement. 2019;15(5):675–85.

83. Jansen WJ, Ossenkoppele R, Knol DL, Tijms BM, Scheltens P, Verhey FRJ, et al. Prevalence of cerebral amyloid pathology in persons without dementia: A meta-analysis. JAMA. 2015;313(19):1924–38.

84. Youn YC, Jang JW, Han SH, Kim HR, Seok JW, Byun JS, et al. 11C-PIB PET imaging reveals that amyloid deposition in cases with early-onset Alzheimer's disease in the absence of known mutations retains higher levels of PIB in the basal ganglia. Clin Interv Aging. 2017;12:1041–8.

85. Tanner JA, Rabinovici GD. Relationship Between Tau and Cognition in the Evolution of Alzheimer's Disease: New Insights from Tau PET. J Nucl Med. 2021;62(5):612–3.

86. Joie R La, Visani A V., Baker SL, Brown JA, Bourakova V, Cha J, et al. Prospective longitudinal atrophy in Alzheimer's disease correlates with the intensity and topography of baseline tau-PET. Sci Transl Med. 2020;12(524):eaau5732

87. Jack CR, Wiste HJ, Weigand SD, Therneau TM, Lowe VJ, Knopman DS, et al. Predicting future rates of tau accumulation on PET. Brain. 2020;143(10):3136–50.

88. Schöll M, Ossenkoppele R, Strandberg O, Palmqvist S, Jögi J, Ohlsson T, et al. Distinct 18F-AV-1451 tau PET retention patterns in early- and late-onset Alzheimer's disease. Brain. 2017;140(9):2286–94.

89. Cho H, Choi JY, Lee SH, Lee JH, Choi YC, Ryu YH, et al. Excessive tau accumulation in the parieto-occipital cortex characterizes early-onset Alzheimer's disease. Neurobiol Aging [Internet]. 2017;53:103–11. Available from: http://dx.doi.org/10.1016/j.neurobiolaging.2017.01.024

90. Pontecorvo MJ, Devous MD, Navitsky M, Lu M, Salloway S, Schaerf FW, et al. Relationships between flortaucipir PET tau binding and amyloid burden, clinical diagnosis, age and cognition. Brain. 2017;140(3):748–63.

91. Ossenkoppele R, Lyoo CH, Jester-Broms J, Sudre CH, Cho H, Ryu YH, et al. Assessment of Demographic, Genetic, and Imaging Variables Associated with Brain Resilience and Cognitive Resilience to Pathological Tau in Patients with Alzheimer Disease. JAMA Neurol. 2020;77(5):632–42.

92. McAleese KE, Colloby SJ, Thomas AJ, Al-Sarraj S, Ansorge O, Neal J, et al. Concomitant neurodegenerative pathologies contribute to the transition from mild cognitive impairment to dementia. Alzheimers Dement. 2021;17(7):1121–33.

93. Edwards L, La Joie R, Iaccarino L, Strom A, Baker SL, Casaletto KB, et al. Multimodal neuroimaging of sex differences in cognitively impaired patients on the Alzheimer's continuum: greater tau-PET retention in females. Neurobiol Aging [Internet]. 2021;105:86–98. Available from: https://doi.org/10.1016/j.neurobiolaging.2021.04.003

94. Buckley RF, Scott MR, Jacobs HIL, Schultz AP, Properzi MJ, Amariglio RE, et al. Sex Mediates Relationships Between Regional Tau Pathology and Cognitive Decline. Ann Neurol. 2020;88(5):921–32.

95. Jack CR, Wiste HJ, Therneau TM, Weigand SD, Knopman DS, Mielke MM, et al. Associations of Amyloid, Tau, and Neurodegeneration Biomarker Profiles with Rates of Memory Decline among Individuals Without Dementia. JAMA. 2019;321(23):2316–25.

96. Ekman U, Ferreira D, Westman E. The A/T/N biomarker scheme and patterns of brain atrophy assessed in mild cognitive impairment. Sci Rep [Internet]. 2018;8(1):8431. Available from: http://dx.doi.org/10.1038/s41598-018-26151-8

97. Van Rossum IA, Vos SJB, Burns L, Knol DL, Scheltens P, Soininen H, et al. Injury markers predict time to dementia in subjects with MCI and amyloid pathology. Neurology. 2012;79(17):1809–16.

98. Tarawneh R, Head D, Allison S, Buckles V, Fagan AM, Ladenson JH, et al. Cerebrospinal fluid markers of neurodegeneration and rates of brain atrophy in early Alzheimer disease. JAMA Neurol. 2015;72(6):656–65.

99. Zetterberg H, Skillbäck T, Mattsson N, Trojanowski JQ, Portelius E, Shaw LM, et al. Association of Cerebrospinal Fluid Neurofilament Light Concentration With Alzheimer Disease Progression. JAMA Neurol [Internet]. 2016;73(1):60-7. Available from: http://archneur.jamanetwork.com/article.aspx?doi=10.1001/jamaneurol.2015.3037

100. Marizzoni M, Ferrari C, Jovicich J, Albani D, Babiloni C, Cavaliere L, et al. Predicting and tracking short term disease progression in amnestic mild cognitive impairment patients with prodromal Alzheimer's disease: Structural brain biomarkers. J Alzheimers Dis. 2019;69(1):3–14.

101. Cardenas VA, Chao LL, Studholme C, Yaffe K, Miller BL, Madison C, et al. Brain atrophy associated with baseline and longitudinal measures of cognition. Neurobiol Aging [Internet]. 2011;32(4):572–80. Available from: http://dx.doi.org/10.1016/j.neurobiolaging.2009.04.011

102. Ossenkoppele R, Smith R, Mattsson-Carlgren N, Groot C, Leuzy A, Strandberg O, et al. Accuracy of Tau Positron Emission Tomography as a Prognostic Marker in Preclinical and Prodromal Alzheimer Disease: A Head-to-Head Comparison Against Amyloid Positron Emission Tomography and Magnetic Resonance Imaging. JAMA Neurol [Internet]. 2021;78(8):961–71. Available from: https://doi.org/10.1001/jamaneurol.2021.1858

103. Cummings J, Lee G, Mortsdorf T, Ritter A, Zhong K. Alzheimer's disease drug development pipeline: 2017. Alzheimers Dement (N Y) [Internet]. 2017;3(3):367–84. Available from: http://dx.doi.org/10.1016/j.trci.2017.05.002

104. Lace G, Savva GM, Forster G, De Silva R, Brayne C, Matthews FE, et al. Hippocampal tau pathology is related to neuroanatomical connections: An ageing population-based study. Brain. 2009;132(5):1324–34.

105. Ferreira D, Nordberg A, Westman E. Biological subtypes of Alzheimer disease: A systematic review and meta-analysis. Neurology. 2020;94(10):436–48.

106. Vila-Castelar C, Guzmán-Vélez E, Pardilla-Delgado E, Buckley RF, Bocanegra Y, Baena A, et al. Examining Sex Differences in Markers of Cognition and Neurodegeneration in Autosomal Dominant Alzheimer's Disease: Preliminary Findings from the Colombian Alzheimer's Prevention Initiative Biomarker Study. J Alzheimers Dis [Internet]. 2020;77(4):1743–53. Available from: https://www.medra.org/servlet/aliasResolver?alias=iospress&doi=10.3233/JAD-200723

107. Fleisher A, Grundman M, Jack CR, Petersen RC, Taylor C, Kim HT, et al. Sex, apolipoprotein E ε4 status, and hippocampal volume in mild cognitive impairment. Arch Neurol [Internet]. 2005;62(6):953–7. Available from: http://archneur.jamanetwork.com/article.aspx?doi=10.1001/archneur.62.6.953

108. Shokouhi S, Taylor WD, Albert K, Kang H, Newhouse PA, Alzheimer's Disease Neuroimaging Initiative. In vivo network models identify sex differences in the spread of tau pathology across the brain. Alzheimers Dement (Amst). 2020;12(1):e12016.

109. Park KH, Noh Y, Choi EJ, Kim H, Chun S, Son YD. Functional connectivity of the hippocampus in early- and vs. late-onset alzheimer's disease. J Clin Neurol. 2017;13(4):387–93.

110. Altmann A, Tian L, Henderson VW, Greicius MD; Alzheimer's Disease Neuroimaging Initiative Investigators. Sex Modifies the APOE -Related Risk of Developing Alzheimer Disease. Ann Neurol. 2014;75(4):563-73.

111. Babapour Mofrad R, Tijms BM, Scheltens P, Barkhof F, van der Flier WM, Sikkes SAM, et al. Sex differences in CSF biomarkers vary by Alzheimer disease stage and APOE ε4 genotype. Neurology. 2020;95(17):e2378-88.

112. La Joie R, Bejanin A, Fagan AM, Ayakta N, Baker SL, Bourakova V, et al. Associations between [18F]AV1451 tau PET and CSF measures of tau pathology in a clinical sample. Neurology. 2018;90(4):e282-90.

113. Grimm A, Biliouris EE, Lang UE, Götz J, Mensah-Nyagan AG, Eckert A. Sex hormone-related neurosteroids differentially rescue bioenergetic deficits induced by amyloid-β or hyperphosphorylated tau protein. Cell Mol Life Sci. 2016;73(1):201-15.

114. Sundermann EE, Panizzon MS, Chen X, Andrews M, Galasko D, Banks SJ, et al. Sex differences in Alzheimer's-related Tau biomarkers and a mediating effect of testosterone. Biol Sex Differ. 2020;11(1):33.

115. Mielke MM, Zetterberg H, Graff-radford J, Vemuri P, Przybelski SA, Blennow K, et al. Comparison of CSF neurofilament light chain,

neurogranin, and tau to MRI markers. Alzheimers Dement. 2021;17(5):801-12.

116. Lin KA, Choudhury KR, Rathakrishnan BG, Marks DM, Petrella JR, Doraiswamy PM, et al. Marked gender differences in progression of mild cognitive impairment over 8 years. Alzheimers Dement (N Y) [Internet]. 2015;1(2):103–10. Available from: http://dx.doi.org/10.1016/j.trci.2015.07.001

117. Sundermann EE, Biegon A, Rubin LH, Lipton RB, Landau S, Maki PM, et al. Does the Female Advantage in Verbal Memory Contribute to Underestimating Alzheimer's Disease Pathology in Women versus Men? J Alzheimers Dis. 2017;56(3):947–57.

118. McCarrey AC, An Y, Kitner-Triolo MH, Ferrucci L, Resnick SM. Sex differences in cognitive trajectories in clinically normal older adults. Psychol Aging. 2016;31(2):166–75.

119. Laws KR, Irvine K, Gale TM. Sex differences in cognitive impairment in Alzheimer's disease. World J Psychiatry. 2016;6(1):54-65.

120. Banks SJ, Andrews MJ, Digma L, Madsen J, Reas ET, Caldwell JZK, et al. Sex differences in Alzheimer's disease: do differences in tau explain the verbal memory gap? Neurobiol Aging [Internet]. 2021;107:70–7. Available from: https://doi.org/10.1016/j.neurobiolaging.2021.05.013

121. Lorius N, Locascio JJ, Rentz DM, Johnson KA, Sperling RA, Viswanathan A, et al. Vascular disease and risk factors are associated with cognitive decline in the Alzheimer disease spectrum. Alzheimer Dis Assoc Disord. 2015;29(1):18–25.

122. Ropele S, Enzinger C, Söllinger M, Langkammer C, Wallner-Blazek M, Schmidt R, et al. The Impact of Sex and Vascular Risk Factors on Brain Tissue Changes with Aging: Magnetization Transfer Imaging Results of the Austrian Stroke Prevention Study. AJNR Am J Neuroradiol [Internet]. 2010;31(7):1297–301. Available from: http://www.ajnr.org/content/31/7/1297.abstract

123. Snyder HM, Asthana S, Bain L, Brinton R, Craft S, Dubal DB, et al. Sex biology contributions to vulnerability to Alzheimer's disease: A think tank convened by the Women's Alzheimer's Research Initiative. Alzheimers Dement, 2016;12(11):1186–96.

124. Holland D, Desikan RS, Dale AM, McEvoy LK, Alzheimer's Disease Neuroimaging Initiative. Higher rates of decline for women and apolipoprotein e ε4 carriers. AJNR Am J Neuroradiol. 2013;34(12):2287–93.

125. Fiford CM, Ridgway GR, Cash DM, Modat M, Nicholas J, Manning EN, et al. Patterns of progressive atrophy vary with age in Alzheimer's disease patients. Neurobiol Aging [Internet]. 2018;63:22–32. Available from: https://linkinghub.elsevier.com/retrieve/pii/S0197458017303718

126. Feczko E, Augustinack JC, Fischl B, Dickerson BC. An MRI-based method for measuring volume, thickness and surface area of entorhinal, perirhinal, and posterior parahippocampal cortex. Neurobiol Aging [Internet]. 2009;30(3):420–31. Available from: https://linkinghub.elsevier.com/retrieve/pii/S0197458007002941

127. Whitwell JL, Dickson DW, Murray ME, Weigand SD, Tosakulwong N, Senjem ML, et al. Neuroimaging correlates of pathologically defined subtypes of Alzheimer's disease: a case-control study. Lancet Neurol [Internet]. 2012;11(10):868–77. Available from: https://linkinghub.elsevier.com/retrieve/pii/S1474442212702004

128. Pontecorvo MJ, Devous MD, Kennedy I, Navitsky M, Lu M, Galante N, et al. A multicentre longitudinal study of flortaucipir (18F) in normal ageing, mild cognitive impairment and Alzheimer's disease dementia. Brain. 2019;142(6):1723–35.

129. Gour N, Felician O, Didic M, Koric L, Confort-gouny S, Gueriot C, et al. Functional Connectivity Changes Differ in Early and Late-Onset Alzheimer's Disease. Hum Brain Mapp. 2014;35(7):2978-94

130. Adriaanse SM, Binnewijzend MAA, Ossenkoppele R, Tijms BM, Flier WM Van Der, Koene T, et al. Widespread Disruption of Functional Brain Organization in Early-Onset Alzheimer's Disease. PLoS One. 2014;9(7):e102995.

131. Filippi M, Basaia S, Canu E, Imperiale F, Meani A, Caso F, et al. Brain network connectivity differs in early-onset neurodegenerative dementia. Neurology. 2017;89(17):1764–72.

132. Kim M, Seo W. Diffusion Tensor Changes According to Age at Onset and Apolipoprotein E Genotype in Alzheimer Disease. Alzheimer Dis Assoc Disord. 2016;30(4):297–304.

133. Insel PS, Mattsson N, Mackin RS, Schöll M, Nosheny RL, Tosun D, et al. Accelerating rates of cognitive decline and imaging markers associated with β-amyloid pathology. Neurology. 2016;86(20):1887–96.

134. Fortea J, Sala-Llonch R, Bartrés-Faz D, Lladó A, Solé-Padullés C, Bosch B, et al. Cognitively preserved subjects with transitional cerebrospinal fluid ß-amyloid 1-42 values have thicker cortex in Alzheimer's disease vulnerable areas. Biol Psychiatry [Internet]. 2011;70(2):183– 90. Available from: http://dx.doi.org/10.1016/j.biopsych.2011.02.017

135. Iacono D, Markesbery WR, Gross M, Pletnikova O, Rudow G, Zandi P, et al. The Nun Study: Clinically silent AD, neuronal hypertrophy, and linguistic skills in early life. Neurology [Internet]. 2009;73(9):665–73. Available from: https://www.neurology.org/lookup/doi/10.1212/WNL.0b013e3181b01077

136. Fan Z, Brooks DJ, Okello A, Edison P. An early and late peak in microglial activation in Alzheimer's disease trajectory. Brain. 2017;140(3):792–803.

137. Kreisl WC, Lyoo CH, Liow J-S, Wei M, Snow J, Page E, et al. 11C-PBR28 binding to translocator protein increases with progression of Alzheimer's disease. Neurobiol Aging [Internet]. 2016;44(12):53–61. Available from: https://linkinghub.elsevier.com/retrieve/pii/S0197458016300458

138. Boerwinkle AH, Wisch JK, Chen CD, Gordon BA, Butt OH, Schindler SE, et al. Temporal Correlation of CSF and Neuroimaging in the Amyloid-Tau-Neurodegeneration Model of Alzheimer Disease. Neurology. 2021;97(1):e76-87.

139. Mattsson N, Insel PS, Palmqvist S, Portelius E, Zetterberg H, Weiner M, et al. Cerebrospinal fluid tau, neurogranin, and neurofilament light in Alzheimer's disease. EMBO Mol Med [Internet]. 2016;8(10):1184-96. Available from: https://onlinelibrary.wiley.com/doi/abs/10.15252/emmm.201606540

140. Smits LL, Pijnenburg YAL, Koedam ELGE, Van Der Vlies AE, Reuling IEW, Koene T, et al. Early onset alzheimer's disease is associated with a distinct neuropsychological profile. J Alzheimers Dis . 2012;30(1):101–8.

141. Van Der Vlies AE, Staekenborg SS, Admiraal-Behloul F, Prins ND, Barkhof F, Vrenken H, et al. Associations between magnetic resonance imaging measures and neuropsychological impairment in early and late onset alzheimer's disease. J Alzheimers Dis. 2013;35(1):169–78.

142. Phillips ML, Stage EC, Lane KA, Gao S, Risacher SL, Goukasian N, et al. Neurodegenerative Patterns of Cognitive Clusters of Early-Onset Alzheimer's Disease Subjects: Evidence for Disease Heterogeneity. Dement Geriatr Cogn Disord. 2019;48(3-4):131–42.

143. Quenon L, Dricot L, Woodard JL, Hanseeuw B, Gilis N, Lhommel R, et al. Prediction of Free and Cued Selective Reminding Test Performance Using Volumetric and Amyloid-Based Biomarkers of Alzheimer's Disease. J Int Neuropsychol Soc. 2016;22(10):991–1004.

144. Grothe MJ, Heinsen H, Amaro E, Grinberg LT, Teipel SJ. Cognitive Correlates of Basal Forebrain Atrophy and Associated Cortical Hypometabolism in Mild Cognitive Impairment. Cereb Cortex. 2016;26(6):2411–26.

145. Ossenkoppele R, Smith R, Ohlsson T, Strandberg O, Mattsson N, Insel PS, et al. Associations between tau, Aβ, and cortical thickness with cognition in Alzheimer disease. Neurology. 2019;92(6):e601–12.